Response to Referee #1

We are very grateful for the referee's critical comments and suggestions, which have helped us improve the paper quality substantially. We have addressed all of the comments carefully as detailed below in our point-by-point responses. Our responses start with "R:".

This paper uses snow sample observations across northern China in January 2014 and aerosol radiation models to examine the reduction of snow albedo due to black carbon, organic carbon and anthropogenic dust. The study suggests different contributions to the snow albedo reductions from these aerosols and suggests that biomass burning may be a major contributor at most snow sampling sites. It also evaluates the model simulations based on the observations. In general, this paper provides useful information, particularly the different performance in snow albedo reduction by three types of aerosols. However, there are still a few limitations. The small sample volume observed over short period at limited sites could make the results questionable. At least discussions about the uncertainties and potential issues in this study are necessary. Corresponding to the limited data, reliable or strong quantitative conclusion is hard to obtain. The authors could provide more quantitative results and discuss the reliability of the findings in the study.

R: We agree with the reviewer that the number of snow sample is small from the only 13 monitoring sites. One reason for the small number of samples in this season (2014) was due to the less snowfall across northern China. Despite with the small snow data samples, we have designed the study carefully by running two models and combing with various other data sets to generate new scientific knowledge. The importance of our study can be reflected in the following aspects:

 (1)Seasonal snow amount at mid-high latitude regions has large spatial variations in any given year. One novelty of the present study is to investigate the spatial and vertical variations of BC in seasonal snow and attribute the light absorption to BC, OC and mineral dust.

(2) Several recent studies have indicated that the mixing states of BC and the irregular morphology of snow grain have large effects in snow albedo reduction (He et al., 2014; Liou et al., 2011, 2014). Based on the comments from this reviewer and from the interactive comments provided by Cenlin He, we have provided a new figure in the revised paper discussing the uncertainties in the mixing states and the irregular morphology of snow grains on snow albedo reduction estimation using SAMDS model simulations (Figure 10).

(3) The title has been changed as "Observations and model simulations of snow albedo reduction in seasonal snow due to insoluble light-absorbing particles during 2014 Chinese survey".

The manuscript is totally rewritten, and more results in discussing the SAMDS for snow albedo reduction due to ILAPs in snow, internal/external mixed BC in snow, and the snow grain shapes were given in the abstract, introduction, methods, results, and the conclusions. Details have already been illustrated in comment 1.

Are the snow samples fresh or aged snow?

R: We have already updated this information in Table 1 and Figure 1.

(2)Snow albedo reduction due to these kinds of aerosols is well known, more quantitative results are needed and more valuable, which could be summarized in the abstract. At current version, it is a little hard for me to summarize the findings I can learn from this paper.

R: We agree with the reviewer that optical properties of black carbon in snow have been investigated in earlier studies (e.g. Liou et al., 2014; Qian et al., 2014; Warren et al., 1980). However, very few studies have focused on light absorption by OC and dust in snow, which is one of the focuses of our study here. We have investigated snow albedo reduction by OC and mineral dust using the SNICAR model and a new SAMDS model. The impact of the uncertainties in the mixing states and the irregular morphology of snow grain on albedo reduction is also illustrated using SAMDS model simulations (Figure 10)..

Page 3, line 11-14, why is Ginoux et al. 2010 cited two times in one sentence (begin and end). This is repeated description and one should be deleted.

R: We have deleted the second citations of Ginoux et al., (2010), and we have also corrected the similar mistakes throughout the manuscript.

Page 4, line 4-5, you use "larger" and "more intense" in the sentence, but I did not see any comparison descriptions around this sentence. What you are comparing?

R: We have added a reference of Guan et al. (2016), which illustrated the relationship between anthropogenic dust and population over global semi-arid regions, and the source attribution of insoluble light-absorbing particles in seasonal snow across northern China. Furthermore, Wang et al. (2013a) also indicates that BC emission sources in China are strongest in far eastern China of our northeast China snow sampling than the other regions across northern China (Figure 11 in Wang et al., 2013a).

Page 4, Line 12-13, why is Light et al. 1998 cited two times in one sentence (begin and end). This is repeated description and one should be deleted.

R: Corrected.

Page 5, line 15-24, you mentioned several campaigns for snow collection. What are the differences or similarities for the findings among them? Also, it shows that there is a snow campaign over the examined region in 2010 carried out by Huang et al. 2011. Why do not you also include the observation from this campaign so that you have enough data samples and you can also compare the differences/similarities in two winters?

R: In this manuscript, we try to focus on the new findings due to ILAPs in snow during 2014 field campaigns more clearly. As a result, we deleted figure 6 and section

3.3. Figure 4 was also modified as figure 4a and 4b based on 2014 snow field campaigns, which weren't published in previous studies.

As Doherty et al., (2015) indicated that with no measure of the interannual variability of the mixing ratio of BC in snow, it is difficult to determine the representativeness of the samples collected in the Arctic survey.

R: We agree with the reviewer. For this reason, we note that further field campaigns on measuring mixing ratio of BC in snow should be performed worldwide in northern Hemisphere. However, these datasets were much useful for climate models to reduce the uncertainty of the climate effects due to BC in snow.

Page 7, line 1-3, is this data criteria enough to prevent contamination? And why do you include site 101 if it does not fit your data criteria?

R: We indicate that the datasets used in this study are criteria enough to prevent contamination. The reason is that the snow sample collection and the analysis procedure were strictly performed followed by Doherty et al. (2010) and Grenfell et al. (2011). Although site 101 is close to the village, we point out that the ILAPs in snow are more representative for the country village regions across northern China.

Page 7, line 5-10, what is the uncertainty introduced due to your visual inspection and data processing method?

R: As shown in Grenfell et al. (2011), visual comparison is best carried out under diffuse reflected illumination with the filters sitting on a white diffusing background. Uncertainties including personal bias involved on measuring BC in snow is approximately a factor of ~1.5-2. The causes of the bias in the visual estimates of the China 2010 field filters vs. those from the expedition reported by Grenfell et al. (2011) is unknown (Grenfell et al., 2011; Wang et al., 2013a).

Page 8, line 1-9, what do some variables (not all) stand for?, such as Ss?

R: The subscript of Ss means sea salt sources. We have added explanations for all the variables that were not labeled in this manuscript.

Page 8, line 17, why do not you introduce Fe when iron is first used in paper?

R: We indicated that Fe in this manuscript is the same as iron (Page 9, line 17) . Another consideration is that when discussing chemical elements, the symbol Fe instead of iron is commonly used.

Page 9, line 4-6, How do you know Microtops II is reliable, or more reliable than CE318?

R: We indicated that Microtops II and CE318 are both effective instruments on measuring aerosol optical depth (AOD) (More et al., 2013; Porter et al., 2001; Zawadzka et al., 2014). However, the major difference between Microtops II and CE318 is that the Microtops II is portable for the field experiments, but CE318 is immovable. For the snow survey, it is better to use the Microtops II instrument

instead of CE318 to measure aerosol optical depth.

Page 9, Line 22, do you mean "in 2014"?

R: We have already corrected this sentence as "Fire locations were based on data provided by the MODIS FIRMS system from October 2013 to January in 2014."

Page 10, line 4-5 and line 19-20, why do the observations and models calculate the albedo at different height (1 m above snow vs at surface)? Also, the downwelling solar radiation in the real sky includes diffuse radiation. How does the model consider the diffuse radiation (such as the contribution from aerosols and clouds in the sky)?

R: Normally the relative position of the sighting laser spot is at a distance of 1m from the optical element for the active field of view for the instrument in strict accordance with the user manual of the SVC HR-1024 spectroradiometer (Figure 6 Setup for FOV map). The direction of the instrument was oriented to the Sun Horizon angles in order to receive more direct solar radiation. The small size of the fore optics greatly reduces errors associated with instrument self-shadowing. Even when the area viewed by the fore optic is outside the direct shadow of the instrument, the instrument still blocks some of the illumination (either diffuse skylight or light scattered off surrounding objects) that would normally be striking the surface under observation for measuring full-sky-irradiance throughout the entire 350 - 2500 nm wavelengths. This spectroradiometer is used for measuring the direct component of solar irradiance because of the minimized relative radiometric errors between total and direct irradiance measurements. For instance, Bi et al. (2013) used a set of broadband radiometers and sun/sky photometers during 2013 field campaign in the middle latitude across northern China to measure the direct and diffuse solar irradiance, and the result indicated that the diffuse solar radiation is 10% lower than the total solar irradiance. Therefore, we indicated that the spectroradiometer in the clean sky condition mainly measured the direct solar irradiance during 2014 snow campaign. The above materials have been added in section 2.4 of the revised paper to present the relative parameter of the spectroradiometer.

Page 11, line 15, the symbol should be μ, please explain its meaning.

R: We have changed the symbol as μ in Page 14, line 16, and μ refers to the escape function in radiative transfer theory (Kokhanovsk and Zege, 2004).

Page 15, line 7-10, both AOD from MODIS and ground are retrieved, please describe clearly.

R: The ground AOD is retrieved by Microtops II sun photometer. We have already indicated that Microtops II sun photometer is an effective instrument on measuring AOD. However, the weakness of this instrument is that it can only precisely measure AOD during the clean sky. So we only measured the ground AOD dataset in six sites. Then we used the MODIS AOD dataset to compare with our ground measurements to indicate the spatial variations of AOD across northern China. The active open fire retrieved from MODIS was also used to show the possible sources of the BC and OC.

Page 15, line 16, colder -> cold

R: corrected.

Page 15, line 23, This sentence is not complete. I believe what you want to say is "..., which with ..."

R: This sentence has been modified as: "In Inner Mongolia, the snow cover was thin and patchy. The average snow depth at sites 90, 91, 93, and 94 was less than 10 cm, which was significantly smaller than those (13 to 20 cm) at sites 95-97 near the northern border of China." in page 18 lines 20-24.

Page 16, line 2-4, "Because less snow fell during the 2014 snow survey period, the surface snow grain radius varied considerably from 0.07 to 1.3 mm.". First, I do not understand this causal relationship, please clarify. Second, what does it compare when using 'less', the same period of other years or other locations?

R: We have revised the sentence as: "The maximum snow depth was found to be 46 cm at site 102 inside a forest near the Changbai Mountains. Snow depth varied from 13 to 46 cm at sites 98 to 102 with an average of 27 cm. R_m of the snow samples varied considerably from 0.07 to 1.3 mm. R_m increased with the snow depth from the surface to the bottom, larger than previously recorded because of snow melting by solar radiation and the ILAPs." in page 19 lines 5-10.

Page 16, line 19-24, why the variations (BC and snow spatial distribution) you found were much higher than the findings from other studies?

R: BC in snow in this manuscript was mostly collected in heavy industrial regions in northern China, where the mixing ratios of BC and OC were much higher than in the other regions of northern China (Flanner et al., 2007; Wang et al., 2013a; Zhao et al., 2014).

Page 17, line 1-8, I cannot catch the main points you would like to deliver here.

R: This section has been completely rewritten for clarification.

Page 17, Figure 5, the sample volume is too small. How reliable are the relationships found here?

R: We have added the datasets of BC measurements in seasonal snow during 2010 field campaign in Figure 5. The caption of Figure 5 was rewritten as "Comparisons between the calculated and optically measured C_{BC}^{est} in surface snow during 2010 and 2014 snow surveys. The datasets of measured C_{BC}^{est} in 2010 from sites 3-40 were reprinted from Wang et al. (2013a).". We have also provided the confidence test of the fitting in Figure 5.

Page 17, line 22-24, I do not understand from Figure 6 how you got this range in OC/BC ratio.

R: See our answer to the next question.

Page 18, line 1-16, it is hard to conclude due to limited data and sites.

R: Following the reviewer's suggestions, we chose to concentrate on the ILAPs in snow and the snow albedo reduction due to internal/external ILAPs in snow, and the snow grain shapes. Therefore, we have deleted figure 6, and added a new figure in discussing the snow albedo reduction due to internal/external mixed BC in snow and difference snow grain shapes as Figure 10 in this revised manuscript.

Page 18, line 18-22. How did you get the observation regarding land-cover type when the land is covered by snow?

R: The land-cover types (Figure 7) were obtained from the Collection 5.1 MODIS global land-cover type product (MCD12C1) at a 0.05°spatial resolution. The dataset included 17 different surface vegetation types (Friedl et al., 2010; Loveland and Belward, 1997). What we wanted to demonstrate is that most of the sampling regions were correlated with human activities, while this manuscript mainly focused on the anthropogenic dust and the other ILAPs in seasonal snow.

(25)Page 19, Line 17-20, why is Wang et al. 2015 cited two times in one sentence (begin and end). This is repeated description and one should be deleted.

R: Corrected.

References:

Bi, J. R., Huang, J. P., Fu, Q., Ge, J. M., Shi, J. S., Zhou, T., and Zhang, W.: Field measurement of clear-sky solar irradiance in Badain Jaran Desert of Northwestern China, J. Quant. Spectrosc. Ra., 122, 194-207, 10.1016/j.jqsrt.2012.07.025, 2013.

Doherty, S. J., Steele, M., Rigor, I., and Warren, S. G.: Interannual variations of light-absorbing particles in snow on Arctic sea ice, J. Geophys. Res.-Atmos., 120, 11391-11400, 2015.

Doherty, S. J., Warren, S. G., Grenfell, T. C., Clarke, A. D., and Brandt, R. E.: Light-absorbing impurities in Arctic snow, Atmos. Chem. Phys., 10, 11647-11680, 2010.

Flanner, M. G., Zender, C. S., Randerson, J. T., and Rasch, P. J.: Present-day climate forcing and response from black carbon in snow, J. Geophys. Res.-Atmos., 112, D11202, 2007.

Friedl, M. A., Sulla-Menashe, D., Tan, B., Schneider, A., Ramankutty, N., Sibley, A., and Huang, X. M.: MODIS Collection 5 global land cover: Algorithm refinements and characterization of new datasets, Remote Sens. Environ., 114, 168-182, 2010.

Ginoux, P., Garbuzov, D., and Hsu, N. C.: Identification of anthropogenic and natural dust sources using Moderate Resolution Imaging Spectroradiometer (MODIS) Deep Blue level 2 data, J. Geophys. Res.-Atmos., 115, D05204, 2010.

Grenfell, T. C., Doherty, S. J., Clarke, A. D., and Warren, S. G.: Light absorption from particulate impurities in snow and ice determined by spectrophotometric analysis of filters, Appl. Opt., 50, 2037-2048, 2011.

Guan, X. D., Huang, J. P., Zhang, Y. T., Xie, Y. K., and Liu, J. J.: The relationship between anthropogenic dust and population over global semi-arid regions, Atmos. Chem. Phys., 16, 5159-5169, 2016.

He, C. L., Li, Q. B., Liou, K. N., Takano, Y., Gu, Y., Qi, L., Mao, Y. H., and Leung, L. R.: Black carbon radiative forcing over the Tibetan Plateau, Geophys. Res. Lett., 41, 7806-7813, 2014.

Huang, J. P., Fu, Q. A., Zhang, W., Wang, X., Zhang, R. D., Ye, H., and Warren, S. G.: Dust and Black Carbon in Seasonal Snow across Northern China, Bull. Amer. Meteor. Soc., 92, 175-181, 2011.

Kokhanovsky, A. A., and Zege, E. P.: Scattering optics of snow, Appl. Opt., 43, 1589-1602, 2004.

Liou, K. N., Takano, Y., and Yang, P.: Light absorption and scattering by aggregates: Application to black carbon and snow grains, J. Quant. Spectrosc. Ra., 112, 1581-1594, 2011.

Liou, K. N., Takano, Y., He, C., Yang, P., Leung, L. R., Gu, Y., and Lee, W. L.: Stochastic parameterization for light absorption by internally mixed BC/dust in snow grains for application to climate models, J. Geophys. Res.-Atmos., 119, 7616-7632, 2014.

Loveland, T. R., and Belward, A. S.: The IGBP-DIS global 1 km land cover data set, DISCover: first results, Int. J. Remote Sens., 18, 3291-3295, 1997.

More, S., Kumar, P. P., Gupta, P., Devara, P. C. S., and Aher, G. R.: Comparison of Aerosol Products Retrieved from AERONET, MICROTOPS and MODIS over a Tropical Urban City, Pune, India, Aerosol. Air. Qual. Res., 13, 107-121, 2013.

Porter, J. N., Miller, M., Pietras, C., and Motell, C.: Ship-based sun photometer measurements using Microtops sun photometers, J. Atmos. Oceanic Technol., 18, 765-774, 2001.

Qian, Y., Wang, H. L., Zhang, R. D., Flanner, M. G., and Rasch, P. J.: A sensitivity study on modeling black carbon in snow and its radiative forcing over the Arctic and Northern China, Environ. Res. Lett., 9, 064001, 2014.

Wang, X., Doherty, S. J., and Huang, J. P.: Black carbon and other light-absorbing impurities in snow across Northern China, J. Geophys. Res.-Atmos., 118, 1471-1492, 2013a.

Wang, X., Pu, W., Zhang, X. Y., Ren, Y., and Huang, J. P.: Water-soluble ions and trace elements in surface snow and their potential source regions across northeastern China, Atmos. Environ., 114, 57-65, 2015.

Warren, S. G., and Wiscombe, W. J.: A Model for the Spectral Albedo of Snow .2. Snow Containing Atmospheric Aerosols, J. Atmos. Sci., 37, 2734-2745, 1980.

Yasunari, T. J., Koster, R. D., Lau, W. K. M., and Kim, K. M.: Impact of snow darkening via dust, black carbon, and organic carbon on boreal spring climate in the Earth system, J. Geophys. Res.-Atmos., 120, 5485-5503, 2015.

Zawadzka, O., Makuch, P., Markowicz, K. M., Zielinski, T., Petelski, T., Ulevicius, V., Strzalkowska, A., Rozwadowska, A., and Gutowska, D.: Studies of aerosol optical depth with the use of Microtops II sun photometers and MODIS detectors in coastal areas of the Baltic Sea, Acta Geophysica, 62, 400-422, 2014.

Zhao, C., Hu, Z., Qian, Y., Leung, L. R., Huang, J., Huang, M., Jin, J., Flanner, M. G., Zhang, R., Wang, H., Yan, H., Lu, Z., and Streets, D. G.: Simulating black carbon and dust and their radiative forcing in seasonal snow: a case study over North China with field campaign measurements, Atmos. Chem. Phys., 14, 11475-11491, 2014.

Response to Cenlin He's comments

We thank Cenlin He for his comments, which have heled us improve the paper quality. We have incorporated these comment into the revised paper as detailed below.

The authors conducted extensive field measurements of BC, OC, and dust concentrations in snow over the northern China and employed the SNICAR and SAMDS model simulations to investigate snow albedo reduction caused by the light-absorbing aerosols. This study provides a valuable observational dataset to improve our understanding in the effects of light-absorbing aerosol deposition on snow albedo reduction. I have a short comment on snow albedo modeling. The authors mentioned that the SAMDS model considers aerosol-snow mixing state and the irregular morphology of snow grain by using asymptotic radiative transfer theory. However, the authors did not provide enough discussions on the effects of BC/dust/OC-snow mixing state and snow grain shape on snow albedo reduction as well as compare with some recent studies. These factors are not trivial in evaluating aerosol-snow albedo effects, in addition to snow grain size and aerosol concentration. For example, recent studies by Liou et al. (2014) and He et al. (2014) developed and applied a stochastic snow model to study BC/dust-induced snow albedo reduction, which explicitly simulates different aerosol-snow mixing states and snow grain shapes. They found that using a realistic snowflake shape reduces BC-induced snow albedo reduction by 20–40% compared to a spherical snow grain, while multiple internal mixing of BC and snow increases the albedo reduction by 40–60% relative to the external mixing. I would suggest discussing these recent findings, which could be very helpful for people to understand potential uncertainty and improvement in snow albedo modeling.

R: We noted that the two references by Liou et al. (2014) and He et al. (2014) are both very important achievements for understanding light absorption by internally mixed BC/dust in snow grains for application to climate models. Therefore, we also used the SAMDS model to simulate the snow albedo change by internal/external mixing of BC and snow associated with the irregular morphology of snow grains using asymptotic radiative transfer theory (Figure 10). The following discussions on snow albedo change due to internal/external mixing states of ILAPs associated with irregular snow grains in snow have been added in the revised manuscript.

1. Introduction
"Warren and Wiscombe (1980) found that a mixing ratio of 10 ng g^{-1} of soot in snow can reduce snow albedo levels by 1%. Light et al. (1998) determined that 150 ng g^{-1} of BC embedded in sea ice can reduce ice albedo levels by a maximum of 30%. 1 ng g^{-1} of BC has approximately the same effect on the albedo of snow and ice at 500 nm as 50 ng g^{-1} of dust (Warren, 1982). Doherty et al. (2013) analyzed field measurements of vertical distributions of BC and other ILAPs in snow in the Arctic during the melt season and found significant melt amplification due to an increased

mixing ratio of BC by up to a factor of 5. Yasunari et al. (2015) suggested that the existence of snow darkening effect in the Earth system associated with ILAPs contributes significantly to enhanced surface warming over continents in northern hemisphere midlatitudes during boreal spring, raising the surface skin temperature by approximately 3–6 K near the snowline. Warren and Wiscombe (1985) pointed out that modeling soot in snow as an "external mixture" (impurities particles separated from ice particles) may underestimate the true effect of the impurities as a given reduction of albedo by about half as much soot, if the soot is instead located inside the ice grains as an "internal mixture". Hansen et al. (2004) and Cappa et al. (2012) noted that for a given BC mass on snow albedo, the internal mixing of BC in snow is a better approximation than external mixing, whereas internal mixing increases the BC absorption coefficient by a factor of two, for better agreement with empirical data. Hadley and Kirchstetter (2012) also indicated that increasing the size of snow grains could decrease snow albedo and amplify radiative perturbation of BC. For a snow grain optical effective radius (R_{eff}) of 100 μm, the albedo reduction caused by 100 ng g^{-1} of BC is 0.019 for spherical snow grains but only 0.012 for equidimensional nonspherical snow grains (Dang et al., 2016). Fierce et al. (2016) pointed out that BC coated with non-absorbing particles absorbs more strongly than the same amount of BC in an uncoated particle, but the magnitude of this absorption enhancement is still a challenge. He et al. (2014) indicated that BC-snow internal mixing increases the albedo forcing by 40–60% compared with external mixing, and coated BC increases the forcing by 30–50% compared with uncoated BC aggregates, whereas Koch snowflakes reduce the forcing by 20–40% relative to spherical snow grains using a global chemical transport model in conjunction with a stochastic snow model and a radiative transfer model."

2.5 Model simulations

The contents the asymmetry factor for calculating the snow albedo change by irregular snow grains have been added in Section 2.5 as: "The theory based on the ray-optics approach shows that g in Equation (11) and B in Equation (13) are 0.89 and 1.27 for spheres, 0.84 and 1.50 for hexagonal plates/columns, and 0.75 and 1.84 for fractal grains, respectively."

3.3 Simulations of snow albedo

"Previous studies indicated that the mixing ratio of BC (10-100 ng g^{-1}) in snow may decrease its albedo by 1-5% (Hadley and Kirchstetter, 2012; Warren and Wiscombe, 1980). Liou et al. (2011) demonstrated that a small BC particle on the order of 1 μm internally mixed with snow grains could effectively reduce visible snow albedo by as much as 5-10% using a geometric-optics surface-wave approach. They also found that internal mixing of BC in snow reduces snow albedo substantially more than external mixing, and the snow grain shape plays a critical role in snow albedo calculations through its forward scattering strength by modeling the positions of BC internally mixed with different snow grain types (Liou et al., 2014).

Figure 10a illustrates the effect of snow shape (fractal grains, hexagonal

plates/columns, and spheres) on snow albedo at the spectral wavelengths of 400 nm-1400 nm with R_{eff} of 100 μm simulated by SAMDS model. As is shown, the differences of snow albedo caused by three snow shapes are remarkable. The snow albedo for spherical snow grains is higher than that for the other two shapes because the scattering by spherical snow grains is more in forward direction and less to the sides, resulting in a larger g and a smaller B as discussed in section 2.5. In addition, the snow albedo reduction for aged snow such as spherical snow grains is larger than fresh snow such as fractal snow grains, and hexagonal plates/colums snow grains with the increased BC in snow. It shows that snow albedo by spherical snow grains is typically lower by 0.017-0.073 than the fractal snow grains, and by 0.008-0.036 than the hexagonal plates/columns snow grains, as a function of BC mixing ratios (0-5000 ng g^{-1}). Dang et al. (2016) assessed the effects of snow grain shapes on snow albedo using the asymmetry factors g of nonspherical ice crystal developed by Fu (2007). They obtained similar result that the albedo reduction caused by 100 ng g^{-1} of BC for spherical snow grains is larger by 0.007 than nonspherical snow grains with the same area-to-mass ratio for R_{eff} of 100 μm.

Figure 10b shows the spectral albedo of snow for the internal/external mixing of BC and snow with R_{eff} of 100 μm for a solar zenith angle θ of 60° as a function of BC mixing ratio. For a given shape (hexagonal plates/columns), we found that snow albedo as a function of BC mixing ratios calculated from this study decreases as the fraction of the internal mixing increases (Figure 10b). In previous studies, the BC mixing ratios in seasonal snow were up to 3000 ng g^{-1} due to heavy industrial activities across northern China, but the lowest mixing ratios of BC were found in the remote northeastern on the border of Siberia, with a median value in surface snow of 100 ng g^{-1} (Huang et al., 2011; Wang et al., 2013a, 2014; Ye et al., 2012). As a result, snow albedo by internal mixing of BC and snow is lower than external mixing by up to 0.036 for 3000 ng g^{-1} BC in snow in the heavy industrial regions across northeastern China, whereas by low to 0.005 for 100 ng g^{-1} BC in snow in the further north China near the border of Siberia. We indicated that the snow grain shape effect on snow albedo between spherical snow grains and fractal snow grains is relatively larger than the effect of the internal/external mixing of BC and snow as a function of the BC mixing ratios. However, He et al. (2014) also pointed out that the snow albedo reductions computed by previous models under assorted assumptions vary by a factor of 2 to 5.".

4 Conclusions

"Then, we indicated that the new spectral snow albedo model (SAMDS) can be used to investigate the snow albedo influenced by the internal/external mixing of BC and snow, irregular morphology of snow grains and the vertical distribution of snow grains. For instance, the snow albedo for spherical snow grains is typically lower than that for the fractal snow grains and hexagonal plates/columns snow grains with R_{eff} of 100 μm. The internal mixing of BC and snow absorbs substantially more light than external mixing. For fresh snow grains of hexagonal plates/columns with R_{eff} of 100 μm, the difference of snow albedo between internal and external mixing of BC and

snow is up to 0.036 for 3000 ng g^{-1} BC in snow in the heavy industrial regions across northeastern China, whereas by low to 0.005 for 100 ng g^{-1} BC in snow in the further north China near the border of Siberia. The spectral albedo of snow reduction caused by OC (20 µg g^{-1}) is larger by up to a factor of 3 for a snow grain size of 800 µm compared to 100 µm by using SAMDS model."
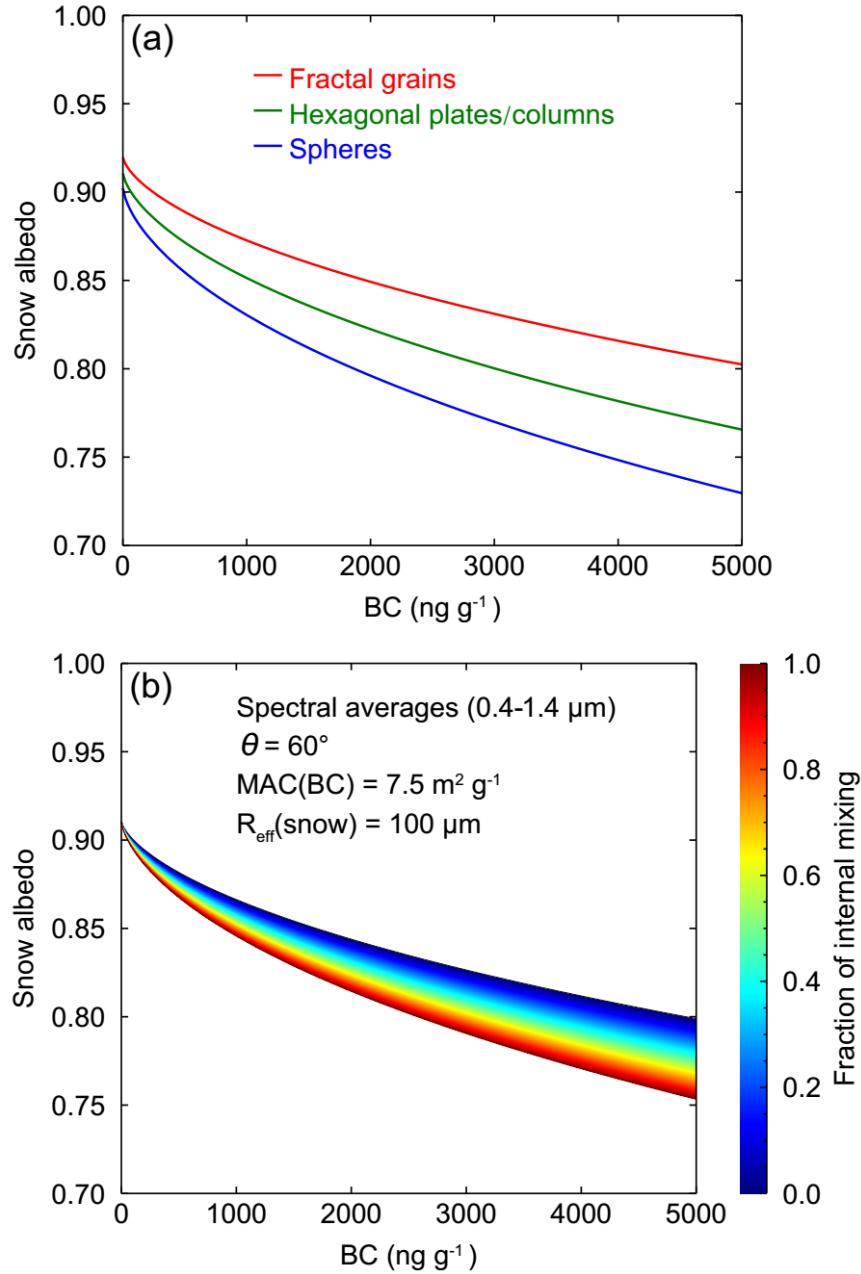
Fig. 10. Spectral albedo of snow as a function of BC mixing ratios in snow by using SMDAS model for: (a) the irregular morphology of snow grains (fractal grains, hexagonal plates/columns, and spheres), (b) internal/external mixing of BC and hexagonal plates/columns snow grains. Also shown are model parameters including integrate spectral wavelengths (400-1400 nm), solar zenith angle (θ), mass absorption coefficient (MAC) of BC, and snow grain optical effective radius (R_{eff}).

References:

Cappa, C. D., Onasch, T. B., Massoli, P., Worsnop, D. R., Bates, T. S., Cross, E. S., Davidovits, P., Hakala, J., Hayden, K. L., Jobson, B. T., Kolesar, K. R., Lack, D. A., Lerner, B. M., Li, S. M., Mellon, D., Nuaaman, I., Olfert, J. S., Petaja, T., Quinn, P. K., Song, C., Subramanian, R., Williams, E. J., and Zaveri, R. A.: Radiative Absorption Enhancements Due to the Mixing State of Atmospheric Black Carbon, Science, 337, 1078-1081, 2012.

Dang, C., Fu, Q., and Warren, S. G.: Effect of Snow Grain Shape on Snow Albedo, J. Atmos. Sci., 73, 3573-3583, 2016.

Doherty, S. J., Grenfell, T. C., Forsstrom, S., Hegg, D. L., Brandt, R. E., and Warren, S. G.: Observed vertical redistribution of black carbon and other insoluble light-absorbing particles in melting snow, J. Geophys. Res.-Atmos., 118, 5553-5569, 2013.

Fierce, L., Bond, T. C., Bauer, S. E., Mena, F., and Riemer, N.: Black carbon absorption at the global scale is affected by particle-scale diversity in composition, Nat. Commun., 7, 2016.

Fu, Q.: A New Parameterization of an Asymmetry Factor of Cirrus Clouds for Climate Models, J. Atmos. Sci., 64, 4140-4150, 2007.

Hadley, O. L., and Kirchstetter, T. W.: Black-carbon reduction of snow albedo, Nat. Clim. Change, 2, 437-440, 2012.

Hansen, J., and Nazarenko, L.: Soot climate forcing via snow and ice albedos, Proc. Nat. Acad. Sci. U.S.A., 101, 423-428, 2004.

He, C. L., Li, Q. B., Liou, K. N., Takano, Y., Gu, Y., Qi, L., Mao, Y. H., and Leung, L. R.: Black carbon radiative forcing over the Tibetan Plateau, Geophys. Res. Lett., 41, 7806-7813, 2014.

Huang, J. P., Fu, Q. A., Zhang, W., Wang, X., Zhang, R. D., Ye, H., and Warren, S. G.: Dust and Black Carbon in Seasonal Snow across Northern China, Bull. Amer. Meteor. Soc., 92, 175-181, 2011.

Light, B., Eicken, H., Maykut, G. A., and Grenfell, T. C.: The effect of included particulates on the spectral albedo of sea ice, J. Geophys. Res.-Oceans, 103, 27739-27752, 1998.

Liou, K. N., Takano, Y., and Yang, P.: Light absorption and scattering by aggregates: Application to black carbon and snow grains, J. Quant. Spectrosc. Ra., 112, 1581-1594, 2011.

Liou, K. N., Takano, Y., He, C., Yang, P., Leung, L. R., Gu, Y., and Lee, W. L.: Stochastic parameterization for light absorption by internally mixed BC/dust in snow grains for application to climate models, J. Geophys. Res.-Atmos., 119, 7616-7632, 2014.

Wang, X., Doherty, S. J., and Huang, J. P.: Black carbon and other light-absorbing impurities in snow across Northern China, J. Geophys. Res.-Atmos., 118, 1471-1492, 2013a.

Wang, X., Xu, B. Q., and Ming, J.: An Overview of the Studies on Black Carbon and Mineral Dust Deposition in Snow and Ice Cores in East Asia, J. Meteorol. Res.-Prc., 28, 354-370, 2014.

Warren, S. G., and Wiscombe, W. J.: A Model for the Spectral Albedo of Snow .2. Snow Containing Atmospheric Aerosols, J. Atmos. Sci., 37, 2734-2745, 1980.

Warren, S. G. and Wiscombe, W. J.: Dirty Snow after Nuclear-War, Nature, 313, 467-470, 1985.

Warren, S. G.: Optical-Properties of Snow, Rev. Geophys., 20, 67-89, 1982.

Yasunari, T. J., Koster, R. D., Lau, W. K. M., and Kim, K. M.: Impact of snow darkening via dust, black carbon, and organic carbon on boreal spring climate in the Earth system, J. Geophys. Res.-Atmos., 120, 5485-5503, 2015.

Ye, H., Zhang, R. D., Shi, J. S., Huang, J. P., Warren, S. G., and Fu, Q.: Black carbon in seasonal snow across northern Xinjiang in northwestern China, Environ. Res. Lett., 7, 044002, 2012.

Response to Referee #2

We greatly appreciate this referee's critical comments and suggestions, which have helped us improve the paper quality substantially. We have addressed all of the comments carefully as detailed below in our point-by-point responses below. Our responses start with "R:".

Due to the high amounts of industrialization in China, there is a need for studies of impurities in seasonal snow. This study is on a Chinese snow survey conducted in 2014. However, it is not clear how much of the data presented in this study has already been published. The authors are recommended to clarify, in much more detail, what data has been previously published, and what are novel results from this study and included in this manuscript. For example, it is not clear whether this study presents new snow chemistry data, or if this data has been published in another manuscript, such as Wang 2015. It is also unclear why the 2010 Chinese Snow survey data is included in the study. Averaging results from the 2010 and 2014 surveys seems inappropriate, especially because the snow conditions/depths appear to vary widely since so many sites did not even have enough snow to resample in 2014. The paper does not appear to be ready for publication in this submission, even with the following revisions. Major restructuring is needed.

R: We admit that the ILAPs and the chemical species in seasonal snow across northern China have already been investigated in previous studies (Huang et al., 2011; Wang et al., 2013a, 2015; Ye et al., 2012, Zhang et al., 2013a). Similar experiments on measuring ILAPs in seasonal snow have also been conducted on the Arctic, Greenland, North America, even in Loess Plateau in recent years (Doherty et al., 2010; 2014; Ming et al., 2009). For instance, a similar paper on the mixing ratios of ILAPs in Arctic snow (Doherty et al., 2010) has been widely used for validating modeled snow BC mixing ratios. There are also heavy loadings of mineral dust in present snow, which could also lead a rapid snow albedo reduction (Yasunari at al., 2015). However, the ability to test model representation of ILAPs in snow via climate modeling is still critical. According to the model simulations by Qian et al. (2014) and Zhao et al. (2014), although the model simulates reasonably well the magnitude of BC mixing ratios in the middle latitudes, the models generally moderately underestimates BC in snow in the clean regions but significantly overestimates BC in some polluted regions. We thus realized that the snow albedo could be reduced remarkably due to the large variations of ILAPs in seasonal snow in those regions across northern China, which could lead large biases of the radiative forcing of ILAPs in seasonal snow due to the model simulations. Based on the above mentioned studies, we think there is a need to investigate the spatial and vertical variations of BC in seasonal snow and attribute the light absorption to BC, OC and mineral dust. Another purpose of the study is to reveal the snow albedo reduced by ILAPs in snow between surface measurements and model simulations using a standard spectroradiometer, two snow/ice radiative models of the Snow, Ice, and Aerosol Radiation (SNICAR) model, and a new radiative model (Spectral Albedo Model for Dirty Snow, or SAMDS).

Based on the comments from all the reviewers, we have made the following major revisions to improve the quality and clarity of the paper:

(1) The title has been changed to "Observations and model simulations of snow albedo reduction in seasonal snow due to insoluble light-absorbing particles during 2014 Chinese survey".

(2) The abstract has been rewritten to accurately reflect the new results.

(3) We have deleted the part of discussion in the Introduction related to radiative forcing of ILAPs. We, however, have added discussion on the internal/external mixing state of BC in snow and different snow grain shapes in affecting snow albedo, which is more correlated with the scope of this manuscript.

(4) The result section was changed from "section 3.1-3.6" to "section 3.1-3.4" as follows:
3.1 The spatial distribution of AOD
3.2 Contributions to light absorption by ILAPs
3.3 Simulations of snow albedo
3.4 Comparison between the observed and modeled snow albedo

(5) We have deleted the Figure 6 and section 3.3, whih discussed the emission sources by using the chemical species in previous version.

(6) We have added analysis on the uncertainty of the snow albedo reduction by the mixed BC in snow by different snow grain shapes. Therefore, a new figure is added as Figure 10 in the revised manuscript to present the snow albedo change due to the internal/external mixing of BC in snow and the snow grain shapes by using the SAMDS model compared with previous studies (He et al., 2014; Liou et al., 2011, 2014).

(7) We have revised the "Conclusions" to better reflect the revised contents.

The novelty of the paper appears to begin in the model comparisons with the albedo surface observations made in 2014. The reader suggests the authors significantly revise the paper to focus solely on the 2014 observations (unless the reader is confused by the text and the 2010 data has not yet been published?).

R: The 2010 snow survey datasets used in this study was deleted. We noted that most of the chemical datasets used in this study were to retrieve the new datasets of sea salt and $K_{Biosmoke}^{+}$ depending on the previous studies, which were not shown by Wang et al. (2015). However, only SO_4^{2-}, NO_3^{-} and NH_4^{+} data from Wang et al. (2015) were reused in the present study to indicate the mass contribution of the ILAPs with the other chemical species in snow across northern China. To make this clear, we have added a section to explain the datasets published by Wang et al., (2015) used in this study.

Additionally, according to the methods used, the reader asks the authors to report the BC as equivalent black carbon (eBC) rather than black carbon. If there is a reason otherwise to report as BC, please explain.

R: We have modified "BC" as "C_{BC}^{est}" or "C_{BC}^{equiv}" in the revised manuscript.

It appears (though clarification is needed from the authors) that a new model, SAMDS, similar to the SNICAR model, is applied here. However, only a small portion of this very long paper is devoted to this section. A short discussion/conclusion at the end needs further expansion. Then for the authors to focus on the observed vs. modeled albedo, as well as provide more information and justification for applying the SAMDS model more widely. The SAMDS model appears to be the main highlight of the paper. The title and paper could be restructured around the SAMDS model.

R: The title of this manuscript has been modified as "Observations and model simulations of snow albedo reduction in seasonal snow due to insoluble light-absorbing particles during 2014 Chinese survey". The manuscript has also been restructured around the SAMDS model throughout the revised manuscript (See abstract, introduction, results, and the conclusions).

The scientific methods used could be explained in a more logical way throughout the methods section of the paper. Also, in the site description, an explanation why the site numbers begin at 90 in 2014 should be given. Also, a map including GPS coordinates and the sampling sites would aid the reader. Additionally, it is stated that the same volume of snow was not collected at all sites. How much volume was filtered at each site? This leads the reader to believe that if the same top volume of snow was not collected at each site, the integrated mass concentration of BC in each snow sample would be different?

R: The site numbers during the snow survey in 2014 have been labeled in Figure 1. We noted that the site numbers beginning at 90 in this study are numbered in chronological order following Wang et al. (2013a) and Ye et al., (2012). Therefore, we have modified the captions in Table 1 and Figure 1 to make this clear. We need to clarify this question about the volume of snow samples. Firstly, enough snow samples have been collected during field campaigns. Secondly, we quickly melt the snow samples in the lab, and filtrated the snow samples by using different liquid snow volume, which depended on the degree of contamination for snow samples. The calculation of C_{BC}^{max}, C_{BC}^{est}, and f_{BC}^{est} are listed as follows:

$$C_{BC}^{max} = \frac{L_{BC}^{max} \times A}{V}$$

$$C_{BC}^{est} = C_{BC}^{max} \times f_{BC}^{est}$$

C_{BC}^{max} (ng g^{-1}): maximum BC is the mass of BC per mass of snow, if all aerosol light absorption at 650–700 nm is due to BC.

C_{BC}^{est} (ng g^{-1}): estimated BC is the estimated true mass of BC per mass of snow, derived by separating the spectrally resolved total light absorption.

f_{BC}^{est}: Fraction of light absorption by true mass of BC per mass of snow.

Yes, the volume is a very important parameter in collecting the ILAPs on the nuclepore filter. However, due to the mass loading of BC (L_{BC}^{max}) can be measured by using the ISSW instrument, we note that the mixing ratios of C_{BC}^{max} and C_{BC}^{est} for each snow samples are definitely comparable based on above calculation. Then, the averaged C_{BC}^{est} for each vertical profile of snowpack is calculated by using following equation:

$$\text{average BC} = \frac{\sum_i (C_{BC_i}^{est} * \rho_i * h_i)}{\sum_i (\rho_i * h_i)}$$

where i is the number of snow layer, $C_{BC_i}^{est}$, ρ_i and h_i are the estimated BC mixing ratio, snow density and snow depth, respectively, at the layer i.

In conclusion, much of the intro and re-presenting of previously published data from the 2010 and 2014 Chinese snow surveys could be removed. And/or better support/clarification for the reason for including it could be included.

R: We have deleted the previously published datasets from 2010 and 2014 in conclusion, and focused more attention on the model simulations, especially for the description of SAMDS model.

Suggestions for Revisions:
The abstract is not currently sufficient. The first sentence states that 92 samples were collected in 2014, however, the 92 points appear to be presented as fewer averages later. The abstract should state how many average values are presented in the study and if the 92 samples were collected across X sites, X snowpits, and at X resolution within the snowpit. Additionally, only surface sample average concentrations are presented in the abstract, how many samples were collected at the surface? And how many in snow pits, and integrated pit samples?

R: We have modified the abstract. The first sentence has been revised as "A snow survey was carried out to collect 13 surface snow samples (10 for fresh snow, and 3 for aged snow), and 79 sub-surface snow samples in seasonal snow at 13 sites in January 2014 across northeastern China. A spectrophotometer and the chemical analysis were used to separate snow particulate absorption by insoluble light-absorbing particles (ILAPs, e.g. black carbon, BC; mineral dust, MD; and organic carbon, OC) in snow, and the snow albedo was measured using a field spectroradiometer during this period."

First of all, at the end of the introduction, previous data published from the 2010 and 2014 Chinese snow survey must be presented clearly. Then, a paragraph outlining what is specifically novel about this study must then be stated. Throughout the manuscript, when previously published data is presented, a reference must be cited for where that data has been published.

R: We have removed all of the datasets from 2010 snow surveys throughout the revised manuscript except for Figure 5, and in the last paragraph we have added discussion on the novelty of this study. We have added the citation and the explanation in the figures very carefully, when used the published datasets by Wang et al., (2015).

Additionally, is this paper the first presentation of the SAMDS model? This should be more clearly stated in the abstract, as this appears to be the main point/novelty of the paper. In general, the paper could be edited to more clearly explain what new data is presented in the study. There are pervasive run-on sentences; the manuscript should be edited to make the language more concise.

R: Yes, the SAMDS model is the first time to be used to reveal the effects of ILAPs, the internal/external mixing of BC and snow, and the snow grain shapes on snow albedo reduction. We have also rewritten the abstract to better illustrate the new

SAMDS model. The revised manuscript is also reconstructed to make the language more concise following the reviewer's comments and suggestions.

The discussion should be expanded to support a more widespread use of the SAMDS model. Also, stating how the model will be disseminated, would aid readers in applying it to their own research. Is there a plan to do so?

R: Yes, the SAMDS model will be definitely disseminated, and we are glad to release the source code after the publication by Zhang et al. (2016). Except the discussion of SAMDS used in this study, the SAMDS model also consider the following processes: (i) mixing states between impurities and snow grains, (ii) the irregular morphology of snow grains and aerosol particles, (iii) specific mineral compositions and size distributions of MD in snow, (iv) aging processes of snow grains and soot aggregates, and (v) multilayers for studying vertical distributions of snow grains and impurities. A detailed description of the SAMDS model will be presented by Zhang et al. (2016). We also note that the SAMDS model can be used to couple with the global climate model (e.g. NCAR Community Atmosphere Model, CAM) to simulate the radiative forcing due to ILAPs in snow and the multiple internal/external mixing of BC in various types of snow grains, which is similar with the previous studies (Flanner et al., 2009; He et al., 2014; Zhao et al., 2014).

Overall, the paper needs major restructuring and revision to portray a logical flow of information. The main weakness is that it is very unclear what is new data and what has previously been published from the 2010 and 2014 surveys and this paper should focus only on what is new.

R: As shown in our responses to the general comments above, we have reconstructed the paper substantially. The main purpose of this manuscript focuses on the spatial variations of ILAPs in seasonal snow during less snow year in 2014, and the discrepancy of snow albedo change by ILAPs in snow and the shapes of snow grains between model simulations and observations.

Specific Line Comments:

Comment 1: Jaffe 1999 cited on Page 3 Line 4 is not included in the bibliography.

R: We have added this reference in the bibliography as follows:

Reference:
Jaffe, D., Anderson, T., Covert, D., Kotchenruther, R., Trost, B., Danielson, J., Simpson, W., Berntsen, T., Karlsdottir, S., Blake, D., Harris, J., Carmichael, G., and Uno, I.: Transport of Asian air pollution to North America, Geophys. Res. Lett., 26, 1999.

Comment 2: Page 4 Line 3: Writing edit: ', with India at' => ' and ' 76.1% in India'

R: revised as suggested.

Comment 3: Page 4 Line 13: 'Among its main light-absorbing impurities' This sentence introduction does not make sense. Could just remove the intro and start with '1ng g-1 of BC'. . ..

R:Revised as suggested.

Comment 4: Page 4 Line 14: 'on the albedo' => 'on the albedo of snow and ice'.

R: Revised as suggested.

Comment 5: Page 4 Line 17: 'owing to' doesn't read well... please alternate words here, as well as multiple other locations in the manuscript. Other suggestions could be, 'due to', etc.

R: We have replaced "owing to" as "due to", "because of", and "Assumption" throughout the revised manuscript.

Comment 6: Page 4 Line 20, first word. Include citation(s) for the previous sentence.

R: Three citations have been added after the first sentence as follow:

Brandt, R. E., Warren, S. G., and Clarke, A. D.: A controlled snowmaking experiment testing the relation between black carbon content and reduction of snow albedo, J. Geophys. Res.-Atmos., 116, 2011.
Hadley, O. L., and Kirchstetter, T. W.: Black-carbon reduction of snow albedo, Nat. Clim. Change, 2, 437-440, 2012.
Warren, S. G. and Wiscombe, W. J.: Dirty Snow after Nuclear-War, Nature, 313, 467-470, 1985.

Comment 7: Page 4 Line 21: In the Bond 2013 paper, sub-title 0.2.3 Synthesis of black carbon climate forcing terms, number 2: "The best estimate of industrial-era climate forcing of black carbon through all forcing mechanisms is +1.1 W m-2 with 90% uncertainty bounds of +0.17 to +2.1 W m-2." Rather than 90 % confidence interval as listed in this manuscript.

R: The sentence has been revised as "Bond et al. (2013) estimated the industrial-era climate forcing of BC through all forcing mechanisms to be approximately +1.1 W m$^-$^{2}, with 90% uncertainty bounds of +0.17 to +2.1 W m^{-2}."

Comment 8: Page 5 Line 9: 'in situ' => 'in situ' and elsewhere in the manuscript.

R: We have removed "in situ" throughout the manuscript, and instead using "field campaigns". Similar corrections have also been made throughout the revised manuscript.

Comment 9: Page 5 Line 20: 'involve' use different word such as 'present' or 'include'

R: We have changed "involve" as "present" in Page 6, line 24.

Comment 10: Page 5 Line 21: Begin new sentence with 'Previously, . . .we analyzed' if some data from the Chinese snow survey in 2014 was already published and include citation. The reader is confused if some of this data has already been published, or if this data is all unpublished and included in this study. If all the data is unpublished, could start the sentence with, 'Here' instead of 'previously', such as

'Here we analyze...' instead of 'analyzed' to convey to the reader this is new data being presented.

R: The introduction has been mostly reconstructed, and the datasets of the chemical species used in this study have been carefully rewritten in section 2.2.

Comment 11: Page 5 Line 21: Here you could explain how this study is different than what has already been published from the Chinese snow survey in 2014.

R: We have rewritten this paragraph in revised manuscript as "To our knowledge, there are only a few studies that compare modeled and observed snow albedo reduction due to ILAPs in snow (Dang et al., 2015; Flanner et al., 2007, 2012; Grenfell et al., 1994; Liou et al., 2014; Warren et al., 1980). In this study, a 2014 snow survey was performed across northeastern China to analyze light absorption of ILAPs in seasonal snow, and the comparison of snow albedo reduction due to internal/external mixed BC in snow and different snow grain shapes. In section 2, we present the experimental procedures, including a new radiative transfer model (Spectral Albedo Model for Dirty Snow, or SAMDS). After describing our methods (Sect. 2), we demonstrate the light absorption by snowpack containing ILAPs across northeastern China for less snow fallen year through a Chinese survey in 2014 following the snow surveys held in 2010 and 2012 across northern China carried out by Huang et al. (2011) and Ye et al. (2012). Then, a comparison of the snow albedo reduction under clear sky conditions measured by using a field spectroradiometer and simulated by the Snow, Ice, and Aerosol Radiation (SNICAR) model and SAMDS model based on two-stream radiative transfer solution is present. The SAMDS model is also used for the computation of light absorption by complex ILAPs in snow for application to analyze the effects of snow grain shapes (fractal grains, hexagonal plates/columns, and spheres) and internal/external mixing of BC and snow on snow albedo. Finally, conclusions are given in section 4.".

Comment 12: Page 6 Line 11: I think it is a bit misleading to say 'we explore climatic effects of ILAPs' as far as the reader can see, albedo reduction is explored, but climate models are not employed. Please rephrase or clarify.

R: See our reply to comment 11 above.

Comment 13: Page 6 Line 13, 'Therefore' => 'Here'. Or clarify if something else is meant.

R: See our reply to comment 11 above.

Comment 14: Page 6 Line 14: Create two sentences. 'campaign. Snow albedo is also. . .' Also, when was the snow campaign? 2014? Please include year for clarity.

R: See our reply to comment 11 above.

Comment 15: Page 6 Line 15: Is this the first presentation of SAMDS? If so rephrase sentence to explain 'SNICAR and 'the new' SAMDS. . .'

R: Yes, this is the first presentation of the SAMDS model, therefore, we have revised the abstract, results, and the conclusions for the SAMDS model. For the revised paper, the sentence has been revised as "In section 2, we present the experimental procedures, including a new radiative transfer model (Spectral Albedo Model for Dirty Snow, or SAMDS). After describing our methods (Sect. 2), we demonstrate the light absorption by snowpack containing ILAPs across northeastern China for less snow fallen year through a Chinese survey in 2014 following the snow surveys held in 2010 and 2012 across northern China carried out by Huang et al. (2011) and Ye et al. (2012). Then, a comparison of the snow albedo reduction under clear sky conditions measured by using a field spectroradiometer and simulated by the Snow, Ice, and Aerosol Radiation (SNICAR) model and SAMDS model based on two-stream radiative transfer solution is present. The SAMDS model is also used for the computation of light absorption by complex ILAPs in snow for application to analyze the effects of snow grain shapes (fractal grains, hexagonal plates/columns, and spheres) and internal/external mixing of BC and snow on snow albedo. Finally, conclusions are given in section 4."

Comment 16: Page 6 Line 19: Include sub-heading for 'Site Introduction'. Also, include the time range the samples were collected in this paragraph, was each site visited once over the month?

R: This sentence has been revised as "In 2014, there was less snowfall in January than in previous years (e.g., 2010), and only 92 snow samples (13 surface snow, and 79 sub-surface snow samples) at 13 sites were collected during this snow survey." The sub-heading has also been revised as "Snow field campaign in January 2014".

Comment 17: Page 7: In the site introduction, please explain why only sites 90 –102 were visited. Why do the numbers begin at 90? Where there 90 sites in 2010 where there was not snow in 2014?

R: We have collected snow samples in 86 sites in the 2010 and 2012 campaigns across northern China (Figure 1 in Ye et al., 2012), and three snow samples were collected in Lanzhou in 2013 winter, which weren't shown in this study. As a result, the sampling sites in this manuscript are numbered in chronological order beginning at 90 followed Wang et al. (2013a), and Ye et al., (2012). We have added one sentence as "The snow sampling sites in this study began at 90, which are numbered in chronological order followed by Wang et al. (2013a) and Ye et al. (2012)."

Comment 18: Page 7: This is troubling to the reader. If different volumes of sample were collected based on how dirty a site was, does this make the measurements comparable? When the sample is filtered, does the volume not matter? How much volume was filtered? The total sample? Please explain.

R: We need to clarify this question. Yes, the volume is a very important parameter in collecting the ILAPs on the nuclepore filter. We recorded the filtration volume (V) and the surface area of the filter loaded by ILAPs (A), and measured the mass loading of BC (L_{BC}^{max}) by using the ISSW instrument, Then, the calculation of C_{BC}^{max}, C_{BC}^{est}, and f_{BC}^{est} are listed as follows:

$$C_{BC}^{max} = \frac{L_{BC}^{max} \times A}{V}$$

$$C_{BC}^{est} = C_{BC}^{max} \times f_{BC}^{est}$$

C_{BC}^{max} (ng g^{-1}): maximum BC is the mass of BC per mass of snow, if all aerosol light absorption at 650–700 nm is due to BC.

C_{BC}^{est} (ng g^{-1}): estimated BC is the estimated true mass of BC per mass of snow, derived by separating the spectrally resolved total light absorption.

f_{BC}^{est}: Fraction of light absorption by true mass of BC per mass of snow.

Therefore, the calculation of the mixing ratio of BC in snow needs to use the volume to convert the mass loading of BC as mixing ratio of BC in snow; details could be found by Grenfell et al. (2011) and Doherty et al. (2010). Another issue is that there were most of drifting sampling sites in Inner Mongolia and Qilian Mountains as indicated by Wang et al. (2010). Drifted snow is wind-blown, and is more likely to have mixed with locally wind-blowing soil during the drifting process. We thus collected "left" and "right" samples at all sites, and all of the datasets from table 1 are the average values from the two adjacent samples through the whole depth of the snowpack. For the above reason, the dirty layers and new fallen snow were collected in all sites separately, and we think the dirty snow for the single layer has not affected the results, even for the filtration processes. Doherty et al. (2010) also indicated that if there was obvious layering, for example a thin top layer of newly fallen snow or drift snow, that layer was collected separately, however thin.

Comment 19: Page 7 Line 13: Wang 2015 => It appears some of the 2014 Chinese snow survey data has been previously published. A more in depth explanation in the introduction section should explain how this study builds on previously published results of the same snow study, and what data is new. Also, please state what chemistry was analyzed in Wang 2015, just stating it was 'similar' to other studies by Hegg et al., is not sufficient. Also, it is not clear with the next sentence, were the major ions described in Wang 2015? This paragraph needs to be re-written to clearly state what has been published and what is new data being presented here. Or if results from Wang 2015 are being applied here in a new analysis.

R: We thank the reviewer for this helpful suggestion. We have added more explanations about the chemical analysis to clarify the difference between this study and the previous study by Wang et al. (2015). The paragraph has been rewritten as follows:

"The major water-soluble ions and trace elements in surface snow samples during this snow survey have already been investigated by Wang et al. (2015). However, the ILAPs in seasonal snow during this survey have not shown yet. For the importance of the ILAPs in snow, we will present the contribution and the emission sources of the ILAPs together with suites of other corresponding chemical constituents in seasonal snow. For instance, Hegg et al., (2009, 2010) analyzed the source attribution of the ILAPs in arctic snow by using a positive matrix factorization (PMF) model consisted with trajectory analysis and satellite fire maps. Briefly, major ions (SO_4^{2-}, NO_3^-, Cl^-, Na^+, K^+, and NH_4^+) were analyzed with an ion chromatograph (Dionex, Sunnyvale, CA), and trace elements of Fe and Al were measured by inductively coupled plasma mass spectrometry (ICP-MS). These analytical procedures have been described elsewhere (Yesubabu et al., 2014). In this paper, the major ions are used to retrieve the sea salt and biosmoke potassium ($K_{Biosmoke}^+$), which datasets were not shown by Wang et al. (2015). However, only SO_4^{2-}, NO_3^-, and NH_4^+ were reprinted from Wang et

al. (2015) to reveal the mass contribution of the ILAPs and the chemical constituents in seasonal snow during this snow survey."

Comment 20: Page 8 Line 11: The first sentence should be rewritten as its not clear to the reader how iron would originate from mineral dust in seasonal snow. Please explain in the text why this assumption is made.

R: As Alfaro et al, (2004) indicated that the light absorption by mineral dust should be highly sensitive to their content in iron oxides (hematite, goethite, etc.) based on Mie theory. Sokolik and Toon, (1999) also pointed out that computations performed with optical models show that the absorbing potential of mineral dust is more sensitive to the presence of strongly absorbing iron oxides such as hematite and goethite than to other minerals. Thus it is now possible to assess the absorption properties of mineral dust by using iron oxide content (Bond et al., 1999). In this study, the sampling sites were positioned 50 km from cities and at least 1 km upwind of approach roads or railways to prevent contamination.
For the above reason, the first sentence has been rewritten as "Recent studies indicated that the light absorption by MD should be highly sensitive to the presence of strongly absorbing iron oxides such as hematite and goethite than to other minerals (Alfaro et al., 2004; Sokolik and Toon, 1999).. Thus it is now possible to assess the absorption properties of MD by using iron oxide content (Bond et al., 1999). In this study, the iron (Hereinafter simply "Fe") in seasonal snow is assumed to be originating from MD during this survey."

Comment 21 Page 9 Line 5: Why is it stated that the Microtops II Sun Photometer was used instead of the CE318? Please explain the significance for stating this and the difference between the two. What does the Microtops II do that the CE318 does not?

R: We indicate that Microtops II and CE318 are both effective instruments on measuring aerosol optical depth (AOD) (More et al., 2013; Porter et al., 2001; Zawadzka et al., 2014). However, the major difference between Microtops II and CE318 is that the Microtops II is portable for the field experiments, but CE318 is immovable. For it's a snow survey, it is better to use the Microtops II instrument instead of CE318 to measure aerosol optical depth.

Comment 22 Page 9 Line 14: include ' in this study'. . . during the 2014 Chinese survey. (If that is what the authors mean, otherwise please clarify).

R: Right, we have replaced this sentence as "To better understand the background weather conditions in the local atmosphere during this snow survey, we used a portable and reliable Microtops II Sun photometer at wavelengths of 340, 440, 675, 870, and 936 nm instead of the CE318 sun tracking photometer to measure the surface AOD in this study."

Comment 23 Page 9 Line 24: Spectroradiometers have been used in a number of other studies than listed here. Please include 'e.g.' and then the citations.

R: We have modified this sentence as "Snow albedo plays a key role in affecting the energy balance and climate in the cryosphere (e.g. Hadley and Kirchstetter, 2012; Liou et al., 2014; Warren and Wiscombe, 1985). Wright et al. (2014) indicated that

the spectral albedo measured by using an Analytical Spectral Devices (ASD) spectroradiometer at 350-2200 nm is in agreement with albedo measurements at the baseline Surface Radiation Network (BSRN). Wuttke et al. (2006a) pointed out that the spectroradiometer instrument is considered as the more capable, rapid, and mobile to conduct spectral albedo measurements during short time periods, especially in the very cold regions (e.g. in the Arctic). The major advantage is the more extensive wavelength range, and the cosine error is less than 5% for solar zenith angles below 85o at the wavelength of 320 nm (Wuttke et al., 2006a, b)."

Comment 24 Page 10 Line 5: How was the spectroradiometer held level? What was the field of view? How did you minimize shadows from the leveling device? What were the solar zenith angles? This data should all be included in the text and solar zenith angles should be presented in a table.

R: Normally the relative position of the sighting laser spot is at a distance of 1m from the optical element for the active field of view for the instrument in strict accordance with the user manual of the SVC HR-1024 spectroradiometer (Figure 6 Setup for FOV map). The nominal filed of view (FOV) lens is 8° to enable the instrument to look at different size targets. The measured solar zenith angles and the other datasets used to simulate snow albedo have been labeled in Figure 11. The direction of the instrument was oriented to the Sun Horizon angles in order to receive more direct solar radiation. The small size of the fore optics greatly reduces errors associated with instrument self-shadowing. Even when the area viewed by the fore optic is outside the direct shadow of the instrument, the instrument still blocks some of the illumination (either diffuse skylight or light scattered off surrounding objects) that would normally be striking the surface under observation for measuring full-sky-irradiance throughout the entire 350-2500 nm wavelengths. This spectroradiometer is used for measuring the direct component of solar irradiance because of the minimized relative radiometric errors between total and direct irradiance measurements. For instance, Bi et al., (2013) used a set of broadband radiometers and sun/sky photometers during 2013 field campaign in the middle latitude across northern China to measured the direct and diffuse solar irradiance, and the result indicated that the diffuse solar radiation is lower than 10% compared with the total solar irradiance. Therefore, we indicated that the spectroradiometer in the clean sky condition mainly measured the direct solar irradiance during 2014 snow campaign. Therefore, the above paragraph was added to present the relative parameter of the spectroradiometer in section 2.4.

Comment 25 Page 11 Line 3: Is this the first presentation of the SAMDS model in publication? If so this needs to be highlighted more in the abstract, title, and especially the text here. Otherwise please include a citation for the SAMDS model.

R: Yes, the SAMDS model is the first time to be presented in open publication. So, we have addressed more information about the snow albedo reduction by the SAMDS model throughout the revised manuscript.

Comment 26: In general it seems this paper could be more focused around the SAMDS model as this appears to be the novelty of the paper.

R: We agree with the reviewer, therefore, we have changed the focus to investigating ILAPs, the internal/external of BC with snow, snow grain shapes in affecting the snow albedo reduction between surface measurements and model simulations.

Comment 27: Page 14 Line 13: This sentence is confusing and needs to be revised. For example: Delete 'For' and begin sentence with 'Most of the snow samples were collected in the afternoon corresponding to the Aqua-MODIS (13:30LT) overpass time. Then the next sentence starting with 'The averaged. . .''

R: The sentence has been revised as: "Most of the snow samples were collected in the afternoon at the Aqua-MODIS (13:30 LT) overpass time in order to compare the local AODs in sampling sites by using an spectroradiometer with the satellite remote sensing. The AOD spatial distribution derived from the Aqua-MODIS satellite over northern China associated with sampling site numbers is shown in Figure 1 during this snow survey."

Comment 28: Page 15 Lines 5 – 10. These sentences need to be restructured and concise.

R: These sentences have been restructured as: "Compared with the retrieved AOD by the remote sensing, the surface measurements of AOD were also conducted during this snow survey. Generally, the measured AOD were gradually higher from Inner Mongolia regions moved to the industrial area across northeastern China."

Comment 29: Page 15 Line 13: Remove 'processes'.

R: We have deleted "processes" as the reviewer's suggestion.

Comment 30: Page 15 Line 21: Please explain 'left and right' samples. Do the authors mean sample duplicates? This sentence needs restructuring.

R: Right. The sentence has been modified as "Two vertical profiles of snow samples ("left" and "right") were collected through the whole depth of the snowpack at all sites to reduce the possible contamination by artificial effects during the sampling process, and the dusty or polluted layers were separately collected during the sampling process.", and the caption of table 1 was added with "… All of the datasets are the average values from the left and right snow samples."

Comment 31 Page 15 Lines 21 - 25: Major run-on sentence, which needs revision.

R: The sentence has been modified as "In Inner Mongolia, the snow cover was thin and patchy. The average snow depth was less than 10 cm from sites 90, 91, 93, and 94, which was significantly lower than that near the northern border of China, ranging from 13 to 20 cm at sites 95-97. The snow samples were collected from drifted snow in Inner Mongolia, and the mass loadings of ILAPs in seasonal snow are mainly due to blowing soil dust. Therefore, the vertical profiles of snow samples mixed with blowing soil from these sites are insufficient to represent the seasonal evolution of wet and dry deposition to snow (Wang et al., 2013a). However, the light absorption of ILAPs is still dominated by OC in these regions, which has been illustrated in the following section."

Comment 32: Page 15 Lines 21 – 25: If the snowpack was so thin and patchy – won't blowing soil/dirt be an issue for the measurements? Please explain how this is accounted for.

R: We indicated that the mass loading of blowing soil could be the dominant factor in snow sampling in Inner Mongolia, when the snowpack was thin and patchy. However, the light absorption of ILAPs in snow is still dominated by OC in these regions.

Comment 33 Page 16: What type of snow was present? Fresh snow or old snow? Please explain using the international snow classification. Also, how soon were samples collected after snow falls? Also, it would be assumed that since the study was conducted in January, during Chinese winter, some sites could have fresh snow, where others could be 'older' snow?

R: We have already updated this information in Figure 1 and Table 1. The fresh snow was defined as the snow fell less than two days.

Comment 34 Page 16 Lines 14 - 19: Run-on sentence again. Please separate into two sentences. 'The results from the 2010 – 2014 Chinese snow surveys are shown in. ...)

R: The sentence has been modified as "To better understand the distribution of C_{BC}^{est} in seasonal snow across northern China, the spatial distribution of C_{BC}^{est} in the surface and average snow measured during this snow survey are shown in Figure 4. The spatial distributions of C_{BC}^{est} in the surface and average snow measured using the ISSW spectrophotometer during the 2014 survey generally ranged from 50 to 3700 ng g^{-1} and 60 to 1600 ng g^{-1}, with the medium values of 260 ng g^{-1}, and 260 ng g^{-1}, respectively. These variations of C_{BC}^{est} were very similar to those of the previous snow campaign by Wang et al. (2013a), however, much higher than those in the Xinjiang region of northwestern China (Ye et al., 2012), along the southern edge of the Tibetan Plateau (Cong et al., 2015), and across North America (Doherty et al., 2014)."

Table 1: Needs to be reorganized by dates collected (i.e. 2010 and 2014). Also include the number of samples incorporated in the average values. Sample depth is confusing. . . so the samples were collected over 5 cm and integrated into one measurement? What about the surface samples were less volume was collected at sites that were particularly dusty/polluted, i.e. Page 7 Line 4. Separate surface samples and snow pit data. Also, it appears

R: We need to clarify that the average snow depth in each site is measured 4 times in nearby locations. If the snow depth is thin and patchy, the snow samples could be collected from the drifted snow (e.g. Inner Mongolia regions), which is higher than the average snow depth in each site. So, we noted that the site average snow depth and the snow sampling depth for each site are both shown in Table 1. Therefore, the sentence has been modified as "Two vertical profiles of snow samples ("left" and "right") were collected through the whole depth of the snowpack at all sites to reduce the possible contamination by artificial effects during the sampling process, and we note that the dusty or polluted layers were separately collected during the sampling process. All of the datasets in seasonal snow from Table 1 are the average values from the two adjacent snow samples through the whole depth of the snowpack.".

Table 2: Include snowpack depth for each site, to see how snow pack depth varied from 2010-2014 as that may have influenced measured BC content. Also, given the method used, should BC = eBC? And was this 2010 data published previously? If so, include a citation. If the 2010 data has been published before, then it appears that there are only 12 new data points in this study from 2014. Why are sites 41 – 46 listed with sample dates but no avg BC value?

R: We agree with the reviewer that the datasets of surface and everaged C_{BC}^{est} in snow in Table 2 has already been published by Wang et al. (2013a). Therefore, we deleted Table 2, and Table 4, and the manuscript mainly focused on the new results in 2014 snow survey.

Table 3: Wasn't this data publishes in Wang 2015, from sub section 2.2 Chemical Speciation Page 7 Line 13? If not, or if so clarify either way, provide references, and explain why the data is being presented again and what is new.

R: We note that only the datasets of SO_4^{2-}, NO_3^-, and NH_4^+ were published in Wang et al. (2015), but the other chemical speciation calculated by the water-soluble ion in section 2.2 was new. However, we indicated that the datasets of SO_4^{2-}, NO_3^-, and NH_4^+ were useful to show the attribution from different sources. We have added the following sentence in Table 2, and Figure 6 as "We noted that the datasets of SO_4^{2-}, NO_3^-, and NH_4^+ were reprinted from Wang et al. (2015).".

Figure 4: Site numbers should be included with the map and the 2014 data should only be presented since the 2010 data is already published? At least a distinction should be made between the 2010 and 2014 data. They should not be averaged together as there are many factors that would influence the differing values. Figure 5: These data do not appear to be normally distributed as they are heavily weighted on the low end, and just a couple larger concentrations. Also provide the p-value to show the significance of the fit.

R: We deleted Figure 4c, 4d, and Figure 6 to concentrate the novelty of this manuscript. We also provided the confidence test of the fit in Figure 5.

Figure 6: Again, like Figure 5, these data do not appear to be normally distributed as they are heavily weighted on the low end, and just a couple larger concentrations. Also provide the p-value to show the significance of the fit. Why is there one red dot at 0.25 AL and 1.5 K+?

R: We have deleted figure 6, and added a new figure in discussing the snow albedo reduction due to internal/external mixed BC in snow and difference snow grain shapes in Figure 10.

Figure 7: This is a nice figure. The land cover legend should be mentioned in the figure legend.

R: We have added the land cover legend in Figure 6 & Figure 7 as "The distribution of 17 different surface vegetation types retrieved from MODIS global land cover type product (MCD12C1) with 0.05 spatial resolution were used in this study."

Figure 8: As in Figure 7, the land cover legend should be mentioned in the figure legend.

R: See our answer to the above question.

Figure 9: Why is only the visible range presented? Please clarify in Figure legend.

R: We have already extended the spectral wavelengths from 400-1400 nm in Figure 8.

Comment 34 Page 16 Lines 14 - 19: The reader doesn't understand this sentence. Are these averaged values from the surface samples?

R: The sentence has been revised as "The spatial distributions of C_{BC}^{est} in the surface and average snow measured using the ISSW spectrophotometer during the 2014 survey generally ranged from 50 to 3700 ng g^{-1} and 60 to 1600 ng $^{g-1}$, with the medium values of 260 ng g^{-1}, and 260 ng g^{-1}, respectively.". Similar mistakes were corrected throughout the revised manuscript.

Comment 34 Page 16 Line 19: Include standard deviations with the ranges. How many samples were in this range?

R: We have changed the sentences as "The spatial distributions of C_{BC}^{est} in the surface and average snow measured using the ISSW spectrophotometer during the 2014 survey generally ranged from 50 to 3700 ng g^{-1} and 60 to 1600 ng $^{g-1}$, with the medium values of 260 ng g^{-1}, and 260 ng g^{-1}, respectively.".

Comment 35: Page 17 Line 5: Include a reference to the table where this data is displayed.

R: We have indicated that the datasets are from table 1.

Comment 36: Page 17 Line 11: Where is this regression value from? Reference figure.

R: The sentence has been revised as "The two results agreed very well (R^2=0.99), indicating that Equation (7) agreed well for this measurement in Figure 5.".

Comment 37: Page 18 Line 2: Pleas explain how photochemical reactions are related to biomass burning contributions of OC?

R: Actually, we didn't separate the contributions to light-absorbing OC from primary and secondary sources because our measurements do no provide such information. Therefore, the emission sources of the carbonaceous aerosols and the chemical species of Figure 6 have been deleted in the revised manuscript.

Comment 37: Page 18 Line 3: p-value? And please include for the other figures.

R: We have deleted Figure 6 and section 3.3 of emission factors. The confidence tests have been added in Figure 5 and their corresponsive results.

Comment 38 Page 19: The reader finds this paragraph confusing. Are the percentages from Figure 7? If the samples were collected in January 2014, why are there seasonal/time references? i.e. Line 11" Sulfate peaks were found in summer. . . this should be clearly tied to the Zhang 2013 reference. If the next sentence, line 12 – 17 (Which is a very long run-on sentence) also refers to Zhang 2013 then this needs to be more clearly stated. The combination of presenting results from this study and Zhang 2013 needs to be reorganized more clearly. For example a paragraph explaining Zhang 2013 could come first, and then compare this study to those. Also Zhang 2013 should probably be more clearly explained in the introduction. Again, it also appears that Wang 2015 already published snow chemistry data from these results? This needs to be more clearly referenced in the paper.

R: The results from this paragraph have been deleted, because this study will mainly focused on the ILAPs in seasonal snow, and its optical effects on snow albedo.

Comment 39 Page 20 Line 1: Include citation for iron originating from industrial emissions.

R: Two citations were added in this sentence as "however, Fe can also originate from industrial emissions, such as the metal and steel industries (Hegg et al., 2010; Ofosu et al., 2012)."

Comment 39 Page 20 Line 3: Is this sentence about 'this' study, or Doherty 2014?

R: The sentence means this study of 2014 snow survey.

Comment 39 Page 20 Line 6: 'Here, light absorption. . . '

R: We have modified this sentence.

Comment 40: Page 21 Line 4- 6: This has already been stated and should be in the methods.

R: The sentences have been moved to the method section as the reviewer's suggestion.

Comment 41 Page 21: The reader is not sure what the authors mean by 'Higher degrees of snow albedo. . .' do they mean more reduction or a high albedo? 'There was a larger reduction in snow albedo for. . .."

R: The sentence has been revised as "A larger reduction in snow albedo by both BC and MD-contaminated snow was found for larger snow grains. . ."

Figure 10: Include labels for A, B, C. Same goes for all other figures.

R: Yes, we have replotted all of the figures in the revised manuscript, and labeled for (a), (b)… very clearly.

Comment 42 Page 22: Why is BC now refereed to as the ' BC mixing ratios'. Please clarify where this change in terminology was introduced.

R: We have unified all of mixing ratios and BC as C_{BC}^{est}, which are consistent with the previous studies by Doherty et al. (2010, 2015) and Wang et al. (2013a).

Comment 43: Overall, ILAPs is not used consistently in the paper as light absorbing aerosols is written out many times. The reader suggests to standardize this.

R: We have standardized the light absorbing aerosols as ILAPs throughout the revised manuscript.

Comment 44 Page 23 Lines 23 – 35: Please explain why, " . . .this study shows that the spectral albedo of snow reduction caused OC levels to increase?" Shouldn't the reduction in spectral albedo be a result of the OC levels?

R: This study indicated that the snow albedo reduction is not only correlated with the increased mixing ratios of OC in Figure 9c, but also highly correlated with the different snow grain sizes (e.g. snow grain size of 800 μm compared to 100 μm). Therefore, the sentence has been edited as "The radiative transfer modeling results presented by Zhang et al. (2016) and measurement results of this study show that the spectral albedo of snow reduction due to the increased OC mixing ratios (above 20 μg g^{-1}) is larger for a factor of 3 by assuming the snow grain size of 800 μm compared to 100 μm.".

Comment 45: The paper needs a lot of reorganization. For a 25 page paper, one page of Discussion does not seem adequate. Rename Subtitle 4, "Conclusions".

R: The conclusions have already renamed, and more discussion has been updated.-

Comment 46 Page 24 Line 4: Include the 13 sites also in the abstract. This description from lines 3 – 7 should be included in the site description and does not need to be repeated in the conclusion. Comment 47: Page 24 Line 22: Please state the range in latitudes covered in this study in the site description. Did the 13 sites cover a large latitudinal gradient?

R: The conclusion has been rewritten the same as comments 48.

Comment 48 Page 25 Line 13: The last sentence of the entire manuscript seems like an odd conclusion, 'to include OC as an input parameter in the SNICAR model'. Why not argue for the use of the SAMDS model? Does it not include OC as an input parameter? A better conclusion would be to compare the SAMDS and SNICAR models. Is the reason the SNICAR model is suggested to incorporated OC because it is widely used? Did the authors try incorporating OC as an input parameter in the off-line SNICAR code? The discussion and conclusion of this manuscript needs revision.

R: The conclusions were totally rewritten as follows:
"In this study, a snow survey was performed in January 2014, and 92 snow samples were collected at 13 sites across northern China. We found that higher AODs measured using a sun photometer and remote sensing devices showed that heavily

polluted areas remain in industrial regions across northern China. The measured C_{BC}^{est} through the 2014 survey via the ISSW spectrophotometer in surface and average snow of 50 to 3700 and 60 to 1600 ng g^{-1}, with the medium values of 260 ng g^{-1}, and 260 ng g^{-1}, respectively, were much larger than those of previous snow field campaigns. The chemical composition analysis showed that the mass contributions in seasonal snow was dominated by OC and MD. However, assuming the MACs for BC, OC, and Fe are 6.3, 0.3, and 0.9 m^2 g^{-1}, respectively, at 550 nm, light absorption was still dominated by BC and OC in seasonal snow during the entire campaign. The light-absorbing contribution of the MD was larger at high latitudes than at low latitudes due to strong winds transporting snow. Then, we present a new spectral snow albedo model (SAMDS) for simulating the surface albedo of snow with deposited ILAPs by using the asymptotic analytical radiative transfer theory. Given the measured BC, MD and OC mixing ratios of 100-5000 ng g^{-1}, 2000-6000 ng g^{-1}, and 1000-30000 ng g^{-1} in surface snow across northeastern China, we ran the models at a solar zenith angle θ of 60°, and the results indicated that the albedo of fresh snow at 550 nm is generally in a range of 0.95-0.75 with R$_{eff}$ of 100 μm. This model can also be used to investigate the snow albedo influenced by the internal/external mixing of BC and snow, irregular morphology of snow grains and the vertical distribution of snow grains and impurities for multilayer snow. For a given shape (spheres, hexagonal plates/columns, and fractal particles), it shows that snow albedo for spherical snow grains is typically lower than that for the fractal snow grains and hexagonal plates/columns snow grainswith R$_{eff}$ of 100 μm. The internal mixing of BC and snow absorbs substantially more light than external mixing. For fresh snow grains of hexagonal plates/columns with R$_{eff}$ of 100 μm, the difference of snow albedo between internal and external mixing of BC and snow is up to 0.036 for 3000 ng g^{-1} BC in snow in the heavy industrial regions across northeastern China, whereas by low to 0.005 for 100 ng g^{-1} BC in snow in the further north China near the border of Siberia. The spectral albedo of snow reduction caused by OC (20 μg g^{-1}) is larger by up to a factor of 3 for a snow grain size of 800 μm compared to 100 μm by using SAMDS model.

A comparison between measured and simulated snow albedos was conducted. Generally, the snow albedos measured from a spectroradiometer and simulated using the SNICAR and SAMDS models agreed well at the lower mixing ratios of BC, MD, and OC. However, a large discrepancy in snow albedo between the model simulations and surface measurements for heavy loading of ILAPs in snow was found by using R$_m$. We demonstrate that the simulated snow albedo reduction by SMDAS and SNICAR models is significantly enhanced by using R$_{eff}$ of snow grains compared with R$_m$, especially in the case of near-infrared wavelengths. Although the MAC of OC is much lower than that of BC, we found that OC was a major absorber in snow due to its high mixing ratio from human activities occurring across northeastern China. Moreover, 5000 ng g^{-1} of OC was found to reduce the snow albedo by 0.016-0.059 depending on the snow grain size and aging period. Therefore, we suggest that the mixing ratio of OC should be added as an input parameter to the SNICAR model for determining snow albedos.

Although the SAMDS model might be useful to researchers who are conducting studies involving ILAPs and snow interaction and feedback in snow albedo change, we indicate that further snow surveys across northern China should be performed for the following reasons: (1) large variations of ILAPs in seasonal snow across northern China can lead higher uncertainties of snow albedo reduction, especially in the industrial regions, and (2) we only measured the snow albedo at 6 sampling sites by

using the spectroradiometer in the clear sky condition due to much less snow fallen in January 2014 than that in previous years. Comparing model simulations with the observations, we found that R_{eff} could seemingly be enhanced by the high mixing ratios of ILAPs in snow, however, we note that further snow surveys on measuring snow albedo should be conducted to reveal this phenomenon. Finally, there are large uncertainties in simulating snow albedo reduction and radiative forcing due to the ILAPs mixed with snow/ice and the irregular morphology of snow grains, the potential snow albedo change for aged snow should be investigated in the following snow surveys accordingly to test the capability of SAMDS model, which will provide more valuable and useful information for the climate models.".

References:

Alfaro, S. C., Lafon, S., Rajot, J. L., Formenti, P., Gaudichet, A., and Maille, M.: Iron oxides and light absorption by pure desert dust: An experimental study, J. Geophys. Res.-Atmos., 109, 2004.

Bi, J. R., Huang, J. P., Fu, Q., Ge, J. M., Shi, J. S., Zhou, T., and Zhang, W.: Field measurement of clear-sky solar irradiance in Badain Jaran Desert of Northwestern China, J. Quant. Spectrosc. Ra., 122, 194-207, 2013.

Bond, T. C., Bussemer, M., Wehner, B., Keller, S., Charlson, R. J., and Heintzenberg, J.: Light absorption by primary particle emissions from a lignite burning plant, Environ. Sci. Technol., 33, 3887-3891, 1999.

Bond, T. C., Doherty, S. J., Fahey, D. W., Forster, P. M., Berntsen, T., DeAngelo, B. J., Flanner, M. G., Ghan, S., Karcher, B., Koch, D., Kinne, S., Kondo, Y., Quinn, P. K., Sarofim, M. C., Schultz, M. G., Schulz, M., Venkataraman, C., Zhang, H., Zhang, S., Bellouin, N., Guttikunda, S. K., Hopke, P. K., Jacobson, M. Z., Kaiser, J. W., Klimont, Z., Lohmann, U., Schwarz, J. P., Shindell, D., Storelvmo, T., Warren, S. G., and Zender, C. S.: Bounding the role of black carbon in the climate system: A scientific assessment, J. Geophys. Res.-Atmos., 118, 5380-5552, 2013.

Cong, Z., Kang, S., Kawamura, K., Liu, B., Wan, X., Wang, Z., Gao, S., and Fu, P.: Carbonaceous aerosols on the south edge of the Tibetan Plateau: concentrations, seasonality and sources, Atmos. Chem. Phys., 15, 1573-1584, 2015.

Dang, C., Brandt, R. E., and Warren, S. G.: Parameterizations for narrowband and broadband albedo of pure snow and snow containing mineral dust and black carbon, J. Geophys. Res.-Atmos., 120, 5446-5468, 2015.

Doherty, S. J., Dang, C., Hegg, D. A., Zhang, R. D., and Warren, S. G.: Black carbon and other light-absorbing particles in snow of central North America, J. Geophys. Res.-Atmos., 119, 12807-12831, 2014.

Doherty, S. J., Steele, M., Rigor, I., and Warren, S. G.: Interannual variations of light-absorbing particles in snow on Arctic sea ice, J. Geophys. Res.-Atmos., 120, 11391-11400, 2015.

Doherty, S. J., Warren, S. G., Grenfell, T. C., Clarke, A. D., and Brandt, R. E.: Light-absorbing impurities in Arctic snow, Atmos. Chem. Phys., 10, 11647-11680, 2010.

Flanner, M. G., Liu, X., Zhou, C., Penner, J. E., and Jiao, C.: Enhanced solar energy absorption by internally-mixed black carbon in snow grains, Atmos. Chem. Phys., 12, 4699-4721, 2012.

Flanner, M. G., Zender, C. S., Hess, P. G., Mahowald, N. M., Painter, T. H., Ramanathan, V., and Rasch, P. J.: Springtime warming and reduced snow cover from carbonaceous particles, Atmos. Chem. Phys., 9, 2481-2497, 2009.

Flanner, M. G., Zender, C. S., Randerson, J. T., and Rasch, P. J.: Present-day climate forcing and response from black carbon in snow, J. Geophys. Res.-Atmos., 112, D11202, 2007.

Grenfell, T. C., Doherty, S. J., Clarke, A. D., and Warren, S. G.: Light absorption from particulate impurities in snow and ice determined by spectrophotometric analysis of filters, Appl. Opt., 50, 2037-2048, 2011.

Grenfell, T. C., Warren, S. G., and Mullen, P. C.: Reflection of Solar-Radiation by the Antarctic Snow Surface at Ultraviolet, Visible, and near-Infrared Wavelengths, J. Geophys. Res.-Atmos., 99, 18669-18684, 1994.

Hadley, O. L., and Kirchstetter, T. W.: Black-carbon reduction of snow albedo, Nat. Clim. Change, 2, 437-440, 2012.

He, C. L., Li, Q. B., Liou, K. N., Takano, Y., Gu, Y., Qi, L., Mao, Y. H., and Leung, L. R.: Black carbon radiative forcing over the Tibetan Plateau, Geophys. Res. Lett., 41, 7806-7813, 2014.

Hegg, D. A., Warren, S. G., Grenfell, T. C., Doherty, S. J., and Clarke, A. D.: Sources of light-absorbing aerosol in arctic snow and their seasonal variation, Atmos. Chem. Phys., 10, 10923-10938, 2010.

Hegg, D. A., Warren, S. G., Grenfell, T. C., Doherty, S. J., Larson, T. V., and Clarke, A. D.: Source Attribution of Black Carbon in Arctic Snow, Environ. Sci. Technol., 43, 4016-4021, 2009.

Huang, J. P., Fu, Q. A., Zhang, W., Wang, X., Zhang, R. D., Ye, H., and Warren, S. G.: Dust and Black Carbon in Seasonal Snow across Northern China, Bull. Amer. Meteor. Soc., 92, 175-181, 2011.

Jaffe, D., Anderson, T., Covert, D., Kotchenruther, R., Trost, B., Danielson, J., Simpson, W., Berntsen, T., Karlsdottir, S., Blake, D., Harris, J., Carmichael, G., and Uno, I.: Transport of Asian air pollution to North America, Geophys. Res. Lett., 26, 1999.

Liou, K. N., Takano, Y., and Yang, P.: Light absorption and scattering by aggregates: Application to black carbon and snow grains, J. Quant. Spectrosc. Ra., 112, 1581-1594, 2011.

Liou, K. N., Takano, Y., He, C., Yang, P., Leung, L. R., Gu, Y., and Lee, W. L.: Stochastic parameterization for light absorption by internally mixed BC/dust in snow grains for application to climate models, J. Geophys. Res.-Atmos., 119, 7616-7632, 2014.

Ming, J., Xiao, C. D., Cachier, H., Qin, D. H., Qin, X., Li, Z. Q., and Pu, J. C.: Black Carbon (BC) in the snow of glaciers in west China and its potential effects on albedos, Atmos. Res., 92, 114-123, 2009.

More, S., Kumar, P. P., Gupta, P., Devara, P. C. S., and Aher, G. R.: Comparison of Aerosol Products Retrieved from AERONET, MICROTOPS and MODIS over a Tropical Urban City, Pune, India, Aerosol. Air. Qual. Res., 13, 107-121, 2013.

Ofosu, F. G., Hopke, P. K., Aboh, I. J. K., and Bamford, S. A.: Characterization of fine particulate sources at Ashaiman in Greater Accra, Ghana, Atmos. Pollut. Res., 3, 301-310, 2012.

Porter, J. N., Miller, M., Pietras, C., and Motell, C.: Ship-based sun photometer measurements using Microtops sun photometers, J. Atmos. Oceanic Technol., 18, 765-774, 2001.

Qian, Y., Wang, H. L., Zhang, R. D., Flanner, M. G., and Rasch, P. J.: A sensitivity study on modeling black carbon in snow and its radiative forcing over the Arctic and Northern China, Environ. Res. Lett., 9, 064001, 2014.

Sokolik, I. N., and Toon, O. B.: Incorporation of mineralogical composition into models of the radiative properties of mineral aerosol from UV to IR wavelengths, J. Geophys. Res.-Atmos., 104, 9423-9444, 1999.

Wang, X., Doherty, S. J., and Huang, J. P.: Black carbon and other light-absorbing impurities in snow across Northern China, J. Geophys. Res.-Atmos., 118, 1471-1492, 2013a.

Wang, X., Huang, J. P., Zhang, R. D., Chen, B., and Bi, J. R.: Surface measurements of aerosol properties over northwest China during ARM China 2008 deployment, J. Geophys. Res.-Atmos., 115, D00k27, 2010.

Wang, X., Pu, W., Zhang, X. Y., Ren, Y., and Huang, J. P.: Water-soluble ions and trace elements in surface snow and their potential source regions across northeastern China, Atmos. Environ., 114, 57-65, 2015.

Warren, S. G. and Wiscombe, W. J.: Dirty Snow after Nuclear-War, Nature, 313, 467-470, 1985.

Warren, S. G., and Wiscombe, W. J.: A Model for the Spectral Albedo of Snow .2. Snow Containing Atmospheric Aerosols, J. Atmos. Sci., 37, 2734-2745, 1980.

Wright, P., Bergin, M., Dibb, J., Lefer, B., Domine, F., Carman, T., Carmagnola, C., Dumont, M., Courville, Z., Schaaf, C., and Wang, Z. S.: Comparing MODIS daily snow albedo to spectral albedo field measurements in Central Greenland, Remote Sens. Environ., 140, 118-129, 2014.

Wuttke, S., Seckmeyer, G., and Konig-Lang, G.: Measurements of spectral snow albedo at Neumayer, Antarctica, Ann. Geophys., 24, 7-21, 2006b.

Wuttke, S., Seckmeyer, G., Bernhard, G., Ehramjian, J., McKenzie, R., Johnston, P., and O'Neill, M.: New spectroradiometers complying with the NDSC standards, J. Atmos. Oceanic Technol., 23, 241-251, 2006a.

Yasunari, T. J., Koster, R. D., Lau, W. K. M., and Kim, K. M.: Impact of snow darkening via dust, black carbon, and organic carbon on boreal spring climate in the Earth system, J. Geophys. Res.-Atmos., 120, 5485-5503, 2015.

Ye, H., Zhang, R. D., Shi, J. S., Huang, J. P., Warren, S. G., and Fu, Q.: Black carbon in seasonal snow across northern Xinjiang in northwestern China, Environ. Res. Lett., 7, 044002, 2012.

Yesubabu, V., Srinivas, C. V., Hariprasad, K. B. R. R., and Baskaran, R.: A Study on the Impact of Observation Assimilation on the Numerical Simulation of Tropical Cyclones JAL and THANE Using 3DVAR, Pure Appl. Geophys., 171, 2023-2042, 2014.

Zawadzka, O., Makuch, P., Markowicz, K. M., Zielinski, T., Petelski, T., Ulevicius, V., Strzalkowska, A., Rozwadowska, A., and Gutowska, D.: Studies of aerosol optical depth with the use of Microtops II sun photometers and MODIS detectors in coastal areas of the Baltic Sea, Acta Geophysica, 62, 400-422, 2014.

Zhang, R., Hegg, D. A., Huang, J., and Fu, Q.: Source attribution of insoluble light-absorbing particles in seasonal snow across northern China, Atmos. Chem. Phys., 13, 6091-6099, 2013a.

Zhang, X. L., Wu, G. J., Kokhanovsky, A., Yao, T. D., and Tong D.: Spectral albedo parameterization for dirty snow with considering mirco-physicochemical properties of impurities - Part I: Theory and preliminary evaluation, 2016.

Zhao, C., Hu, Z., Qian, Y., Leung, L. R., Huang, J., Huang, M., Jin, J., Flanner, M. G., Zhang, R., Wang, H., Yan, H., Lu, Z., and Streets, D. G.: Simulating black

carbon and dust and their radiative forcing in seasonal snow: a case study over North China with field campaign measurements, Atmos. Chem. Phys., 14, 11475-11491, 2014.

Observations and model simulations of sSnow albedo reduction in seasonal snow due to insoluble light-absorbing particles during 2014 Chinese survey~~anthropogenic dust and carbonaceous aerosols across northern China~~

Xin Wang[1], Wei Pu[1], Yong Ren[1], Xuelei Zhang[2], Xueying Zhang[1], Jinsen Shi[1], Hongchun Jin[1], Mingkai Dai[1], Quanliang Chen[3]

[1] Key Laboratory for Semi-Arid Climate Change of the Ministry of Education, College of Atmospheric Sciences, Lanzhou University, Lanzhou, 730000, China
[2] Key Laboratory of Wetland Ecology and Environment, Northeast Institute of Geography and Agroecology, Chinese Academy of Sciences, Changchun 130102, China
[3] College of Atmospheric Science, Chengdu University of Information Technology, and Plateau Atmospheric and Environment Laboratory of Sichuan Province, Chengdu 610225, China

Correspondence to: X. Wang (wxin@lzu.edu.cn)

Abstract.

A snow survey was carried out to collect 13 surface snow samples (10~~9~~ for fresh snow, and 3 for aged snow), and 79 sub-surface snow samples in seasonal snow at 13 sites in January 2014 across ~~northeast~~northeastern China. A spectrophotometer and the chemical analysis were used to separate snow particulate absorption by insoluble light-absorbing particles (ILAPs, ~~~(~~e.g. black carbon, BC; mineral dust, MD~~organic carbon, OC~~; and organic carbon, OC~~mineral dust, MD~~) in snow, and the snow albedo was measured by using a field spectroradiometer during this period~~s~~. In this study, a~~A~~ new radiative transfer model (Spectral Albedo Model for Dirty Snow, or SAMDS) is developed to ~~model~~ simulate the spectral albedo ~~reduction due to ILAPs of~~in snow based on the asymptotic radiative transfer theory. The comparison between SAMDS and the Snow, Ice, and Aerosol Radiation (SNICAR) model indicates that the spectral albedos of pure snow derived from these models agree well, however, there is a slight tendency for the SNICAR model values to become lower than SAMDS model values when BC and MD are considered.~~The results indicate that~~ Given the measured BC, MD and OC mixing ratios of 100-5000 ng g^{-1}, 2000-6000 ng g^{-1}, and 1000-30000 ng g^{-1} in surface snow across northeastern China, the snow albedo of fresh snow at 550 nm with a snow grain optical effective radius (R_{eff}) of 100 μm is generally in a range of 0.95-0.75 by using SAMDS model. ~~t~~The snow albedo reduction due to spherical snow grains assumed as~~for aged snow due to spherical~~aged snow ~~grains~~ is graduately larger than fresh snow ~~for~~such as ~~Koch snowflake~~fractal snow grains, and hexagonal plates/colums snow grains associated with the increased BC in snow. For typically BC mixing ratios of 100 ng g^{-1} in remote areas and 3000 ng g^{-1} in heavy industrial areas across northern China, ~~an effective radius of 100 μm,~~the snow albedo ~~reduction caused by 100 ppb of~~for ~~~~internal ~~mixed BC~~mixing of BC and snow ~~is XX, but only~~

~~XX~~is lower by 0.005 and 0.036 than that ~~for~~of external ~~mixed BC~~mixing for hexagonal plates/columns snow grains with R_{eff} of 100 μm. ~~A comparison between SAMDS and the Snow, Ice, and Aerosol Radiation (SNICAR) model indicated that the spectral albedos of pure snow derived from these models agreed well, however, a slight tendency for the SNICAR model values to become lower than SAMDS model values when BC and MD mixing ratios range from 1 to 5 μg g^{-1} and 4 to 6 μg g^{-1}, respectively.~~ The result also shows that the simulated snow albedos by both SAMDS and SNICAR agree well with the observed values at low ILAPs mixing ratios, but tend to be higher compared with surface observations at high ILAPs mixing ratios.

~~This study offers not only an explanation for the discrepancy of the snow albedo reduction between modeled and observed snow albedo reduction due to ILAPs in snow, but also demonstrates the enhancement of the model simulations of the snow albedo reduction by using the optical effective radii (R_{eff}) of snow grains than that the measured snow grian radii due to SMDAS and SNICAR models, especially in the case of near-infrared wavelengths.~~ ~~A survey was performed to collect 92 seasonal snow samples at 13 sties across northern China in January 2014, and the mixing ratios of Insoluble Light Absorbing Particles (ILAPs, e.g. black carbon, organic carbon, and mineral dust (MD) in seasonal snow were measured by using an integrating sphere/integrating sandwich spectrophotometer (ISSW), and the chemical analysismethods. Based on the surface measurements of ILAPs in snow, a new radiative transfer model (Spectral Albedo Model for Dirty Snow, or SAMDS) is developed to simulate the spectral albedo reduction due to ILAPs in snow based on the asymptotic radiative transfer theory. We calculate that XX XX %, and XX XX % of snow albedo reduction in surface snow resides within the concentrations of BC and~~

MD in the ranges of XX ng g, and XX ng g, respectively. A comparison between SAMDS and the SNICAR models indicated that the snow albedo can reduce 1-3%, 2-5%, and 2-4% due to ng g, XXX ng g, and xxx ng g of black carbon (BC), and mineral dust (MD) in snow. We note that tThe organic carbon (OC) is also another key parameter in affecting snow albedo of 1-5% due to XXX ppb in snow due to SDAMS model simulation. For a given shape (Koch snowflake, hexagonal plates/columns, and spheres), the snow albedo reduction due to spherical snow grains is graduately larger than Koch snowflake, and hexagonal plates/colums with the increased concentration of BC in snow. The internal mixing of BC in snow absorbs substantially higher than the external mixing at the wavelengths of 400 nm -1400 nm. In addition to the BC and AD parameters in the Snow, Ice, and Aerosol Radiation (SNICAR) model, the OC content in snow is considered an initial parameter for calculating snow albedo through a new radiative transfer model (Spectral Albedo Model for Dirty Snow, or SAMDS). The spectral albedo of snow reduction caused by OC (20 $\mu g\ g^{-1}$) is up to a factor of 3 for a snow grain size of 800 μm compared to 100 μm. We find a larger difference in snow albedo levels between the model simulations and surface measurements for higher insoluble light absorbing impurities (ILAPs) using the measured snow grain radii. Compared with the observed snow albedo, we also note that the optical effective radii (R_{eff}) of snow grains can significantly enhance the model simulations of snow albedo reduction than that the measured snow grian radii due to SMDAS and SNICAR models, especially in the case of near-infrared wavelengths.

1   Introduction

Mineral dust (MD), black carbon (BC) and organic carbon (OC) are three insoluble light-absorbing particles (ILAPs) that play key roles in regional and global climate (Bond et a., 2013; Dang et al., 2014; Flanner et al., 2007, 2009; Hansen et al., 2005; IPCC, 2013; Li et al., 2016; McConnell, 2007~~Jaffe et al., 1999~~). ~~Anthropogenic dust (AD) is a major form of mineral dust.~~ The ~~AD~~ MD particles ~~content~~ can influence air quality and human health through emission, transport, removal, and deposit processes (Aleksandropoulou et al., 2011; Chen et al., 2013; Huang et al., 2014, 2015a, 2015b; Kim et al., 2009; Li et al., 2009; Mahowald and Luo, 2003; Zhang et al., 2005~~, 2015~~). ~~AD~~ They~~MD particles~~ also act as cloud condensation nuclei that affect cloud formation (Coz et al., 2010; Givati and Rosenfeld, 2004; Rosenfeld et al., 2001) and deliver various trace nutrients to terrestrial and marine ecosystems (Acosta et al., 2011; Mahowald et al., 2005; Qiao et al., 2013). The Taklimakan and Gobi desert, and several other deserts are well known to be major dust sources across northern China, and MD particles can be lifted in the atmosphere and transported to the downwelling regions via wet and dry depositions (Chen et al., 2013; Huang et al., 2008; Jaffe, et al., 1999; Wang et al., 2008; Zhang et al., 2003). But recent studies indicated that the anthropogenic dust emissions from disrupted soils by human activities, such as deforestation, overgrazing, agricultural and industrial activities, are not well constrained (Aleksandropoulou et al., 2011; Tegen and Fung, 1995; Tegen et al., 2002, 2004; Thompson et al., 1988), which differs from natural MD originating from desert regions (Che et al., 2011, 2013, 2015a; Goudie and Middleton, 2001; Li et al., 2012; Park and Park, 2014; Pu et al., 2015; Wallach and Fischer, 1970; Wang et al., 2008, 2010b). For instance, Kamani et al. (2015)~~Ginoux et al. (2010) estimated that MD due to anthropogenic dust activities accounts for 25% of dust aerosols using observational~~

data from MODIS Deep Blue satellite products combined with a land-use fraction dataset (Ginoux et al., 2010). Anthropogenic dust originates primarily from urban and regional sources, especially during the winter,Recent studies indicated that and anthropogenicMD   dust influenced by anthropogenic activities has already been

5   enriched with heavy metals and other toxic elements (Kamani et al., 2015; Li et al., 2013; Wang et al., 2015; Zhang et al., 2013). Northeastern China and surrounding regions are generally regarded as industrial areas most affected by human activities. Because anthropogenic dust emissions from disturbed soils are not well constrained, we define mineral dust from areas disrupted by human activities, such as deforestation,

10   overgrazing, agricultural and industrial activities, as anthropogenic dust (Aleksandropoulou et al., 2011; Tegen and Fung, 1995; Tegen et al., 2002, 2004; Thompson et al., 1988), which differs from natural mineral dust originating from desert regions (Che et al., 2011, 2013, 2015a; Goudie and Middleton, 2001; Li et al., 2012; Park and Park, 2014; Pu et al., 2015; Wallach and Fischer, 1970; Wang et al.,

15   2008, 2010b). This assumption is consistent with the results of a recent study by Huang et al. (2015a), who found that anthropogenic dust contributions to regional emissions in eastern China are 91.8%, with and 76.1% in India at 76.1% (e.g., Figure 10 in Huang et al., 2015a). This may be due to larger population densities, which are characterized by more intense human activity in eastern China and India (Guan et al.,

20   2016; Huang et al., 2015a; Wang et al., 2013a; Zhang et al., 2013).)

Compared to ADMD, carbonaceous aerosols, such as BC and OC, generated from the incomplete combustion of fossil fuels and from biomass burning are also major anthropogenic pollutants. ILAPs deposited on snow have been found to shorten the

25   snow cover season by decreasing the snow albedo and accelerating snow melt

(Flanner et al., 2007, 2009). ~~Warren and Wiscombe (1980) found that a mixing ratio of 10 ng g^{-1} of soot in snow can reduce snow albedo levels by 1%. Light et al. (1998) determined that 150 ng g^{-1} of BC embedded in sea ice can reduce ice albedo levels by a maximum of 30% (Light et al., 1998). Among its main light-absorbing impurities, 1 ng g^{-1} of BC has approximately the same effect on the albedo of~~ <u>snow and ice at 500</u> ~~nm as 50 ng g^{-1} of dust (Warren, 1982). Doherty et al. (2013) analyzed field measurements of vertical distributions of BC and other ILAPs in snow in the Arctic during the melt season and found significant melt amplification owing to an increased mixing ratio of BC by up to a factor of 5.~~

It is widely known that small snow albedo changes can have significant effects on global warming patterns, involving changes in snow morphology, sublimation, and melt rates (~~Brandt et al., 2011; Hadley and Kirchstetter, 2012; Warren and Wiscombe, 1985~~<u>Brandt et al., 2011; Hadley and Kirchstetter, 2012; Warren and Wiscombe, 1985</u>). <u>Warren and Wiscombe (1980) found that a mixing ratio of 10 ng g^{-1} of soot in snow can reduce snow albedo levels by 1%. Light et al. (1998) determined that 150 ng g^{-1} of BC embedded in sea ice can reduce ice albedo levels by a maximum of 30%. 1 ng g^{-1} of BC has approximately the same effect on the albedo of snow and ice at 500 nm as 50 ng g^{-1} of dust (Warren, 1982). Doherty et al. (2013) analyzed field measurements of vertical distributions of BC and other ILAPs in snow in the Arctic during the melt season and found significant melt amplification due to an increased mixing ratio of BC by up to a factor of 5. Yasunari et al. (2015) suggest<u>ed</u>~~s~~ that the existence of snow darkening effect in the Earth system associated with ~~dust, BC, and OC~~<u>ILAPs</u> contributes significantly to enhanced surface warming over continents in northern hemisphere midlatitudes during boreal spring, raising the surface skin temperature by approximately 3–6 K near the snowline. Warren and Wiscombe</u>

(1985) pointed out that modeling soot in snow as an "external mixture" (impurities particles separated from ice particles), may underestimate the true effect of the impurities as a given reduction of albedo by about half as much soot, if the soot is instead located inside the ice grains as an "internal mixture". Hansen et al. (2004) and Cappa et al. (2012) noted that for a given BC mass on snow albedo, the internal mixing of BC in snow is a better approximation than external mixing, whereas internal mixing increases the BC absorption coefficient by a factor of two, for better agreement with empirical data. Hadley and Kirchstetter (2012) also indicated that increasing the size of snow grains could decrease snow albedo and amplified the radiative perturbation of BC. For a snow grain optical effective radius (R_{eff}) of 100 μm, the albedo reduction caused by 100 ng g^{-1} of BC is 0.019 for spherical snow grains but only 0.012 for equidimensional nonspherical snow grains (Dang et al., 2016). Fierce et al. (2016) pointed out that BC coated with non-absorbing particles absorbs more strongly than the same amount of BC in an uncoated particle, but the magnitude of this absorption enhancement is still a challenge. He et al. (2014) indicated that BC-snow internal mixing increases the albedo forcing by 40–60% compared with external mixing, and coated BC increases the forcing by 30–50% compared with uncoated BC aggregates, whereas Koch snowflakes reduce the forcing by 20–40% relative to spherical snow grains using a global chemical transport model in conjunction with a stochastic snow model and a radiative transfer model.

Climate models have indicated that the reduction in surface albedo caused by BC leads to global warming and nearly global melting of snow and ice (Hansen and Nazarenko, 2004). Recent modeling studies have estimated regional and global radiative forcing caused by ILAPs deposited on snow by reducing the surface albedo (Flanner, 2013; Flanner et al., 2007; Hansen and Nazarenko, 2004; Jacobson, 2004;

Koch et al., 2009; Qian et al., 2015; Zhao et al., 2014). Flanner et al. (2012) demonstrated that the simulated global-mean fraction of BC residing within ice grains of surface snow increases the global BC/snow radiative forcing by 34–86% relative to paired control simulations that apply external optical properties to all BC. Bond et al. (2013) estimated the industrial-era climate forcing of BC through all forcing mechanisms to be approximately +1.1 W m^{-2}, with 90% uncertainty boundsconfidence limits of +0.17 to +2.1 W m^{-2}. This value includes the net effect of BC on radiation, clouds, and snow albedo, which have been found to heavily impact the earth's climate (Bond et al, 2013; IPCC, 2013; Li et al., 2016). Recent modeling studies have estimated regional and global radiative forcing caused by ILAPs deposited on snow by reducing the surface albedo (Flanner, 2013; Flanner et al., 2007; Hansen and Nazarenko, 2004; Jacobson, 2004; Koch et al., 2009; Qian et al., 2015; Zhao et al., 2014).

Climate models have indicated that the reduction in surface albedo caused by BC leads to global warming and nearly global melting of snow and ice (Hansen and Nazarenko, 2004). Regional forcing by BC contamination in snow in snow-covered regions, e.g., the Arctic and Himalayas (0.6 and 3.0 W m^{-2}, respectively), is comparable to carbon dioxide levels (1.5 W m^{-2}) in the atmosphere since the pre-industrial period (Flanner et al., 2007). The efficacy of radiative forcing due to BC deposited on snow has been estimated to be as high as 236% (Hansen et al., 2005).

Although AD MD is a less efficient absorber than BC and OC, in situ field campaigns measurements on collectingof seasonal snow samples across northern China and the Himalayas have shown high AD MD loadings (Guan et al., 2015; Kang et al., 2016; Wang et al., 2012; Wang et al., 2013a). In some regions, especially areas with thin

9

and patchy snow cover and mountainous regions, soil dust significantly decreases the snow albedo, exceeding the influence of BC. However, models did~~o~~ not capture these potentially large sources of local dust in snowpack and may overestimate BC forcing processes (Painter et al., 2007, 2010, 2012). Recently, several seasonal snow collection campaigns were performed across northern China, the Himalayas, North America, Greenland and the Arctic (Cong et al., 2015; Dang and Hegg, 2014; Doherty et al., 2010, 2014; Huang et al., 2011; Xu et al., 2009, 2012; Zhao et al., 2014). However, determining the effects of ~~light absorbing impurities~~ILAPs on snow albedo reduction continues to ~~involve~~ present numerous challenges (Huang et al., 2011; Wang et al., 2013a, 2015; Ye et al., 2012; Zhang et al., 2013a).

To our knowledge, there are only a few studies that compare modeled and observed snow albedo reduction due to ILAPs in snow (Dang et al., 2015; Flanner et al., 2007, 2012; Grenfell et al., 1994; Liou et al., 2014; Warren et al., 1980~~Ref.~~). ~~We analyzed observed ILAPs in seasonal snow through a Chinese survey in 2014 following a snow campaign held in 2010 across northern China carried out by Huang et al. (2011). The area is seasonally covered with snow for approximately 3-6 months from late fall to early spring (Wang et al., 2014). Our sampling sites were located across northeastern China and were positioned far from the northern boundaries of desert regions, such as the Gobi Desert in southern Mongolia and the Badain Jaran and Tengger Deserts in northwestern China (Li et al., 2009). Zhang et al. (2013), using a positive matrix factorization (PMF) receptor model, showed that industrial pollution sources are a major factor affecting seasonal snow across northeastern China. Huang et al. (2015a) developed a new technique for distinguishing anthropogenic dust from natural dust based on Cloud-Aerosol Lidar and Infrared Pathfinder Satellite Observation (CALIPSO) dust and planetary boundary layer (PBL) height retrievals along with a~~

land-use dataset. The authors found that the annual mean contribution of anthropogenic dust in eastern China is approximately 91.8% owing to recent urbanization and human activity (Huang et al., 2015a). In this paper In this study, a 2014 snow survey was performed across northeastern China to analyze light absorption of ILAPs in seasonal snow, and the comparison of snow albedo reduction due to internal/external mixed BC in snow and different snow grain shapes. This paper is organized as follows. In section 2, we present the, experimental procedures, including a new radiative transfer model (Spectral Albedo Model for Dirty Snow, or SAMDS). After describing our methods (Sect. 2) In section 3, wwe demonstrateed explore the climatic effects light absorption by snowpack containing of ILAPs (including BC, OC, and AD) on seasonal snow across northeast northeastern China for less snow fallen year through a Chinese survey in 2014 following the snow surveys held in 2010 and 2012 across northern China carried out by Huang et al. (2011), and Ye et al. (2012). Then, a comparison of the snow albedo reduction under clear sky conditions measured by using a field spectroradiometer and simulated by collected through surface measurements and the Snow, Ice, and Aerosol Radiation (SNICAR) model and SAMDS model based on two-stream radiative transfer solution is present. The SAMDS model is also used for the computation of light absorption by complex ILAPs in snow for application to analyze the effects of aggregates and snow grain shapes (fractal particles grains, hexagonal plates/columns, and spheres) with the snow albedo reduction due to and internal and /external mixing structures of BC and snow on snow albedo. Finally, conclusions are Concluding and discussing remarks are given in section 4. across northeastern China, which are highly correlated with industrial pollution resulting from human activity. Therefore, ILAPs in seasonal snow are examined during a snow campaign, and the snow albedo is measured using an

11

HR-1024 field spectroradiometer and simulated using two radiative transfer models (i.e., SNICAR and SAMDS).

2 Experimental procedures

2.1 Snow field campaign in January 2014 January

In 2014, there was less snowfall in January than in previous years (e.g., 2010), and only 92 snow samples (13 surface snow, and 79 sub-surface snow samples) at 13 sites were collected during this snow survey. There were 10 fresh snow, and 3 aged snow for surface snow. In 2014, there was less snowfall in January than in previous years (e.g., 2010), and only 92 snow samples at 13 sites were collected. The snow sampling sites in this study were began at 90 (see Figure 1 and Table 1), which are numbered in chronological order followed by Wang et al. (2013a), and Ye et al. (2012). Samples from sites 90-93 were collected from grassland and cropland areas in Inner Mongolia. Sites 94-98 and sites 99-102 were located in the Heilongjiang and Jilin provinces, respectively, which are the most heavily polluted areas in northern China during winter. The snow sampling routes were similar to those used in the previous survey conducted in 2010 across northern China (Huang et al., 2011). To prevent contamination, the sampling sites were positioned 50 km from cities and at least 1 km upwind of approach roads or railways; the only exception was site 101, which was positioned downwind and close to villages. Two vertical profiles of snow samples ("left" and "right") were collected through the whole depth of the snowpack at all sites to reduce the possible contamination by artificial effects during the sampling process, and we note that the dusty or polluted layers were separately collected during the sampling process. We gathered the "left" and "right" snow samples at vertical intervals of snow samples every 5 cm for each layer from the surface to the bottom

12

~~unless a particularly dusty or polluted layer was present.~~ All of the datasets of C_{BC}^{equiv}, C_{BC}^{equiv}, ~~and~~ C_{BC}^{est} in seasonal snow from ~~T~~table 1 are the average values from the two adjacent snow samples through the whole depth of the snowpack. Snow grain sizes (R_m) were measured by visual inspection on millimeter-gridded sheets viewed through a magnifying glass. The snow samples were kept frozen until the filtration process was initiated. In a temporary lab based in a hotel, we quickly melted the snow samples in a microwave, let them settle for 3-5 minutes, and then filtered the resulting water samples through a 0.4-μm nuclepore filter to extract particulates. ~~and~~

2.2 Chemical speciation

The major water-soluble ions and trace elements in surface snow samples during this snow survey have already been investigated by Wang et al. (2015). However, the ILAPs in seasonal snow during this survey have not shown yet. For the importance of the ILAPs in snow, we will present the contribution and discuss the potential ~~the~~ emission sources of the ILAPs together with suites of other corresponding chemical constituents in seasonal snow. For instance, Hegg et al.~~,~~ (2009, 2010) ~~shown that~~analysed the source attribution of the ILAPs in arctic snow by using a positive matrix factorization (PMF) model consisted with trajectory analysis and satellite fire maps. ~~The chemical analysis of snow samples from the 2014 Chinese survey was described by Wang et al. (2015), and it was similar to the analysis applied for snow samples described by Hegg et al. (2009, 2010).~~ Briefly, major ions (SO_4^{2-}~~SO42~~, NO_3^-~~NO₃⁻~~, Cl⁻, ~~⁻~~Na⁺, K⁺, and NH_4^+~~NH4⁺~~) were analyzed with an ion chromatograph (Dionex, Sunnyvale, CA), and trace elements of Fe and Al were measured by inductively coupled plasma mass spectrometry (ICP-MS). These analytical procedures

13

have been described elsewhere (Yesubabu et al., 2014). In this paper, the major ions are used to retrieve the sea salt ~~components aerosol~~ and biosmoke potassium ($K^+_{Biosmoke}$) ~~$K^+_{Biosmoke}$~~ $K^+_{Biosmoke}$, which datasets were not shown by Wang et al. (2015). However, only SO_4^{2-}, NO_3^- ~~SO_4^{2-}, NO_3^-~~, and NH_4^+ ~~NH_4^+~~ were reprinted from Wang et al. (2015) to reveal the mass contribution of the ILAPs~~S~~ and the chemical constituents in seasonal snow during this snow survey. Previous studies have revealed considerable variations in iron (Fe) of 2-5% in dust (Lafon et al., 2006), although Al is more stable than Fe in the earth's crust. Hence, we retrieved the mass concentration of ~~minerals~~ MD via the Al concentration assuming a fraction of 7% ~~when estimating the~~in MD~~dust levels~~ (Arhami et al., 2006; Lorenz et al., 2006; Zhang et al., 2003). Sea salt was estimated following the method presented in Pio et al. (2007):

$$Sea\ salt = Na^+_{Ss}+Cl^-+0.12Na^+_{Ss}+0.038Na^+_{Ss}+0.038Na^+_{Ss}+0.25Na^+_{Ss}, \tag{1}$$

where subscript Ss means sea salt~~–~~ sources, ~~where~~ Na_{Ss} was calculated using the following formula (Hsu et al., 2009):

$$Na_{Ss} = Na_{Total} - Al\times(Na/Al)_{Crust}. \tag{2}$$

Following Hsu et al. (2009), the contribution of ~~$K^+_{Biosmoke}$~~ $K^+_{Biosmoke}$ was determined using the following equations:

$$K^+_{Biosmoke} = K_{Total} - K_{Dust} - K_{Ss}, \tag{3}$$

$$K_{Dust} = Al\times(K/Al)_{Crust}, \tag{4}$$

$$Na_{Ss} = Na_{Total} - Al\times(Na/Al)_{Crust}, \tag{5}$$

$$K_{Ss} = Na_{Ss}\times0.038, \tag{6}$$

where ~~$K^+_{Biosmoke}$~~ $K^+_{Biosmoke}$, K_{Dust}, and K_{Ss} refer to biosmoke potassium, dust-derived potassium, and sea-salt-derived potassium, respectively. Equations (4), (5), and (6) were derived from Hsu et al. (2009) and Pio et al. (2007).

14

2.3 Spectrophotometric analysis

Recent studies indicated that the light absorption by MD should be more sensitive to the presence of strongly absorbing iron oxides such as hematite and goethite than to other minerals (Alfaro et al., 2004; Sokolik and Toon, 1999)~~As Alfaro et al., (2004) indicated that the light absorption by mineral dust~~MD ~~should be highly sensitive to their content in iron oxides (hematite, goethite, etc.) based on Mie theory. Sokolik and Toon., (1999) also pointed out that computations performed with optical models show that the absorbing potential of mineral dust~~MD ~~is more sensitive to the presence of strongly absorbing iron oxides such as hematite and goethite than to other minerals (Sokolik and Toon, 1999)~~. Thus it is now possible to assess the absorption properties of ~~mineral dust~~MD by using iron oxide content (Bond et al., 1999). In this study, the iron (Hereinafter ~~Hereafter~~ simply "Fe"~~the same as Fe~~) in seasonal snow is assumed to be originating ~~originated~~ from ~~mineral dust~~MD during this survey, which followed the procedures performed by Wang et al., (2013a). ~~Assuming that iron originated from mineral dust in seasonal snow, w~~We measured the mixing ratios of BC and OC using an integrating sphere/integrating sandwich spectrophotometer (ISSW), which was first described by Grenfell et al. (2011) and used by Doherty et al. (2010, 2014) and Wang et al. (2013a)~~ to measure mixing ratios of BC and OC~~. The equivalent BC (C_{BC}^{equiv} C_{BC}^{equiv}), maximum BC (C_{BC}^{max} C_{BC}^{max}), estimated BC (C_{BC}^{est} C_{BC}^{est}), fraction of light absorption by non-BC ILAPs (f_{non-BC}^{est} f_{non-BC}^{est}), and absorption Ångstrom exponent of all ILAPs ~~–~~($Å_{tot}$) were described by Doherty et al. (2010). Previous studies have concluded that ~~light-absorbing particles~~ILAPs are primarily derived from BC, OC, and ~~Fe~~iron (Fe). The mass loadings of BC (L_{BC}) and OC (L_{OC})~~and OC~~ were calculated using the following equation:

$$\tau_{tot}(\lambda) = \beta_{BC}(\lambda) \times L_{BC} + \beta_{OC}(\lambda) \times L_{OC} + \beta_{Fe}(\lambda) \times L_{Fe}. \tag{7}$$

Here, $\tau_{tot}(\lambda)$ refers to the measured optical depth. L_{BC} and L_{OC} ~~L_{BC} and L_{OC}~~ can be determined from this equation assuming that the mass absorption coefficients~~mass absorption efficiencies~~ (MACs~~β~~) for BC, OC, and Fe are 6.3, 0.3, and 0.9 $m^2 g^{-1}$,

5   respectively, at 550 nm and that the absorption Ångstrom exponents (Å or AAE) for BC, OC and Fe are 1.1, 6, and 3, respectively (e.g., Equations (2) and (3) in Wang et al., 2013a).

2.4   Aerosol optical depth and snow albedo measurements

10   The Microtops Ⅱ Sun photometer has been widely used to measure aerosol optical depth (AOD) in recent years (More et al., 2013; Porter et al., 2001; Zawadzka et al., 2014), and is recognized as a very useful tool for validating aerosol retrievals from satellite sensors.~~We used a portable and reliable Microtops Ⅱ Sun photometer at wavelengths of 340, 440, 675, 870, and 936 nm instead of the CE318 sun tracking photometer (Holben et al., 2006) to measure the in situ~~surface aerosol optical depth

15   ~~(AOD).~~ Ichoku et al. (2002b) and Morys et al. (2001) provided a general description of the Microtops Ⅱ Sun photometer's design, calibration, and performance. ~~The Microtops Ⅱ Sun photometer has been widely used in recent years (de Mourgues et al., 1970; Porter et al., 2001; Zawadzka et al., 2014) and is recognized as a very useful tool for validating aerosol retrievals from satellite sensors. A Microtops Ⅱ Sun~~

20   ~~photometer was calibrated following the methods presented by Morys et al. (2001) and Ichoku et al. (2002b).~~ To better understand the background weather conditions in the local atmosphere during this snow survey, we used a portable and reliable Microtops Ⅱ Sun photometer at wavelengths of 340, 440, 675, 870, and 936 nm instead of the CE318 sun tracking photometer to measure the surface AOD in this

study~~., a Microtops II Sun photometer was used during the 2014 Chinese survey~~in ~~this study.~~ AOD measurements were collected in cloud-free conditions between 11:00 am and 1:00 pm (Beijing local time) to prevent the effects of optical distortions due to large solar zenith angles. ~~We used~~Then, the Moderate Resolution Imaging Spectroradiometer (MODIS) on the Aqua and Terra satellites was used to retrieve the AOD and fire spot datasets (Kaufman et al., 1997; Zhang et al., 2013b; Zhao et al., 2014). The retrieved MODIS AOD is reliable and accurate when applied to three visible channels over vegetated land and ocean surfaces (Chu et al., 2002; Ichoku et al., 2002a; Remer et al., 2002). Fire locations are based on data provided by the MODIS FIRMS system from October ~~2014~~2013 to January ~~2015~~2014. The land-cover types (Figures 6 and 7) were obtained from the Collection 5.1 MODIS global land-cover type product (MCD12C1) at a 0.05° spatial resolution and included 17 different surface vegetation types (Friedl et al., 2010; Loveland and Belward, 1997).

Snow albedo plays a key role in affecting the energy balance and climate in the cryosphere (e.g. Hadley and Kirchstetter, 2012; Liou et al., 2014; Warren and Wiscombe, 1985). Wright et al. (2014) indicated that the spectral albedo measured by using an Analytical Spectral Devices (ASD) s~~S~~pectroradiometer~~s~~ at 350-2200 nm is in agreement with albedo measurements at the baseline Surface Radiation Network (BSRN). Wuttke et al. (2006a) pointed out that the spectroradiometer instrument is considered as ~~the~~ more capable, rapid, and mobile to conduct spectral albedo measurements during short time periods, especially in the very cold regions (e.g. in the Arctic). The major advantage is the more extensive wavelength range, and the cosine error is less than 5% for solar zenith angles below 85° at the wavelength of 320 nm~~have been used to measure the surface spectral albedo~~ (~~Kotthaus et al., 2014;~~

17

Wright et al., 2014; Wuttke et al., 2006a, b). In ~~the 2014 Chinese survey~~this study, snow albedo measurements were obtained using a HR-1024 field -spectroradiometer (SVC, Spectra Vista Corporation, Poughkeepsie, NY, USA). This instrument has a spectral range of 350-2500 nm with resolutions of 3.5 nm (350--1000 nm), 9.5 nm (1000--1850 nm), and 6.5 nm (1850--2500 nm). Normally, the relative position of the spectroradiometer is at a distance of 1m from the optical element for the active field of view ~~According to previously described procedures, we measured the snow albedo 1 m above the ground~~ (Carmagnola et al., 2013). A standard "white" reflectance panel with a VIS–SWIR broadband albedo of 0.98 (P_λ) was used to measure the reflectance spectra along with the target. The reflectance spectra of surface snow (R_s) and the standard panel (R_p) were measured at least ten times. Then, the snow albedo (α) was calculated as follows:

$$\alpha = (R_s/R_p) \times P_\lambda. \tag{8}$$

The nominal filed of view (FOV) lens is 8° to enable the instrument to look at different size targets. In order to receive more direct solar radiation, t~~T~~he direction of the instrument was oriented to the Sun~~.~~ Horizon angles to measure snow albedo~~in order to receive more direct solar radiation~~. The small size of the fore optics greatly reduces errors associated with instrument self-shadowing. Even when the area viewed by the fore optic is outside the direct shadow of the instrument, the instrument still blocks some of the illumination (either diffuse skylight or light scattered off surrounding objects) that would normally be striking the surface under observation for measuring full-sky-irradiance throughout the entire 350--2500 nm wavelengths. Further information on HR-1024 field spectroradiometer use and on the calibration procedure can be found in Wright et al. (2014).~~.~~ The measured solar zenith angles and the other parameters ~~datasets~~ used to simulate snow albedo in this study have been

2.5   Model simulations

BC and ~~dust~~ MD sensitivity effects on the snow albedo simulated by the Snow, Ice, and Aerosol Radiation (SNICAR) model have been validated through recent simulations and field measurements (Flanner et al., 2007, 2009; Qian et al., 2014; Zhao et al., 2014). We used the offline SNICAR model to simulate the reduction in surface snow albedo resulting from ILAPs contamination (Flanner et al., 2007), and we compared the results with our spectroradiometer surface measurements. The SNICAR model calculates the snow albedo as the ratio of the upward and downward solar flux at the snow surface. The measured parameters, including the measured snow grain radius (R_m), snow density, snow thickness, solar zenith angle θ, and mixing ratios of BC and ~~AD~~MD, were used to run the SNICAR model under clear sky conditions. The visible and near-infrared albedos of the underlying ground were 0.2 and 0.4, respectively, as derived from MODIS remote sensing. The ~~mass absorption cross section (~~MAC~~)~~ of BC was assumed to be 7.5 m^2 g^{-1} at 550 nm.

The Spectral Albedo Model for Dirty Snow (SAMDS) for calculating spectral snow albedo as a function of the snow grain radius, the mixing ratios of ILAPs (BC, ~~AD~~MD, and OC), and ~~mass absorption efficiencies~~MACs of impurities was used and is based on asymptotic radiative transfer theory. A detailed description of asymptotic analytical radiative transfer theory for ~~snowpack~~SAMDS ~~was~~could be found ~~presented~~ by Zhang et al. (2016).~~This model explicitly considers (i) mixing states between impurities and snow grains, (ii) the irregular morphology of snow grains and aerosol particles, (iii) specific mineral compositions and size distributions of dust in snow, (iv) aging processes of snow grains and soot aggregates, and (v) multilayers for~~

Briefly, the surface albedo can be calculated using the following asymptotic approximate analytical solution derived from radiative transfer theory (Kokhanovsk and Zege, 2004; Rozenberg, 1962; Zege et al., 1991):

$$R_d(\lambda) = \exp(-4S(\lambda)\mu(v_0)). \tag{9}$$

Here, $R_d(\lambda)$ ~~$R_d(\lambda)$~~ is the plane albedo, v_0 ~~v_0~~ is the solar zenith angle, and $u(v_0)$ $\mu(v_0)$ refers to the escape function in radiative transfer theory, and can be parameterized following Kokhanovsky and Zege (2004):

$$\mu(v_0) = \frac{3}{7}(1+2\cos v_0), \tag{10}$$

where λ ~~λ~~ is the wavelength, $S(\lambda)$ $S(\lambda)$ is the similarity parameter, and

$$S(\lambda) = \sqrt{\frac{\sigma_{abs}}{3\sigma_{ext}(1-g)}}. \tag{11}$$

Here, σ_{abs} and σ_{ext} σ_{abs} ~~and~~ σ_{ext} are the absorption and extinction coefficients, respectively, and g ~~g~~ is the asymmetry parameter (the average cosine of the phase function of the medium).

According to Equations (18) and (25) in Kokhanovsky and Zege (2004), the extinction coefficients of particles can be expressed as follows:

$$\sigma_{ext} = \frac{l_{tr}}{1-g} = \frac{3C_v}{2r_{eff}}, \tag{12}$$

where l_{tr} l_{tr} is the photon transport path length, C_v C_v is the volumetric snow particle concentration, and r_{ef} r_{eff} is the effective grain size, which is equal to the radius of the volume-to-surface equivalent sphere: $r_{ef} = \dfrac{3\overline{V}}{4\overline{A}}$ $r_{eff} = \dfrac{3\overline{V}}{4\overline{A}}$, where $\overline{V}$ and $\overline{A}$ $\overline{V}$ ~~and~~ $\overline{A}$ are the average volume and average cross-sectional (geometric shadow) area of snow grains, respectively.

The absorption coefficient σ_{abs} σ_{abs} in Equation (11) for arbitrarily shaped and weakly absorbing large grains is proportional to the volume concentration (Kokhanovsky and Zege, 2004):

$$\sigma_{abs}=B \cdot \frac{4\pi k(\lambda)}{\lambda} \cdot C_v, \qquad (13)$$

5   where $k(\lambda)$ $k(\lambda)$ is the imaginary component of the complex refractive index for ice, and B B is a factor that is only dependent on the particle shape. The theory based on the ray-optics approach shows that g in Equation (11) and B in Equation (13) are 0.89 and 1.27 for spheres, 0.84 and 1.50 for hexagonal plates/columns, and 0.75 and 1.84 for fractal grains, respectively.

10   The total absorption coefficient, σ_{abs} σ_{abs}, can be derived from the absorption by snow, S_{abs}^{snow} σ_{abs}^{snow}, and the absorption by ~~light-absorbing impurities~~ILAPs (, σ_{abs}^{dust}

σ_{abs}^{BC}, σ_{abs}^{MD}~~dust~~, and σ_{abs}^{OC}): S_{abs}^{dust}, S_{abs}^{BC}, ~~and~~ S_{abs}^{OC}:

$$\sigma_{abs}=\sigma_{abs}^{snow} + \sigma_{abs}^{BC} + \sigma_{abs}^{MD\text{dust}} + \sigma_{abs}^{BC} + \sigma_{abs}^{OC}. \qquad (14)$$

The hemispherical reflectance with a zenith angle v_0 can be expressed as follows:

$$R_d(\lambda) = \exp(-$$

$$4 \cdot \sqrt{\frac{4B}{9(1-g)} \cdot \frac{2\pi \cdot r_{eff}}{\lambda} \cdot k(\lambda) + \frac{\rho_{ice} \cdot 2r_{eff}}{9(1-g)} \cdot MAC_{abs}^{BC} \cdot C_{BC}^* + \frac{\rho_{ice} \cdot 2r_{eff}}{9(1-g)} \cdot MAC_{abs}^{dustMD} \cdot C_{dustMD}^* + \frac{\rho_{ice} \cdot 2r_{eff}}{9(1-g)} \cdot MAC_{abs}^{OC} \cdot C_{OC}^*} \cdot \tfrac{3}{7}(1+2\cos v_0)) \quad , \qquad \text{for}$$

$$\exp(-\sqrt{94.746 \cdot \frac{r_{eff}}{\lambda} \cdot k(\lambda) + 5.163 \cdot r_{eff} \cdot (MAC_{abs}^{BC} \cdot C_{BC}^* + MAC_{abs}^{dustMD} \cdot C_{dustMD}^* + MAC_{abs}^{OC} \cdot C_{OC}^*) \cdot (1+2\cos v_0)}) \quad , \qquad \text{for}$$

spherical grains;

$$= \exp\left(-4.95 \cdot \sqrt{\frac{\pi \cdot r_{eff} \cdot (k(\lambda) + \alpha \cdot C_{dustBC}^* + \beta \cdot C_{BCMD}^* + \chi \cdot C_{OC}^*)}{\lambda}} \cdot (1+2\cos v_0)\right) \quad , \qquad \text{for hexagonal grains;}$$

(15)

$$\exp\left(-4.38 \cdot \sqrt{\frac{\pi \cdot r_{eff} \cdot (k(\lambda) + \alpha \cdot C_{dustBC}^* + \beta \cdot C_{BCMD}^* + \chi \cdot C_{OC}^*)}{\lambda}} \cdot (1+2\cos v_0)\right), \qquad \text{for fractal grains.}$$

~~A detailed description of asymptotic analytical radiative transfer theory for snowpack was presented by Zhang et al. (2016).~~ Previous studies have also shown that the spectral snow albedo is more sensitive to snow grain size and light conditions than BC contamination and snow depths at near-infrared wavelengths (Warren, 1982). Therefore, the snow grain optical effective radius (R_{eff}) was retrieved based on the spectral albedo measured at $\lambda=1.3$ μm ~~(Table 4)~~, where snow grain size dominates the snow albedo variations and the effects of ~~light absorbing particles~~ILAPs at this wavelength are negligible (Warren and Wiscombe, 1980).

3   Results

3.1   The spatial distribution of AOD

The AOD is a major optical parameter for aerosol particles and a key factor affecting global climate (Holben et al., 1991, 2001, 2006; Smith et al., 2014; Srivastava and Bhardwaj, 2014). Most of the snow samples were collected in the afternoon at the Aqua-MODIS (13:30 LT) overpass time in order to compare the local AODs in sampling sites by using an spectroradiometer with the satellite remote sensing. The AODs spatial distribution derived from the Aqua-MODIS satellite over northern China ~~from October to January~~ associated with sampling site numbers is shown in Figure 1 during this snow survey. ~~For most of the snow samples collected in the afternoon at the Aqua-MODIS (13:30 LT) overpass time, the averaged spatial AOD distribution was derived from the Aqua-MODIS satellite "Aerosol" product during the sampling period across northern China. The AOD spatial distribution over northern China is shown in Figure 1 for the period from October to January.~~ The average AOD in the studied area ranged from 0.1 to 1.0 and exhibited strong spatial inhomogeneity. The largest AODs (up to approximately 1.0) retrieved from the MODIS satellite were

23

associated with anthropogenic pollution over northeastern China during the 2014 sampling period. These large values, which exceeded 0.6, were related to local air pollution from industrial areas (Che et al., 2015b; Wang et al., 2010a). In contrast, the MODIS-Aqua results indicate that the smallest AOD~~s~~ (as low as 0.1) at 550 nm were found over the Gobi Desert in Inner Mongolia and were related to strong winter winds. Similar patterns in the retrieved MODIS AOD were found by Zhao et al. (2014) and Zhang et al. (2013b). Although previous studies have indicated that AOD~~s~~ ~~in~~ across northeast~~ern~~ern China are among the highest in East Asia (Ax et al., 1970; Bi et al., 2014; Che et al., 2009; Routray et al., 2013; Wang et al., 2013b; Xia et al., 2005, 2007), field experiments of aerosol optical properties across northeastern China have been limited. Compared with the retrieved AOD by the remote sensing, the surface measurements of AOD were also conducted during this snow survey. Generally, the measured AOD were gradually higher from Inner Mongolia regions moved to the industrial area across ~~northeast~~northeastern China. ~~To evaluate the accuracy of the AODs, in situ AOD measurements were collected during the snow sampling period in January 2014. The in situ AOD measurements were generally consistent with the spatial AOD distribution retrieved from MODIS across northern China, although the retrieved AOD was slightly higher than that retrieved from the in situ measurements in the study area.~~ In Inner Mongolia, the average AOD was less than 0.25 for sites ~~1~~ XX90 to ~~6~~ XX93 under clear sky conditions. We found large discrepancy ~~variations~~ of 40-50% in the same area within ~~in~~ the 1-hour measurements collected from sites ~~6a~~ 95a~~XX~~ and ~~6b~~XX95b, which could be possibly~~; these variations were~~ correlated with regional biomass burning ~~processes~~. However, AOD~~s~~ exceeded 0.3 at sites ~~9~~ XX98 and ~~12~~XX101, which were significantly influenced by anthropogenic air pollution from industrial areas across northern China. MODIS active fires are often spatially

distributed over northeastern China and mainly result from human activities during cold~~er~~ seasons.

3.2 ~~Sampling statistics~~ Contributions to light absorption by ILAPs

Generally, we only collected the aged surface snow in three sites, while fresh surface snow ~~were~~was collected in the other sites during this snow survey in January 2014. C_{BC}^{est}~~C_{BC}^{est}~~, C_{BC}^{max}~~C_{BC}^{max}~~, C_{BC}^{equiv}~~C_{BC}^{equiv}~~, f_{nonBC}^{est}~~f_{non-BC}^{est}~~, $Å_{tot}$ and snow parameters, such as snow depth, snow density, measured snow grain radius (R_m), and snow temperature, are given in Table 1 and Figure 3 for each snow layer following Wang et al. (2013a). ~~Average C_{BC}^{est}, C_{BC}^{max}, and C_{BC}^{equiv} values were calculated using "left" and "right" samples for each layer.~~ In Inner Mongolia~~Generally~~, t~~T~~he snow cover was thin and patchy ~~in Inner Mongolia, and t~~. The average snow depth at sites 90, 91, 93, and 94 was less than 10 cm, which was significantly smaller than those (13 to 20 cm) at sites 95-97 near the northern border of China~~The average snow depth was less than 10 cm from sites 90, 91, 93, and 94, which are~~was significantly lower than that near the northern border of China, ranging from 13 to 20 cm at sites 95-97~~. The snow samples were collected from drifted snow in Inner Mongolia, and the mass loadings of ILAPs in seasonal snow are mainly due to blowing soil dust. Therefore, the vertical profiles of snow samples mixed with blowing soil from these sites are insufficient to represent the seasonal evolution of wet and dry deposition to snow (Wang et al., 2013a). However, the light absorption of ILAPs is still dominated by OC in these regions, which ~~will be~~has been illustrated in the following section.~~, which are slightly lower than that near the northern border of China, ranging from 13 to 20 cm at sites 95-97.The snow cover was thin and patchy in Inner Mongolia, and the average snow depth was less than 10 cm from sites 90, 91, 93, and 94, which slightly higher values~~

25

near the northern border of China, ranging from 13 to 20 cm at sites 95-97. The maximum snow depth was found to be 46 cm at site 102 inside a forest near the Changbai Mountains. Snow depth varied from 13 to 46 cm at sites 98 to 102 with an average of 27 cmThe maximum snow depth of 46 cm at site 102 was found in a forest near the Changbai Mountains, averaging 27 cm and varying from 13 to 46 cm at sites 98 to 102. Because less snow fell during the 2014 snow survey period than that in 2010Because less snow fell during the 2014 snow survey period, R_m of the surface snow samples grain radius varied considerably from 0.07 to 1.3 mm. R_mThe snow grain size increased with the snow depth from the surface to the bottom and was, larger than that previously recorded in previous studies because of snow melting by solar radiation and the ILAPs (Hadley and Kirchstetter, 2012; Motoyoshi et al., 2005; Painter et al., 2013; Pedersen et al., 2015). The snow density exhibited little geographical variation across northern China at 0.13 to 0.38 g cm^{-3}. High snow densities result from melting or snow aging. Similar snow densities have been found in the Xinjiang region in northern China (Ye et al., 2012). AtIn this studysite 90, we only collected one layer of snow samples from central Inner Mongolia, and $C_{BC}^{est}$the BC mixing ratio was 3304 ng g^{-1} forin aged snow. Along the northern Chinese border at sites 91-95, C_{BC}^{est}BC contamination in the cleanest snow ranged from 3027 to 260 ng g^{-1}; only a few values exceeded 200 ng g^{-1}. The f_{nonBC}^{est} f_{non-BC}^{est} value varied remarkably from 29 to 78%, although BC was still a major absorber in this region. Heavily polluted sites were located in industrial regions across northeastern China (sites 99-102). The surface snow C_{BC}^{est} BC in this region ranged from 51008 to 3651700 ng g^{-1}, and the highest C_{BC}^{est} BC in the sub-surface layer of the four sites (?? Check the sites and the values) was 2900882 ng g^{-1} in Table 1. In addition, the

fraction of total particulate solar absorption due to ~~f^{est}_{nonBC}~~ $f^{est}_{non\text{-}BC}$ was typically 35-74%, indicating significant light-absorbing contributions by~~that light absorption in snow is mainly attributable to~~ OC and ~~AD~~MD from human activity in the heavily polluted areas. Å$_{tot}$ ranged from 2.1 to 4.8. A higher Å$_{tot}$ is a good indicator of soil dust, which is primarily driven by the composition of mineral or soil dust. In contrast, a lower Å$_{tot}$ of 0.8-1.2 indicates that ILAPs~~light-absorbing particulates~~ in the snow are dominated by BC (Bergstrom et al., 2002; Bond et al., 1999).

To better understand the ~~BC~~ distribution of ~~C^{est}_{BC}~~ C^{est}_{BC} in seasonal snow across northern China, ~~an~~ the spatial distribution of ~~interannual comparison of~~ ~~C^{est}_{BC}~~ C^{est}_{BC} ~~the BC content~~ in the surface and average snow measured during th~~is~~e snow ~~2010 and 2014 Chinese~~ survey~~s was performed, and the results~~ are shown in Figure 4 ~~and Table 2~~. The spatial distributions of ~~C^{est}_{BC}~~ C^{est}_{BC} ~~BC~~ in the surface and average snow measured using ~~an~~ the ISSW spectrophotometer during the 2014 survey generally ranged from 5~~0~~3 to ~~3651~~ 3700 ng g^{-1} and 6~~0~~2 to 16~~00~~35 ng g^{-1}, with the medium values of 260 ng g^{-1}, and 260 ng g^{-1}, respectively~~respectively~~. These variations of ~~C^{est}_{BC}~~ C^{est}_{BC} were very similar to those of the previous snow campaign by ~~, as shown in Figure 4 (~~Wang et al.~~,~~ (2013a), ~~although~~ however, ~~they were~~ much higher than those in the Xinjiang region of northwestern China (Ye et al., 2012), along the southern edge of the Tibetan Plateau (Cong et al., 2015), and ~~in~~ across North America (Doherty et al., 2014). ~~In the 2014 Chinese survey, we only collected one layer of snow samples from central Inner Mongolia, and the BC mixing ratio was 334 ng g^{-1} in aged snow. Along the northern Chinese border at sites 91-95, BC contamination in the cleanest snow ranged from 27 to 260 ng g^{-1}; only a few values exceeded 200 ng g^{-1}. The~~

value varied remarkably from 29 to 78%, although BC was still a major absorber in this region. Heavily polluted sites were located in industrial regions across northeastern China (sites 99-102). The surface snow BC in this region ranged from 508 to 3651 ng g^{-1}, and the highest BC in the sub-surface layer of the four sites was 2882 ng g^{-1}. In addition, the fraction of total particulate solar absorption due to f_{nonBC}^{est} was typically 35-74%, indicating that light absorption in snow is mainly attributable to OC and AD from human activity.

Figure 5 compares C_{BC}^{est} the BC mixing ratio values measured via the ISSW method with the calculations during 2010 (Wang et al., 2013a) and 2014 snow surveys. Ideally, the C_{BC}^{est} BC content calculated using Equation (7) should be equal to that measured via the ISSW method. The two results agreed very well (R^2=0.99), indicating that Equation (7) worked agreed well for this measurement in Figure 5. Thus, the C_{BC}^{est} BC content measured via the ISSW method was was found to be reasonable and reliable. To compare with the mixing ratio of OC calculated from Equation (7), we used the calculated C_{BC}^{est} BC mixing ratios listed in Figures 6-78 and Table 23 in the following sections.

3.3 Emission factors

Typically, chemical components in seasonal snow originate from different emission sources. For example, OC and BC are emitted from the incomplete combustion of fossil fuels and biofuels. K$^+$ is a good tracer of biomass burning (Cachier et al., 1995), whereas NO$_3^-$ and SO$_4^{2-}$ originate primarily from diesel oil and gasoline combustion and from coal burning with sulfur. NH$_4^+$ is an important indicator of fertilizer used in agricultural processes. OC/BC ratios are used to represent possible emission sources of biomass burning (Bond et al., 2013; Cao et al., 2007; Cong et al., 2015; Novakov et

al., 2005). The OC/BC ratio in the sampled surface snow ranged from 1.4 to 17.6 (Figure 6); a very high OC/BC ratio (17.6) was found at site 90, suggesting that biomass burning may have been a major contributor of OC through photochemical reactions during the 2014 Chinese survey. A relatively high correlation (R^2=0.87, n=13) was observed between OC and BC, indicating similar emission sources at all sampling sites except for those in central Inner Mongolia, as shown in Figure 6a. These results are consistent with those of previous studies (Ming et al., 2010). The strong correlations between NH_4^+/SO_4^{2-} and NH_4^+/NO_3^- shown in Figures 6b and 6c (R^2=0.91 and R^2=0.94, respectively; n=12) suggest that fine particles characterized as $(NH_4)_2SO_4$ and NH_4NO_3 were derived from more intense agricultural and human activities occurring near farmland areas (Ianniello et al., 2011). It is widely accepted that crustal Al originates from mineral or soil dust (Wedepohl, 1995). Therefore, the weak correlation between K^+ and Al could be explained by different emission sources of K^+ and Al (Figure 6d) often attributed to biomass burning and mineral or soil dust, respectively, in local or remote regions. Sampling site 101 (red dot in Figure 6d) is positioned very close to a village. As a result, we found a much higher K^+ than Al value owing due to high biomass burning via human activity in winter.

3.4 Mass contributions of chemical components

In Figure 6, the sampling areas were located in grasslands, croplands, and urban and built-up regions across northern China that are likely influenced by human activity (Huang et al., 2015a).The land cover types (Figure 7) were obtained from the Collection 5.1 MODIS global land cover type product (MCD12C1) at a 0.05° spatial resolution and included 17 different surface vegetation types (Friedl et al., 2010; Loveland and Belward, 1997). The sampling areas were located in grasslands, croplands, and urban and built-up regions across northern China that are likely

~~influenced by human activity (Huang et al., 2015a).~~ According to Table 2~~3~~ and Figure 6~~7~~, the NH_4^+ ~~NH_4^+~~ concentrations emitted from agricultural sources at all sites accounted for less than 2.8% because the sites were positioned 50 km from cities. However, large fractions of both SO_4^{2-}, and NO_3^- ~~SO_4^{2-} and NO_3^-~~ were observed, varying from 14.8 to 42.8% at all sites, with the highest fraction of 24.2-42.8% found in industrial areas. These results show that SO_4^{2-}, and NO_3^- ~~SO_4^{2-} and NO_3^-~~ made the greatest contributions to the total chemical concentration in the surface snow and are significant anthropogenic emissions ~~sources~~ of fossil-fuel combustion in heavy industrial areas. More specifically, the largest ~~AD~~ MD contribution ranged from 35.3 to 46% at sites 91 to 95 ~~owing~~ due to strong winds during winter; the ~~AD~~ MD fractions were only 5.7 to 31% at the other sites. Fractions of BC and OC were similar to those above, showing that biomass burning was a major source during winter in the sampling region. Zhang et al. (2013b) showed that OC and BC fractions vary more widely in the winter than other seasons ~~owing~~ due to industrial activity in China. Sulfate peaks were found in summer (15.4%), whereas nitrate peaks were observed in spring (11.1%). ~~Potassium~~ ($K_{Biosmoke}^+$ ~~$K^+_{biosmoke}$~~) was found to be a good tracer of biomass burning, ranging from 1.3 to 5.1% along the northern Chinese border compared to lower values found at lower latitudes (1.5-2.3%), and it exhibited much higher contributions in Inner Mongolia and along the northern Chinese border ~~owing~~ due to increased emissions from cooking, open fires, and agricultural activities. The fraction of sea salt ~~aerosol~~ was found to range from 6.3 to 20.9%. Wang et al. (2015) showed that higher Cl^-/Na^+ ratios in seasonal snow found in the 2014 Chinese survey were 1–2 times greater than those of seawater, implying that they constituted a significant source of anthropogenic Cl^- ~~(Wang et al., 2015)~~.

~~3.5   BC, OC and AD contributions to light absorption~~

30

As described by Wang et al. (2013a), light absorption by ILAPs can be determined from ISSW measurements combined with a chemical analysis of ~~iron~~ Fe concentrations by assuming that the light absorption of dust is dominated by ~~iron~~ (Fe~~)~~; however, ~~iron~~ Fe can also originate from industrial emissions, such as the metal and steel industries (Hegg et al., 2010; Ofosu et al., 2012). Doherty et al. (2014) used a similar method to distinguish ~~between~~ contributions of ILAPs~~light absorbing impurities~~ in snow in central North America. Although heavy ~~AD~~MD loading was observed in 2014 snow survey~~the study region~~, the fraction of light absorption due to ~~AD~~MD (assumed to exist as goethite) was generally less than 10% across northeastern China (Figure 7~~8~~), which was much smaller than that observed in the Qilian Mountains (e.g., Figure 11 of Wang et al., 2013a). Here, l~~L~~ight absorption was mainly dominated by BC and OC in snow in January 2014. By contrast, the fraction of light absorption due to BC varied from 48.3 to 88.3% at all sites, with only one site dominated by OC (site 90 in central Inner Mongolia). Compared to the light absorption patterns in the Qilian Mountains, ~~iron~~ MD played a less significant role in particulate light absorption in snow across the northeastern China sampling area.

3.~~6~~ 3 Simulations of s~~S~~~~Comparisons between the observed and modeled~~ snow albedo ~~reduction~~

Snow albedo reduction due to BC has been examined in previous studies (Brandt et al., 2011; Hadley and Kirchstetter, 2012; Yasunari et al., 2010). Here, a new radiative transfer model (SAMDS) is developed to assess the effects of ILAPs in snow, the snow grain shapes, and the internal/external mixing of BC and snow on snow albedo based on the asymptotic radiative transfer theory. ~~However, few observations of the BC, OC, and ADMD mixing effects on snow albedo reduction in seasonal snow at~~

31

~~middle latitudes exist. In this study, we measured the snow albedo at six sites under~~ ~~clear conditions. A comparison of T~~the snow albedos derived from the SNICAR and SAMDS models are~~is~~ presented in Figure 8~~9~~. ~~Spectral snow albedos measured in our~~ ~~experiments and simulated through the SNICAR and SAMDS models are shown in~~ ~~Figure 12~~1. We ran the models at a solar zenith angle θ of 60 ~~°C~~, which is ~~consistent~~ comparable with our experimental method for measuring snow albedo ~~and with~~ ~~ILAPs~~light-absorbing impurities across northeastern China. The BC MAC used in the two models was 7.5 m^2 g^{-1} at 550 nm, which was assumed in the most recent climate assessment and is appropriate for freshly emitted BC (Bond and Bergstrom, 2006; Bond et al., 2013; Warren, 1982). Mixing ratios of BC, ~~OC~~MD, and ~~OC~~dust were chosen to exhibit the following ranges: 0.1-5 µg g^{-1}, 2-6 µg g^{-1}, and 1-30 µg g^{-1} ~~0-5 µg~~ ~~g^{-1}, 0-30 µg g^{-1}, and 0-6 µg g^{-1}~~, respectively, encompassing the values measured in snow surfaces across northeastern China in this study and in previous research (Doherty et al., 2010, 2014; Wang et al., 2013a, 2014; Warren and Wiscombe, 1980; Ye et al., 2012~~Warren and Wiscombe, 1980~~) ~~and in this study~~. ~~The BC MAC used in~~ ~~this study was 7.5 m^2 g^{-1} at 550 nm, which was assumed in the most recent climate~~ ~~assessment and is appropriate for freshly emitted BC (Warren, 1982; Bond and~~ ~~Bergstrom, 2006; Bond et al., 2013).~~ Results showed that the albedo of fresh snow at 550 nm with R$_{eff}$ of 100 µm simulated by SAMDS is generally in a range of 0.95-0.75 for ILAPs-contaminated snow across northeastern China (Figure 8). ~~The~~ ~~visible and near-infrared albedos of underlying ground surfaces were 0.2 and 0.4,~~ ~~respectively, according to the MODIS data.~~ The spectral albedos of pure snow derived from the SNICAR (dash line~~s~~) and SAMDS (solid line~~s~~) models agree~~d~~ well. However, there ~~was~~ is a slight tendency for the SNICAR model values to become lower than SAMDS model values when BC and ~~dust mixing ratios~~MD range from 1

~~to 5 µg g⁻¹ and 4 to 6 µg g⁻¹, respectively~~are considered. The 1.~~5-2.5~~3% deviation between the SNICAR and SAMDS modeled snow albedos at 550 nm for ~~higher~~ BC mixing ratios of 1-5 µg g⁻¹ indicates that albedo reduction by ILAPs~~light absorbing impurities~~ in the SNICAR model was greater than that ~~of~~in the SAMDS model. This deviation is in part due to the different parameterization of snow grain shapes, mixing states of snow and BC, and physical-chemical properties of impurities between the two models (Zhang et al., 2016). More notably, snow albedos decrease~~d~~ significantly within the UV-visible wavelength, especially for the higher OC (dotted lines) ~~contents~~ mixing ratios in Figure 8~~9~~. This may be attributed to the fact that OC strongly absorbs UV-visible radiation and masks BC absorption for high AAE of OC, which decreases remarkably with increasing wavelengths (Warren and Wiscombe, 1980).

As is shown in Figure 9~~10~~, we also estimated the reduction in the spectrally weighted snow albedo for different R_{eff} values using the SNICAR and SAMDS models. ~~There was a~~A larger reduction in snow albedo by both BC and MD-contaminated snow was found for larger snow grains ~~Higher degrees of snow albedo reduction by both BC and dust-contaminated snow were generally found for larger snow grains~~ (Figure 9~~10~~a-b). For example, snow albedo reduction attributable to 1 µg g⁻¹~~000 ng g⁻¹~~, 1 µg g⁻¹, and 10 µg g⁻¹ for BC, ~~dust~~MD, and OC, respectively, was 37%, 41%, and 38% greater in 200 µm snow grains (0.081, 0.0019, and 0.047) than that in 100 µm snow grains (0.059, 0.0013, and 0.034). Both the SNICAR and SAMDS models indicated that the snow albedo is more sensitive to BC, especially ~~during~~at lower ILAP~~-~~s mixing ratios~~periods~~. For example, 200 ng g⁻¹ of BC decreased 0.03~~the~~ snow albedo ~~by 3.4% for~~at an ~~optical effective radius~~R_{eff} of 200 µm, which is much larger than the snow albedo reduction of 0.003 and 0.018 ~~of~~by 2000 ng g⁻¹~~2 µg g⁻¹ for~~ ~~of dust~~MD and OC at R_{eff}~~an optical effective radius~~ of 200 µm. As Hadley and Kirchstetter

(2012) noted, compared with pure 55 μm snow grains, 300 ng g^{-1} of BC contamination and growth of R$_{eff}$ to 110 μm cause a net albedo reduction of 0.11 (from 0.82 to 0.71), causing snow to absorb 61% more solar energy. The difference of snow albedo reductions between SNICAR and SAMDS models increases as BC mixing ratio as well as R$_{eff}$ increases (Figure 9a). However, the snow albedo reduction simulated by SNICAR is not always larger than that by SAMDS when the input contaminant is MD instead of BC (Figure 9b). For example, for R$_{eff}$ of 100 μm, the snow albedo reduction for SAMDS is higher than that for SNICAR at MD mixing ratio < 2600 ng g^{-1}, but lower than that for SNICAR at MD mixing ratio > 2600 ng g^{-1}. The turning point of MD mixing ratio is not constant and depends on the value of R$_{eff}$. The complex difference may be a result of the different input optical properties of MD between SAMDS and SNICAR models (Flanner et al., 2007; Zhang et al., 2016). SAMDS model also considers the effect of OC on snow albedo, which is not included in SNICAR model. The albedo reduction by OC is nonnegligible due to its high loading. As is shown, 5000 ng g^{-1} of OC was found to reduce the snow albedo by 0.016-0.059 depending on the snow grain size (50-800 μm).

~~As Hadley and Kirchstetter (2012) noted, compared with pure 55 μm snow, 300 ng g^{-1} of BC contamination and growth to 110 μm causes a net albedo reduction of 0.11 (from 0.82 to 0.71), causing snow to absorb 61% more solar energy (Hadley and Kirchstetter, 2012).~~

Previous studies have also indicated that the mixing ratio of BC (10-100 ng g^{-1}) in snow may decrease its albedo by 1-5% ~~depending on its aging process~~ (Hadley and Kirchstetter, 2012; Warren and Wiscombe, 1980~~; Hadley and Kirchstetter, 2012~~). Liou et al. (2011) demonstrated that a small BC particle on the order of 1 μm internally mixed with snow grains could effectively reduce visible snow albedo by as

much as 5-10% using a geometric-optics surface-wave approach for the computation of light absorption and scattering by complex and inhomogeneous particles for application to aggregates and snow grains with external and internal mixing structures. They also found that internal mixing of BC in snow reduces snow albedo substantially more than external mixing, and the snow grain shape plays a critical role in snow albedo calculations through its forward scattering strength by modeling the positions of BC internally mixed with different snow grain types (Liou et al., 2014). Figure 11 shows the snow albedo reduction due to three shapes of snow grains (fractal particles, hexagonal plates/columns, and spheres) and the internal/external mixing of BC snow for a solar zenith angle θ of 60⁰ as a function of BC mixing ratios computed by SMDAS model. The top panel of Figure 10a1 illustrates the effect of snow shape (fractal grains, hexagonal plates/columns, and spheres) on the snow albedo reduction at the spectral wavelengths of 400 nm-1400 nm with R_{eff} of 10070 μm simulated by SAMDS model. As is shown, the differences of snow albedo caused by three snow shapes areis remarkable. The snow albedo for spherical snow grains is higher than that for the other two shapes, which is because that, the scattering by spherical snow grains is more in forward direction and less to the sides, resulting in a larger g and a smaller B as discussed in section 2.5. In addition, the snow albedo reduction for aged snow such as spherical snow grains is graduately larger than fresh snow such as fractal snow grains, and hexagonal plates/colums snow grains with the increased BC in snow. It shows that snow albedo by spherical snow grains is typically decreaselower by 0.0175-0.0763 than the fractal snow grains, and by 0.008-0.036 than the, and 0.0087-0.0361 as a function of BC mixing ratios (0-5000 ng g⁻¹), which is comparedthan that with by the fractal snow grains and hexagonal plates/columns snow grains as a function of BC mixing ratios (0-5000 ng g^{-1}). Dang et al. (2016)

35

assessed the effects of snow grain shape on snow albedo using the asymmetry factors g of nonspherical ice crystal developed by Fu (2007). They obtained similar result that the albedo reduction caused by 100 ng g^{-1} of BC for spherical snow grains is larger by 0.007 than nonspherical snow grains with the same area-to-mass ratio for R$_{eff}$ of 100 μm. Figure 10b shows the spectral albedo of snow for the internal/external mixing of BC and snow with R$_{eff}$ of 100 μm for a solar zenith angle θ of 60° as a function of BC mixing ratio. For a given shape (hexagonal plates/columns), we ~~find~~ found that snow albedo as a function of BC mixing ratios calculated from this study decreases as the fraction of the internal mixing increases (Figure 10~~1~~b). In previous studies, the BC mixing ratio~~ss~~ in seasonal snow ~~were~~is up to 3000 ng g^{-1} ~~ppb~~ due to heavy industrial activities across northern China, but the lowest ~~concentrations~~mixing ratios of BC were found in the remote ~~northeast~~northeastern on the border of Siberia, with a median ~~concentration~~value in surface snow of 100 ng g^{-1} ~~ppb~~ (Huang et al., 2011; Wang et al., 2013a, 2014; Ye et al., 2012). As a result, snow albedo by internal mixing of BC and ~~~~snow is lower than external mixing by up to 0.03~~6~~ for 3000 ng g^{-1} ~~ppb~~ BC in snow in the heavy industrial regions across ~~northeast~~northeastern China, whereas by low to 0.00~~5~~4 for 100 ng g^{-1}~~ppb~~ BC in snow in the further north China near the border of Siberia ~~and the northern part Xinjiang province~~. We indicated that the snow grain shape effect on snow albedo ~~reduction~~ between spher~~ical~~e~~s~~ snow grains and fractal ~~particles for~~ snow grains ~~on absorption~~ is relatively larger than the effect of the internal ~~and~~ /external mixing ~~states~~ of BC and~~in~~ snow as a function of the BC ~~concentration~~mixing ratios. However, He et al. (2014) also pointed~~s~~ out that the snow albedo reductions computed by previous models under assorted assumptions vary by a factor of 2 to 5.["]

3.4   Comparison~~s~~ between the observed and modeled snow albedo

Although the snow albedo reduction due to ILAPs has been investigated by model simulations in recent studies (Brandt et al., 2011; Flanner et al., 2007; Hadley and Kirchstetter, 2012; Liou et al., 2011, 2014; Warren and Wiscombe, 1980), we note that there were still limited field campaigns on collecting snow samples and measuring ILAPs in seasonal snow associated with the snow albedo reduction at the middle latitudes in northern hemisphere (Doherty et al., 2010, 2014; Wang et al., 2013a; Ye et al., 2012). In this study, we measured the snow albedo at six sites under clear sky conditions during this snow survey, and the comparison of snow albedo reduction between surface measurements and the SNICAR and SAMDS models based on Toon et al.'s (1989) two-stream radiative transfer solution was investigated in Figure 11. Previous studies have also indicated that the mixing ratio of BC (10-100 ng g^{-1}) in snow may decrease its albedo by 1-5% depending on its aging process (Warren and Wiscombe, 1980; Hadley and Kirchstetter, 2012; Hansen and Nazarenko, 2004). {Warren, 1985 #2053}

Figure 121 compares snow albedo values under clear sky conditions collected through surface measurements and the SNICAR and SAMDS models based on Toon et al.'s (1989) two-stream radiative transfer solution. The model input parameters including θ, R_m, R_{eff}, and the mixing ratios of BC (C_{BC}^{est}), MD (C_{MD}) and OC (C_{OC}) were also are listeddisplayed in Figure 11 in Tables 1 and 4. The MAC of BC used in the ISSW iswas 6.3 m^2 g^{-1} at 550 nm, although a value of 7.5 iswas used in the SNICAR and SAMDS models. Thus, the mixing ratiovalue of BC C_{BC}^{est} was was corrected by dividing it by 1.19 (see Figure 11) when BC was used as the input parameter to the snow albedo models (Wang et al., 2013a). The snow albedos measured at 550 nm varied considerably from 0.99 to 0.61 owing due to different mixing ratios of ILAPs and snow parameters, such as snow grain size. The snow albedos predicted by the

37

SNICAR and SAMDS models agreed well at each site based on the same input parameters. The snow albedos of the SNICAR and SAMDS models retrieved ~~from~~ with ~~measured snow grain sizes~~R_m complemented the surface measurements for lower ~~mixing ratios~~values of C_{BC}^{est} ~~BC~~, C_{MD} ~~OC~~, and ~~AD~~C_{OC} (Figure 11a-d)~~MD~~. The highest C_{BC}^{est} ~~BC~~ values ~~mixing ratios~~ were ~~1461~~1500 ng g^{-1} (corrected value of 1200 ng g^{-1}) and ~~3651~~3700 ng g^{-1} (corrected value of 3100 ng g^{-1})~~ng g^{-1}~~ at sites 98 and 101, respectively, across industrial regions~~, with median values found in integrated layers of 264 and 1635 ng g^{-1}, respectively~~. The OC and ~~dust~~MD mixing ratios were as high as ~~3200~~13.3 ~~µg~~ng g^{-1} and ~~32~~3900 ~~µg~~ng g^{-1} in this region. There, ~~The higher AD~~MD mixing ratios ~~are consistent with previous studies conducted by Zhang et al. (2013) and Huang et al. (2015a), who indicated that AD~~MD is highly correlated with anthropogenic air pollution originating from human activity across northeastern China. Thus, w~~we found a larger difference in snow albedo of up to 0.2 at higher C_{BC}^{est}, C_{MD}, and C_{OC}~~BC, OC, and AD~~MD values~~contents~~ between the surface measurements and the modeled albedos by both SAMDS and SNICAR models ~~for~~with ~~the measured snow grain sizes~~the input of R_m (red and blue solid lines in Figure 11e-f)~~ at sites 91, 98, and 101~~. When the snow albedo ~~reduction in albedo caused by ILAP~~slight-absorbing impurities at the inferred wavelength simulated by ~~by~~using R_m~~measured snow grain size~~ was not accounted for, we also calculated the snow albedos ~~from~~by the SAMDS and SNICAR~~SNICAR and SAMDS~~ models by using ~~the optical effective size~~R_{eff} as shown in Figure 12~~11~~ (light red and blue~~blue and red~~ shaded bands)~~, and~~. Results showed that, compared with the snow albedos simulated by using R_m~~,~~ these values were more approximate to the surface measurements~~consistent with~~, especially at near-infrared wavelengths, although still a slight higher than the surface measurements (gray shaded bands)~~, especially at~~

near-infrared wavelengths. This may be attributed to the fact that the R_{eff} optical effective size at these three two sampling sites was much larger than R_m the measured grain size. We innovatively suppose , indicating that, for the same snow grains, the radiative perturbation of ILAPs light-absorbing impurities was are amplified able to

5   enhance with the R_{eff} in spite of the same R_m snow grain optical effective size. Nevertheless, due to the limited measurements of snow albedo, this supposition is quite uncertain and needed to be verified by numerous field measured snow albedos. As indicated in Figure 1 Combinations of the results of Figure 9 and Figure 112 1, that BC, OC, and A D MD are three types of ILAPs found in snow that can reduce spectral

10   snow albedo levels and. r Reduced snow albedo due to ILAPs in our measurements were generally comparable to the modeled effects that found in the commonly used SAMDS SNICAR and commonly used SNICAR SAMDS models (Flanner et al., 2007; Zhang et al., 2016) when the mixing ratios of ILAPs are not quite high. , Therefore we indicate that, 100-500 ng g^{-1} of BC can lower the snow albedo by

15   0.014 2-0.039 6% relative to pure snow with a snow grain size of 1 2 00 μm according to our snow field campaign, and A D MD was found to be a weak absorber owing due to its lower A D MD MAC, supporting previous observations made by Warren and Wiscombe (1980). The OC MAC is was also lower and comparable to that of the A D MD. A clear decreasing trend in the surface snow albedo owing due to the high

20   ambient mixing ratios of OC from Inner Mongolia to northeastern China was found. The radiative transfer modeling results presented by Zhang et al. (2016) and measurement results of this study show that the spectral albedo of snow reduction due to the increased OC mixing ratios concentration (above 20 μg g^{-1}) is larger for a factor of 3 by assuming the snow grain size of 800 μm compared to 100 μm.

25   **4   The radiative transfer modeling results presented by Zhang et al. (2016) and**

measurement results of this study show that the spectral albedo of snow reduction caused OC levels (above 20 μg g⁻¹) to increase by a factor of 3 for a snow grain size of 800 μm compared to 100 μm.

~~Discussion and c~~Conclusions

In this study, a snow survey was performed in January 2014, and 92 snow samples were collected at 13 sites across northern China. We found that higher AODs measured using a sun photometer and remote sensing devices showed that heavily polluted areas remain in industrial regions across northern China. The measured C_{BC}^{est} ~~C_{BC}^{est}~~ through the 2014 survey via the ISSW spectrophotometer in surface and average snow of 50~~3~~ to 36~~51~~700 and 60~~2~~ to 16~~3~~500 ng g⁻¹, with the medium values of 260 ng g⁻¹, and 260 ng g⁻¹, respectively, were much larger than those of previous snow field campaigns. The ~~n~~chemical composition analysis~~on BC fraction~~ showed that the mass contributions~~ILAPs~~ in seasonal snow ~~were~~was dominated by OC and MD. However, assuming the MACs for BC, OC, and Fe are 6.3, 0.3, and 0.9 m² g⁻¹~~Assumption of BC and OC mass absorption efficiencies are 6.3 and 0.3 m² g⁻¹~~, respectively, at 550 nm, light absorption was still dominated by BC and OC in seasonal snow during the entire campaign. The light-absorbing contribution ~~fraction~~ of the MD ~~mixing ratios~~ was larger at high latitudes than at low latitudes due to strong winds transporting snow. Then, ~~–~~

~~In this study, a Chinese survey was performed in January 2014. We collected 92 snow samples from 13 sites across northern China. Much less snow had fallen than in previous years; as a result, most of the surface snow samples were collected as aged snow, and snow grain sizes were much larger owing to solar radiation absorbed by ILAPs as a result of settlement processes. Although we selected study locations in~~

~~remote regions located at least 50 km from cities, higher AODs measured using a sun photometer and remote sensing devices showed that heavily polluted areas remain in industrial regions across northern China. The estimated BC mixing ratios measured through the 2014 survey via the ISSW spectrophotometer in surface and average integrated snow of 53 to 3651 and 62 to 1635 ng g^{-1}, respectively, were much larger than those of previous snow field campaigns. The non-BC fraction showed that most of the ILAPs in seasonal snow were dominated by OC and AD. Owing to BC and OC mass absorption efficiencies of 6.3 and 0.3 m^2 g^{-1}, respectively, at 550 nm, light absorption was still dominated by BC and OC in seasonal snow during the entire campaign. AD contributions in snow to light absorption amounted to less than 10%. The large OC/BC ratios and correlation coefficients indicated that these contributions were mainly derived from common sources (e.g., biomass burning). Similarly, NH$_4^+$ was attributed to intense agricultural activity compared to industrial emissions of SO$_4^{2-}$ and NO$_3^-$.~~

~~The fraction of the AD mixing ratios was larger at high latitudes than at low latitudes owing to strong winds transporting snow.~~ ~~In this study,~~ we indicated that the~~present a~~ new spectral snow albedo model (SAMDS) ~~for simulating the surface albedo of snow with deposited ILAPs~~aerosol impurities (e.g. Black carbon, Organic carbon, Mineral dust, volcano ash, and snow algae) by using the asymptotic analytical radiative transfer theory. Given the measured BC, MD and OC mixing ratios of 100-5000 ng g^{-1}, 2000-6000 ng g^{-1}, and 1000-30000 ng g^{-1} in surface snow across northeastern China, we ran the models at a solar zenith angle θ of 60°, and the results indicated that the albedo of fresh snow at 550 nm is generally in a range of 0.95-0.75 with R$_{eff}$ of 100 μm. This model~~ can ~~also~~ be used to investigate the snow albedo influenced by the internal/external mixing of BC and snow~~with impurities~~, irregular morphology of

snow grains and impurities , aging processes of snow grains and soot aggregates, and the vertical distribution of snow grains and impurities for multilayer snow. Additionally, the properties of different snow grain shapes (Fractal particles, Hexagonal plate/column, and spheres) and the internal/external mixing with BC in snow by using SAMDS model might be useful to researchers who are conducting studies involving ILAPs and snow interaction and feed back in snow albedo reduciton. Compare to the SNICAR model, the snow albedo reduction is in agreement with the SAMDS model, different types of impurity could be included in the parameterization in SAMDS model, such as organic carbon and biogenic particles. For instance, the a given shape (spheres, hexagonal plates/columns, and fractal particles), it shows that snow albedo for spherical snow grains is typically lower by 0.017-0.073, and 0.008-0.036 than that for the fractal snow grains and hexagonal plates/columns snow grains as a function of BC mixing ratios (0-5000 ng g^{-1}) with R_{eff} of 100 μm. it shows that snow albedo by spherical snow grains typically decrease by 0.017-0.073, and 0.008-0.036 as a function of BC mixing ratios (0-5000 ng g^{-1}), which is compared with the fractal snow grains and hexagonal plates/columns snow grains. The internal mixing of BC and snow absorbs substantially more light than external mixing subsequently. For fresh snow grains of hexagonal plates/columns with R_{eff} of 100 μm, the difference of snow albedo between internal and external mixing of BC and snow is up to 0.036 for 3000 ng g^{-1} BC in snow in the heavy industrial regions across northeastern China, whereas by low to 0.005 for 100 ng g^{-1} BC in snow in the further north China near the border of Siberia. The spectral albedo of snow reduction caused by OC (20 μg g^{-1}) is larger by up to a factor of 3 for a snow grain size of 800 μm compared to 100 μm by using SAMDS model.

~~Then, OC emitted from biomass burning and SO$_4$$^{2-}$ and NO$_3$$^-$ generated from fossil fuels and biofuels also played key roles in the mixing ratios of chemical components in seasonal snow. Finally, a~~Aa comparison between measured and simulated snow albedos was conducted. ~~Generally, t~~Tthe snow albedos measured from a spectroradiometer and simulated using the SNICAR and SAMDS models agreed well ~~with~~ at the lower mixing ratios of BC, ~~OC~~MD, and ~~AD~~MDOC. However, a large discrepancy in snow albedo ~~levels~~ between the model simulations and surface measurements for heavy loading of ILAPs in snow was found by using ~~the measured snow grain radii~~R$_m$. We demonstrate that the simulated snow albedo reduction by SMDAS and SNICAR models is significantly enhanced by using R$_{eff}$ of snow grains compared with R$_m$, especially in the case of near-infrared wavelengths.~~Instead of the optical effective snow grains in snow~~Based on the snow grain optical effective size, we found ~~good~~ a remarkable improvement of the snow albedo reduction ~~agreement between surface measurements and radiative transfer models. Therefore, the snow grain optical effective size is preferred~~ to present the snow albedo reduction ~~when measurements on snow grain size are available at the near-infrared wavelength.~~

Although the MAC of OC is~~was~~ much lower than that of BC, we found that OC ~~was~~ was a major absorber in snow ~~owing~~ due to its high mixing ratio~~of OC~~ from human activities occurring across northeastern China. Moreover, 5000 ng g^{-1} of OC was found to reduce the snow albedo by ~~1.5%-5%~~0.016-0.059 depending on the snow grain size and aging period. Therefore, we suggest that the mixing ratio of OC should be added as an input parameter to the SNICAR model for determining snow albedos.

Although the SAMDS model might be useful to researchers who are conducting studies involving ILAPs and snow interaction and feedback in snow albedo change,~~Although the SAMDS model can be used to study the snow albedo reduction~~

for dirty snow due to ILAPs, and multiple internal/external mixing stats of BC associated with irregular snow grains, we indicate that further snow surveys across northern China should be performed for the following reasons:. First(1), large variations of ILAPs in seasonal snow across northern China can lead higher uncertainties of snow albedo reduction, especially in the industrial regions,. and (2)Second, we only measured the snow albedo at 6 sampling sites by using the spectroradiometer in the clear sky condition due to much less snow fallen in January 2014 than that in previous years. Comparinge model simulations with the observations, we found that $R_{eff}$the optical effective snow grains could seemingly be enhanced by the high concentrationsmixing ratios of ILAPs in snow, however, we note that further snow surveys on measuring snow albedo should be conducted to reveal this phenomenon. Finally, there are large uncertainties in affectingsimulating snow albedo reduction and radiative forcing due to the ILAPs mixed with snow/ice and the irregular morphology of snow grains, the potential snow albedo reductionchange for aged snow should be investigated in the following snow surveys accordingly to test the capability of SAMDS model, which will provide more valuable and useful information for the climate models.

5

Table 1. Statistics in on seasonal snow variables measured using an ISSW in the study sites. All of the datasets are the average values from the left and right snow samples. The site numbers beginning at 90 in this study are numbered in chronological order followed by Wang et al. (2013a), and Ye et al. (2012).

Site	Layer	Latitude N	Longitude E	Snow type	Site average snow depth (cm)	Sample depth (cm) Top	Bottom	Temperature (°C)	Snow density (g cm^{-3})	R_m (mm)	C_{BC}^{equiv} (ng g^{-1})	C_{BC}^{max} (ng g^{-1})	C_{BC}^{est} (ng g^{-1})	f_{non-BC}^{est} (%)	$\mathring{A}_{tot}$ 450:600 nm
90	1	45°02'44"	116°22'45"	Aged	3	0	5	-14	0.38	0.15	860	530	330 (-, 470)	61 (45, 110)	3.8
91	1	50°02'48"	124°22'41"	Fresh	8	0	5	-25	0.23	0.08	250	200	160 (110, 200)	35 (18, 55)	2.1
	2			Aged		5	10	-25	0.18	0.15	--	--	--	--	--
92	1	50°39'07"	122°23'53"	Fresh	14	0	5	-16	0.17	0.08	80	70	50 (30, 70)	34 (15, 60)	2.3
	2			Aged		5	10	-16	0.18	1.25	110	100	80 (50, 100)	29 (11, 55)	2.2
93	1	50°24'50"	124°54'20"	Fresh	8	0	1	--	--	0.07	170	100	70 (40, 90)	53 (39, 73)	2.5
	2			Aged		2	6	-21	0.21	0.175	310	140	100 (50, 130)	68 (59, 85)	2.7
94	1	50°09'05"	125°46'06"	Fresh	8	0	1	-24	--	0.1	1200	400	260 (110, 360)	78 (69, 91)	2.8
95	1	50°54'43"	127°04'50"	Aged	18	0	3	-22	0.23	0.175	280	110	80 (40, 100)	73 (64, 86)	2.6
	2			Aged		3	8	-23	0.18	0.9	230	80	50 (30, 70)	77 (68, 89)	2.7
	3			Aged		8	13	-25	0.27	1	90	50	30 (10, 40)	71 (55, 92)	3.2
	4			Aged		13	18	-25	0.14	1.3	520	310	130 (-, 240)	75 (54, 148)	4.8
96	1	49°14'21"	129°43'13"	Fresh	13	0	5	-22	0.37	0.08	1300	390	240 (20, 330)	83 (76, 99)	3.4
	2			Aged		5	10	-23	0.25	0.6	230	90	50 (10, 70)	81 (69, 98)	3.3
	3			Aged		10	15	-22	0.22	1	370	130	80 (30, 110)	80 (71, 93)	3.0
97	1	47°39'18"	131°13'10"	Aged	20	0	5	-22	0.36	0.2	1000	360	240 (90, 310)	76 (69, 91)	2.8
	2			Aged		5	10	-18	0.27	1.1	160	80	50 (20, 70)	71 (57, 91)	3.0

Site	Layer	Latitude N	Longitude E	Snow type	Site average snow depth (cm)	Sample depth (cm) Top	Bottom	Temperature (°C)	Snow density (g cm⁻³)	R_m (mm)	C_{BC}^{equiv} (ng g⁻¹)	C_{BC}^{max} (ng g⁻¹)	C_{BC}^{est} (ng g⁻¹)	f_{non-BC}^{est} (%)	$Å_{tot}$ 450:600 nm
	3			Aged		10	15	-14	0.32	0.9	30	20	10 (5, 20)	74 (44, 90)	3.1
98	1	45°25'38"	130°58'55"	Fresh	35	0	5	-20	0.22	0.09	2200	2100	1500 (750, 1800)	32 (16, 65)	2.5
	2			Aged		5	10	-23	0.24	0.5	640	350	240 (120, 310)	58 (46, 79)	2.6
	3			Aged		10	15	-15	0.24	0.75		60	20 (10, 50)	74 (52, 90)	3.1
	4			Aged		15	20	-14	0.26	0.75	60	40	20 (10, 30)	75 (48, 89)	3.1
	5			Aged		20	25	-13	0.28	1.1	430	260	170 (60, 220)	62 (49, 86)	2.8
	6			Aged		25	30	-11	0.29	1.3	350	170	110 (70, 150)	68 (58, 81)	2.5
	7			Aged		30	35	--	0.33	1.3	290	120	70 (40, 100)	75 (65, 87)	2.6
99	1	43°36'10"	125°42'04"	Fresh	13	0	5	-2	0.18	0.085	1500	920	640 (240, 820)	54 (40, 84)	2.8
	2			Aged		5	12	-3	0.23	1.1	5800	3800	2900 (1500, 3600)	51 (39, 74)	2.5
	3			Aged		12	18	-4	0.28	1.1	2800	1400	1100 (630, 1300)	62 (53, 77)	2.3
	4			Aged		18	24	-4	0.28	0.7	2000	1500	1100 (540, 1400)	46 (32, 73)	2.6
100	1	43°30'45"	127°15'34"	Fresh	18	0	2.5	--	0.14	0.075	1700	700	510 (250, 650)	71 (63, 86)	2.6
	2			Aged		2.5	4	-2	0.18	0.25	4100	2900	1700 (–, 2400)	58 (43, 103)	3.6
	3			Aged		4	9	-2	0.23	0.9	1100	560	410 (210, 530)	60 (49, 80)	2.6
	4			Aged		9	15	-3	0.24	0.8	1600	730	540 (270, 690)	66 (57, 83)	2.6
101	1	43°47'25"	125°46'08"	Fresh	22	0	5	-19	0.24	0.07	5600	5100	3700 (1300, 4600)	35 (18, 76)	2.9
	2			Aged		5	10	-17	0.24	0.9	4300	3800	2600 (880, 3300)	40 (24, 79)	2.9
	3			Aged		10	15	-15	0.23	1.1	660	390	310 (210, 390)	46 (33, 63)	2.1
	4			Aged		15	20	-14	0.28	1.3	300	250	190 (110, 240)	39 (21, 67)	2.5
102	1	42°12'34"	126°37'50"	Fresh	46	0	3	-8	0.13	0.07	2100	1700	1400 (810, 1800)	37 (19, 61)	2.3
	2			Aged		3	8	-8	0.26	0.1	590	380	280 (150, 370)	53 (37, 75)	2.6
	3			Aged		8	13	-8	0.24	0.3	2500	2100	1600 (430, 2100)	35 (15, 81)	3.1

Site	Layer	Latitude N	Longitude E	Snow type	Site average snow depth (cm)	Sample depth Top (cm)	Sample depth Bottom (cm)	Temperature (°C)	Snow density (g cm⁻³)	R_m (mm)	C_{BC}^{equiv} (ng g⁻¹)	C_{BC}^{max} (ng g⁻¹)	C_{BC}^{est} (ng g⁻¹)	f_{non-BC}^{est} (%)	$Å_{tot}$ 450:600 nm
	4			Aged		13	18	-8	0.28	0.6	1900	1100	770 (230, 1000)	60 (48, 88)	3.0
	5	45°02'44"	116°22'45"	Aged		18	23	-7	0.32	1	1100	930	450 (200, 520)	60 (47, 82)	2.7
	6			Aged		23	28	-6	0.27	1.2	1500	1300	900 (300, 1200)	38 (21, 80)	2.9
	7	50°02'48"	124°22'41"	Aged		28	33	-5	0.26	1.2	860	490	340 (130, 400)	66 (53, 87)	2.9
	8			Aged		33	38	-5	0.3	1	430	200	110 (30, 160)	74 (61, 95)	3.2
	2	50°39'07"	122°23'53"	Aged		38	43	-4	0.29	0.8	520	250	160 (70, 230)	71 (58, 87)	2.8

49

ID	No	Lat	Long											
93	1	50°24'50"	124°54'20"	8	5	40	41	0.18	1.25	108	97	77(49,97)	29(11,55)	2.2
	2				0	4	–	–	0.07	172	97	70(39,90)	53(39,73)	2.5
94	1	50°00'05"	125°46'06"	8	2	6	21	0.21	0.175	313	136	100(46,128)	68(50,85)	2.7
	2				0	4	24	–	0.1	1173	404	260(108,363)	78(69,91)	2.8
95	1	50°54'43"	127°04'50"	41	0	3	22	0.23	0.175	278	110	75(37,100)	73(64,86)	2.6
	2				3	8	23	0.18	0.9	230	83	54(25,73)	77(68,89)	2.7
	3				8	41	25	0.27	1	61	50	27(7,40)	71(55,92)	3.2
	4				41	18	25	0.44	1.3	524	308	131(–,237)	75(54,148)	4.8
96	1	49°47'41"	126°43'13"	41	0	5	22	0.37	0.08	1340	385	241(21,332)	83(76,99)	3.4
	2				5	41	23	0.55	0.6	234	58	45(6,74)	81(60,98)	3.3
	3				41	41	22	0.22	1	371	126	78(26,144)	80(71,93)	3.0
97	1	47°39'18"	131°13'0"	20	0	5	22	0.36	0.2	1005	362	236(93,306)	76(60,91)	2.8
	2				5	41	18	0.27	1.1	160	79	45(15,65)	46(15,65)	3.0
	3				41	40	44	0.32	0.9	32	23	9(3,18)	74(44,90)	3.1
98	1	45°25'38"	130°58'55"	35	0	15	20	0.22	0.09	2154	2080	1461(754,1818)	32(16,65)	2.5
	2				5	5	23	0.24	0.5	641	349	241(123,307)	58(46,79)	2.6
	3				41	41	44	0.24	0.75	97	55	25(10,45)	74(52,90)	3.4
	4				0	41	44	0.26	0.75	61	36	16(7,31)	75(48,86)	3.4
	5				5	20	41	0.28	1.1	432	264	166(62,221)	62(49,86)	2.8
	6				20	25	41	0.59	1.3	848	465	117(66,148)	68(58,81)	2.5
	7				25	30	41	0.33	1.3	288	418	72(37,104)	75(65,87)	
99	1	43°36'01"	125°42'04"	41	30	35	–	0.18	0.085	1459	922	636(235,823)	54(40,84)	2.5
	2				0	5	2	0.23	1.1	5847	3778	2882(1549,3559)	51(39,74)	2.3
	3				5	12	3	0.28	1.1	2795	1360	1059(630,1306)	62(53,77)	2.6
	4				12	18	4	0.28	0.7	2027	1518	1105(537,1384)	46(32,73)	

100	1	43°30'45"	127°15'34"	18	0	2.5	1	0.14	0.075	1739	703	508 (250, 651)	71 (63, 98)	2.6
	2				2.5	4	2	0.18	0.25	4126	2891	1729 (—, 2371)	58 (43, 103)	3.6
	3				4	6	2	0.23	0.9	1092	564	414 (208, 529)	60 (49, 80)	2.6
	4				6	15	3	0.24	0.8	1601	728	541 (266, 691)	66 (57, 83)	2.6
101	1	43°47'25"	125°46'08"	22	0	5	14	0.24	0.07	5634	5070	3651 (1333, 4644)	35 (18, 76)	2.7
	2				5	10	11	0.24	0.9	4318	3826	2575 (882, 3284)	40 (24, 79)	2.9
	3				10	15	15	0.23	1.1	657	389	313 (206, 386)	46 (33, 63)	3.4
	4				15	20	14	0.38	1.3	297	254	188 (108, 239)	39 (21, 67)	3.5
102	1	42°12'34"	126°37'50"	46	0	3	8	0.14	0.07	2109	1421	1357 (808, 1755)	37 (19, 61)	3.3
	2				3	8	8	0.36	0.1	594	377	279 (149, 371)	53 (37, 75)	2.6
	3				8	13	8	0.24	0.3	2513	2088	1623 (425, 2120)	35 (15, 81)	3.1
	4				13	18	8	0.38	0.6	1022	1073	773 (229, 1013)	60 (48, 88)	3.6
	5				18	23	7	0.32	1	1112	629	450 (197, 590)	60 (47, 82)	2.7
	6				23	28	6	0.27	1.2	1466	1281	903 (300, 1167)	38 (21, 80)	2.9
	7				28	33	5	0.26	1.2	858	493	344 (133, 457)	66 (53, 87)	2.9
	8				33	38	5	0.3	1	426	197	109 (27, 163)	74 (61, 95)	3.2
	9				38	43	4	0.29	0.8	524	245	157 (67, 220)	71 (58, 87)	2.8

Table 2. Estimates of integrated snowpack BC content in seasonal snow in the study sites for 2010 and 2014. (change as surface and average BC)

Site	Date sampled (2014)		Snowpack average Integrated BC (ng g^{-1})
90	10 Jan		334
91	13 Jan		161
92	14 Jan		65
93	15 Jan		94
94	15 Jan		260
95	16 Jan		62
96	17 Jan		140
97	18 Jan		105
98	19 Jan		264
99	23 Jan		1507
100	24 Jan		592
101	26 Jan		1635
102	27 Jan		583

		53

Table 23. Chemical species (ng g^{-1}) in surface snow for sites across northeastern China in January 2014. The datasets of SO_4^{2-}, NO_3^-, and NH_4^+ were reprinted fromoriginated from Wang et al. (2015).

Site	ADMD	BC	OC	K$^+_{biosmoke}$	SO$_4^{2-}$	NO$_3^-$	NH$_4^+$	Sea salt
90	1900	380	6700	327	1685	213	22	868
91	1700	180	590	179	853	465	36	827
92	1300	60	280	150	511	105	19	456
93	1700	80	450	213	718	387	90	960
94	3300	300	2700	118	1335	550	28	554
95	2000	90	600	164	587	523	39	669
96	2300	280	3900	309	1285	493	91	1227
97	2400	280	2400	173	1163	407	38	753
98	3900	1600	13300	633	3096	747	195	2516
99	3000	770	4700	372	3379	1492	155	2310
100	3800	570	4000	260	4237	2258	487	2195
101	3500	4200	32000	1337	12382	2364	–	5131
102	5800	1700	2400	488	8034	3631	769	4420

Table 4. Measured and calculated snow grain sizes for sites in northeastern China in January 2014.

Site	Measured Snow grain radius (μm)	Calculated R$_{eff}$ using SAMDS (μm)	Calculated R$_{eff}$ using SNICAR (μm)
90	150	203-236	168-197
91	80	178-220	148-183
93	70	73-80	60-65
95	175	148-188	123-156
98	90	248-302	209-259
101	70	362-446	312-390
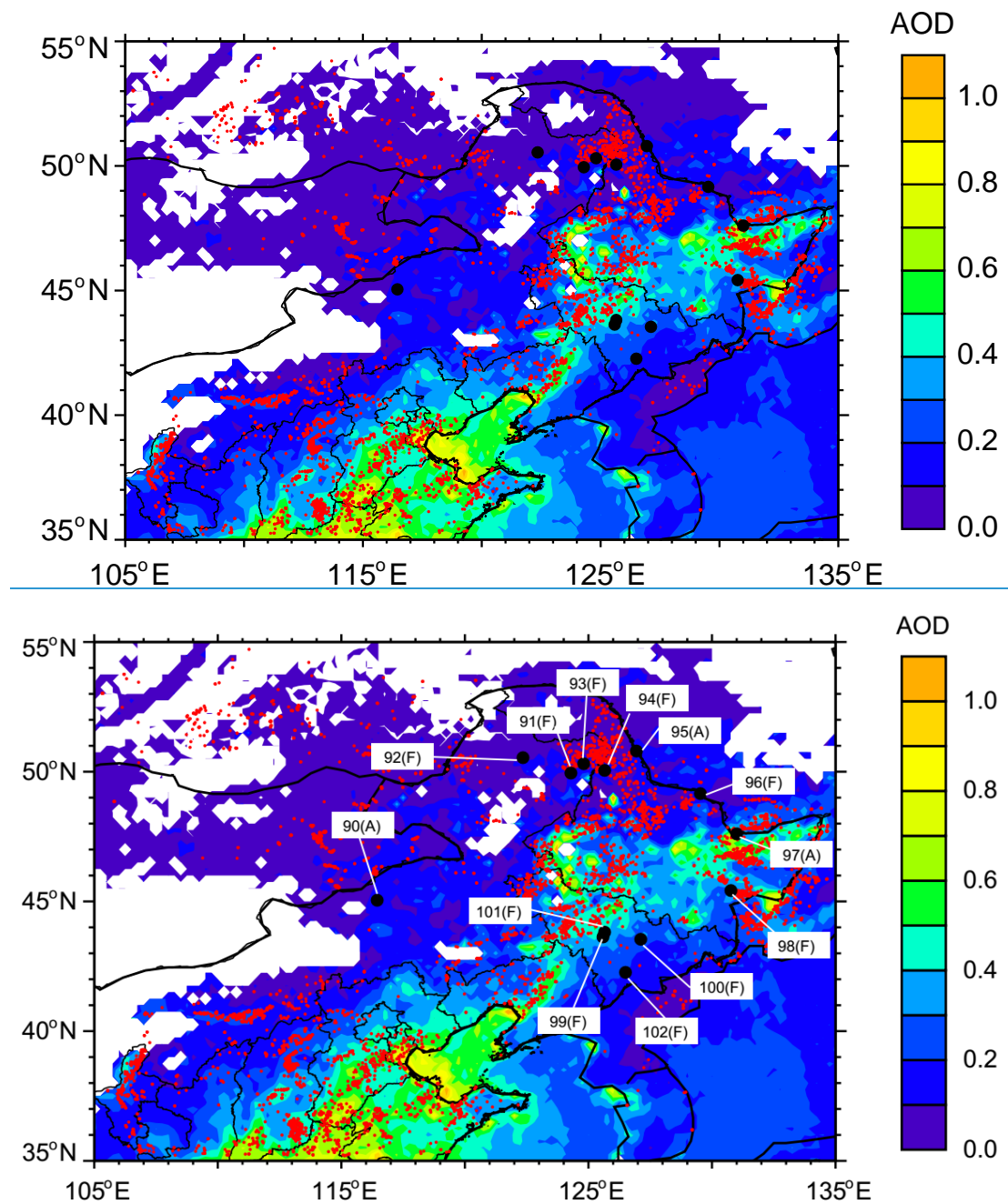
Fig. 1. Spatial distribution of the averaged AOD retrieved from Aqua-MODIS over northern China from October 2013 to January 2014.; Tthe red regions dots are MODIS active fire locations,; the black dots are the sampling locations. The site

55

numbers beginning at 90 in this study are numbered in chronological order followed by Wang et al. (2013a), and Ye et al. (2012). The "A" and "F" refer to aged snow and fresh snow, respectively.
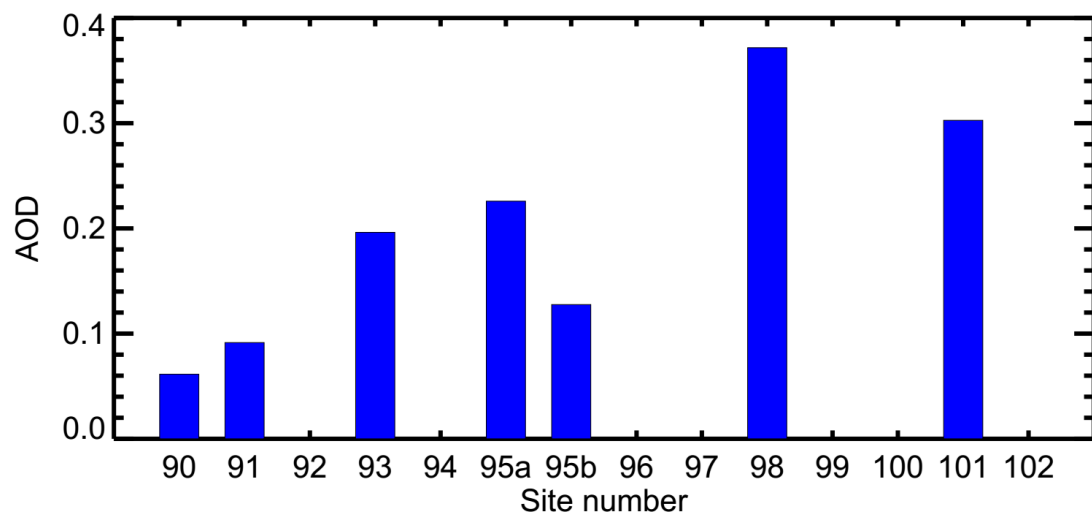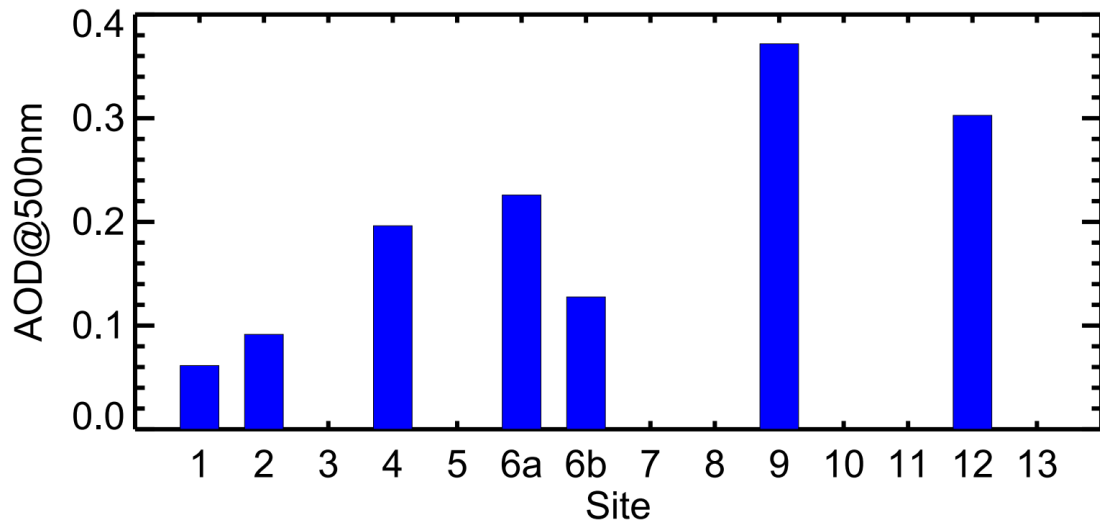
Fig. 2. The variation in AOD at 500 nm at different sites measured using a Microtops Π Sun photometer over northeastern China in January 2014.

Temperature (°C)   Snow density (g cm⁻³)   Snow grain radius (mm)

Temperature (°C)   Snow density (g cm⁻³)   Rm (mm)
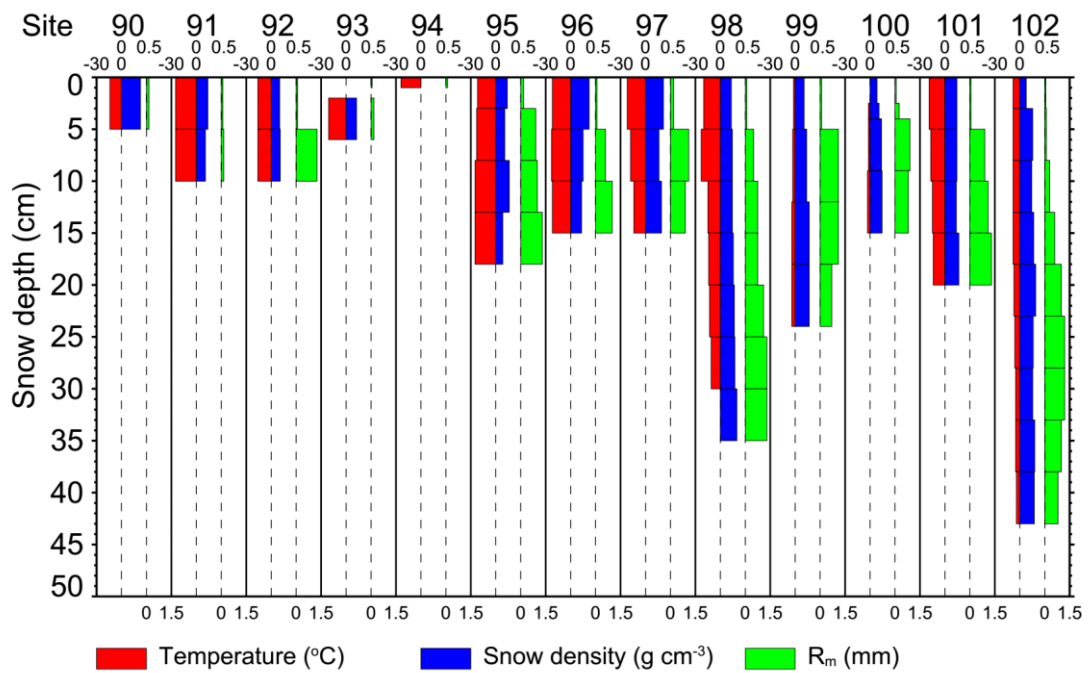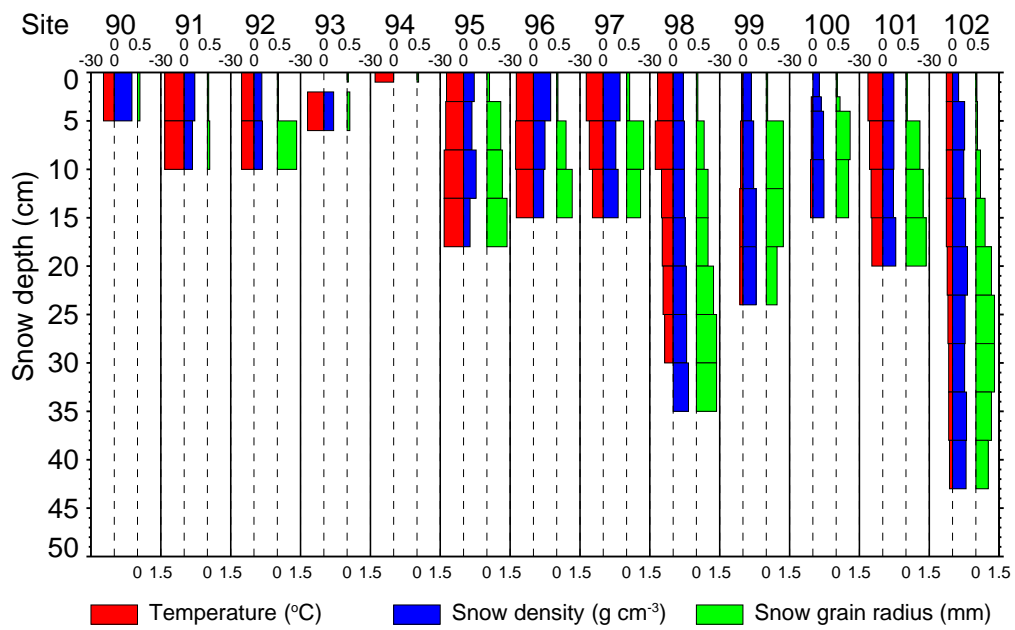
Fig. 3. Vertical temperature, snow density, and measured snow grain radius (R_m) profiles at each site during the 2014 Chinese snow survey.
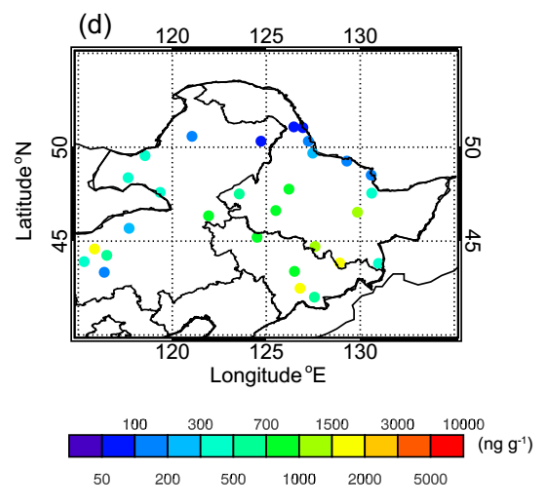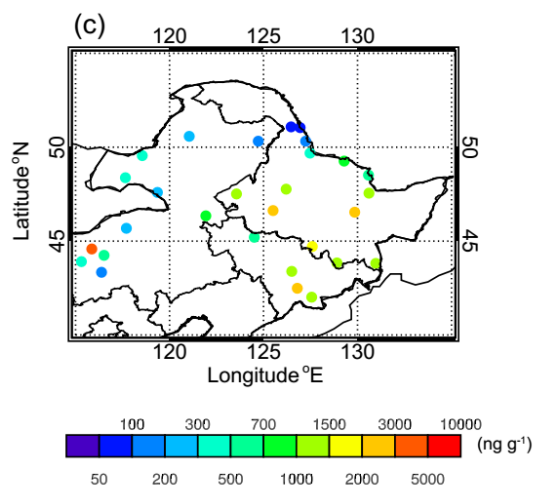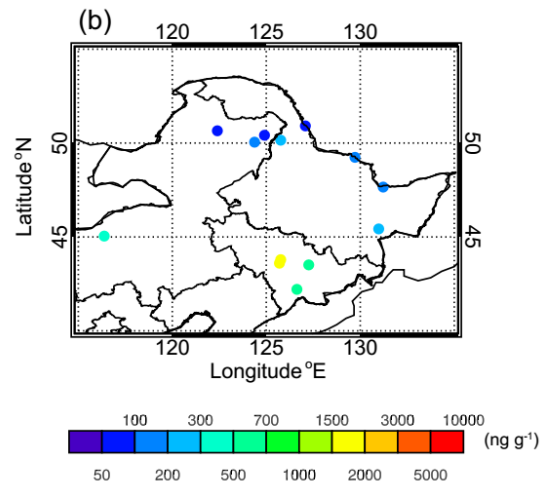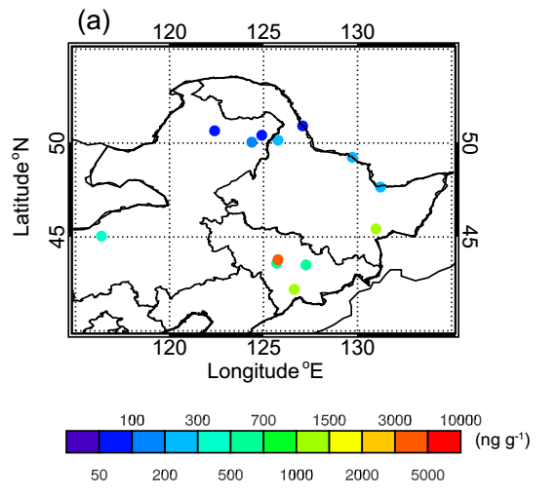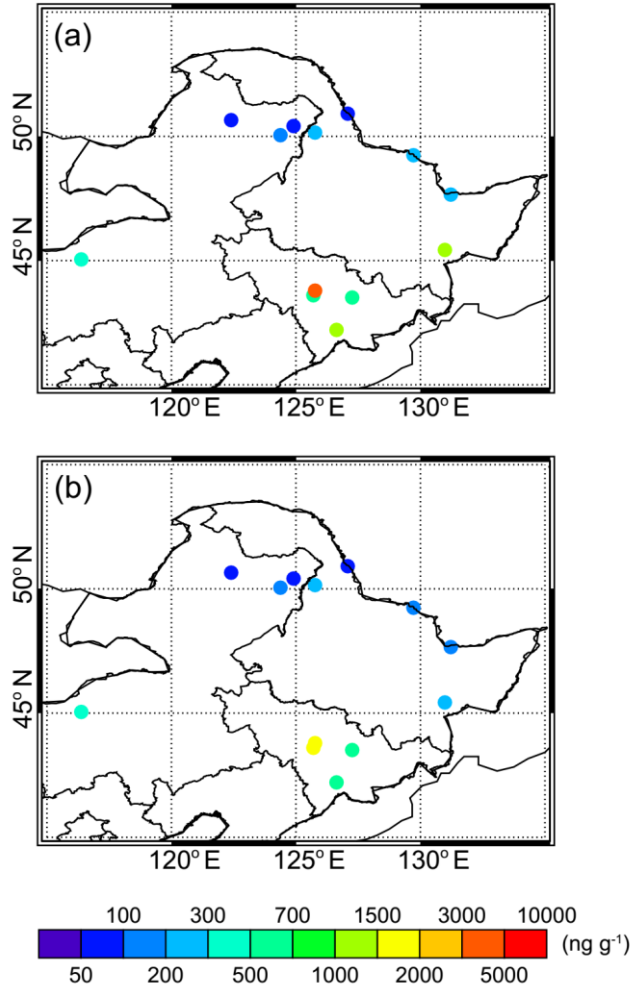
Fig. 4. The spatial distribution of C_{BC}^{est} in the (a) surface and (b) average snow ~~Surface (a, c) and averaged and integrated (b, d) BC content in seasonal snow~~ in 2014 ~~and 2010~~ across north~~east~~ern China.
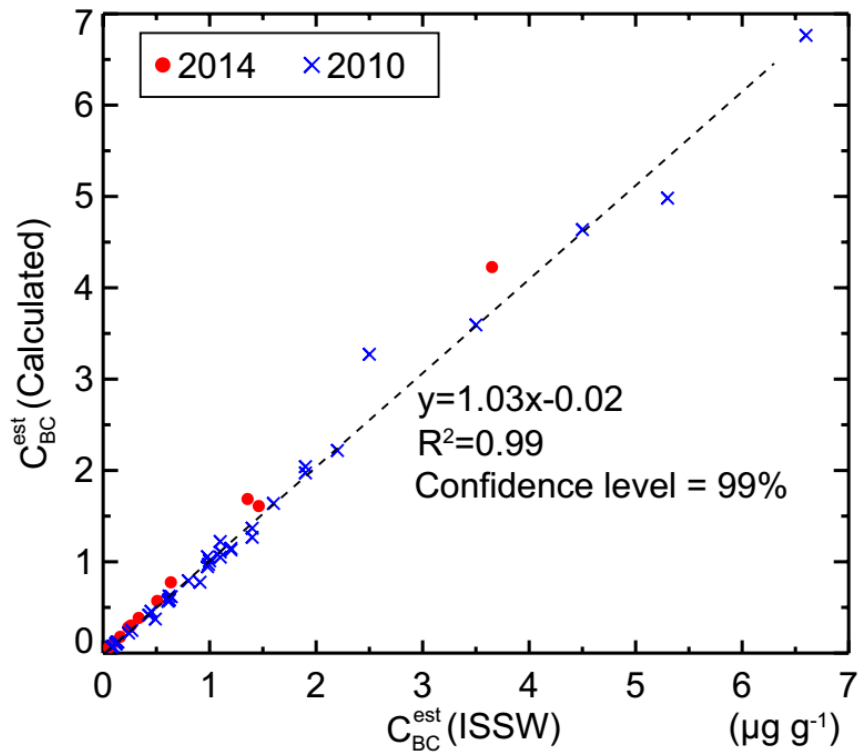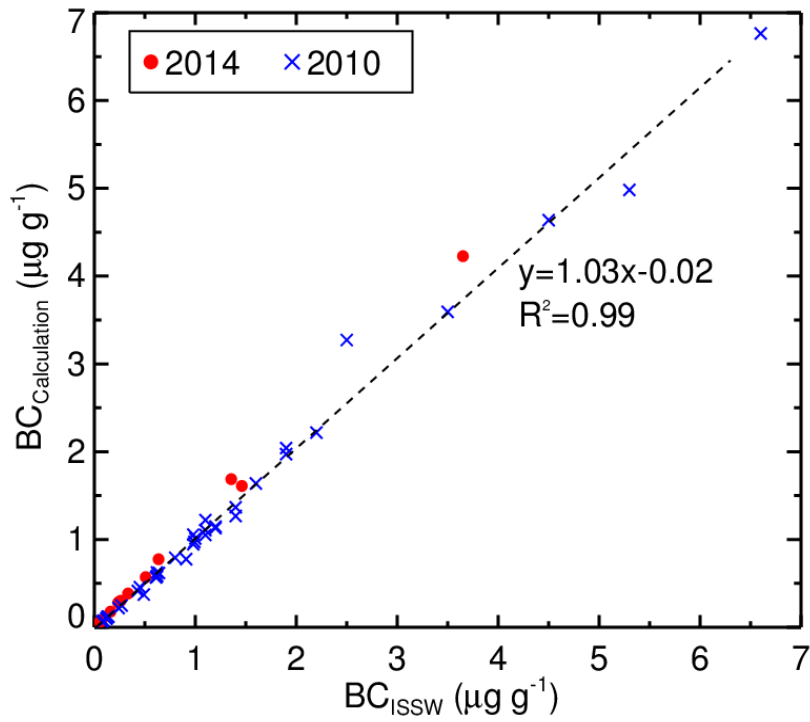
Fig. 5. Comparisons between the calculated and optically measured C_{BC}^{est} ~~BC contents~~ in surface snow <ins>during 2010 and 2014 snow surveys</ins>~~in January 2014~~. <ins>The datasets of</ins>

measured C_{BC}^{est} in 2010 from sites 3-40 were reprinted from Wang et al. (2013a). ~~The datasets in 2010 were originated from sites 3-40 in Wang et al. (2013).~~

Fig. 6. Ratios of OC and BC, NH_4^+ and SO_4^{2-}, NH_4^+ and NO_3^-, and K^+ and Al in surface snow in January 2014.

Composition (%)
- AD
- BC
- OC
- K⁺$_{biosmoke}$
- SO_4^{2-}
- NO_3^-
- NH_4^+
- Seasalt

0 Water	5 Mixed Forest	10 Grasslands	15 Snow and Ice
1 Evergreen Needleleaf	6 Closed Shrublands	11 Permanent Wetlands	16 Bare orsparesly vegetate
2 Evergreen Broadleaf	7 Open Shrublands	12 Croplands	254 Unclassified
3 Deciduous Needleleaf	8 Woody Savannas	13 Urban and Built-up	
4 Deciduous Broadleaf	9 Savannas	14 Cropland Mosaics	

Fig. 67. The major components include ~~AD~~MD, BC, OC, $K^+_{Biosmoke}$ ~~biomass smoke potassium~~, secondary ~~aerosol~~ ions (SO_4^{2-}, NO_3^-, and NH_4^+ ~~sulfate, nitrate, and ammonium~~), and sea salt in the surface snow samples collected in January 2014. The distribution of 17 different surface vegetation types retrieved from MODIS global land cover type product (MCD12C1) with 0.05 spatial resolution ~~were~~was used in this study. The datasets of SO_4^{2-}, NO_3^-, and NH_4^+ were reprinted from~~originated from~~ Wang et al. (2015).

Absorption (%)
- BC
- OC
- AD

0 Water
1 Evergreen Needleleaf
2 Evergreen Broadleaf
3 Deciduous Needleleaf
4 Deciduous Broadleaf

5 Mixed Forest
6 Closed Shrublands
7 Open Shrublands
8 Woody Savannas
9 Savannas

10 Grasslands
11 Permanent Wetlands
12 Croplands
13 Urban and Built-up
14 Cropland Mosaics

15 Snow and Ice
16 Bare orsparesly vegetate
254 Unclassified

Absorption (%)
- BC
- OC
- MD

0 Water
1 Evergreen Needleleaf
2 Evergreen Broadleaf
3 Deciduous Needleleaf
4 Deciduous Broadleaf

5 Mixed Forest
6 Closed Shrublands
7 Open Shrublands
8 Woody Savannas
9 Savannas

10 Grasslands
11 Permanent Wetlands
12 Croplands
13 Urban and Built-up
14 Cropland Mosaics

15 Snow and Ice
16 Bare orsparesly vegetate
254 Unclassified

Fig. 78. The light absorption of ILAPs in surface snow in January 2014. The distribution of 17 different surface vegetation types retrieved from MODIS global land cover type product (MCD12C1) with 0.05 spatial resolution werewas used in this study.
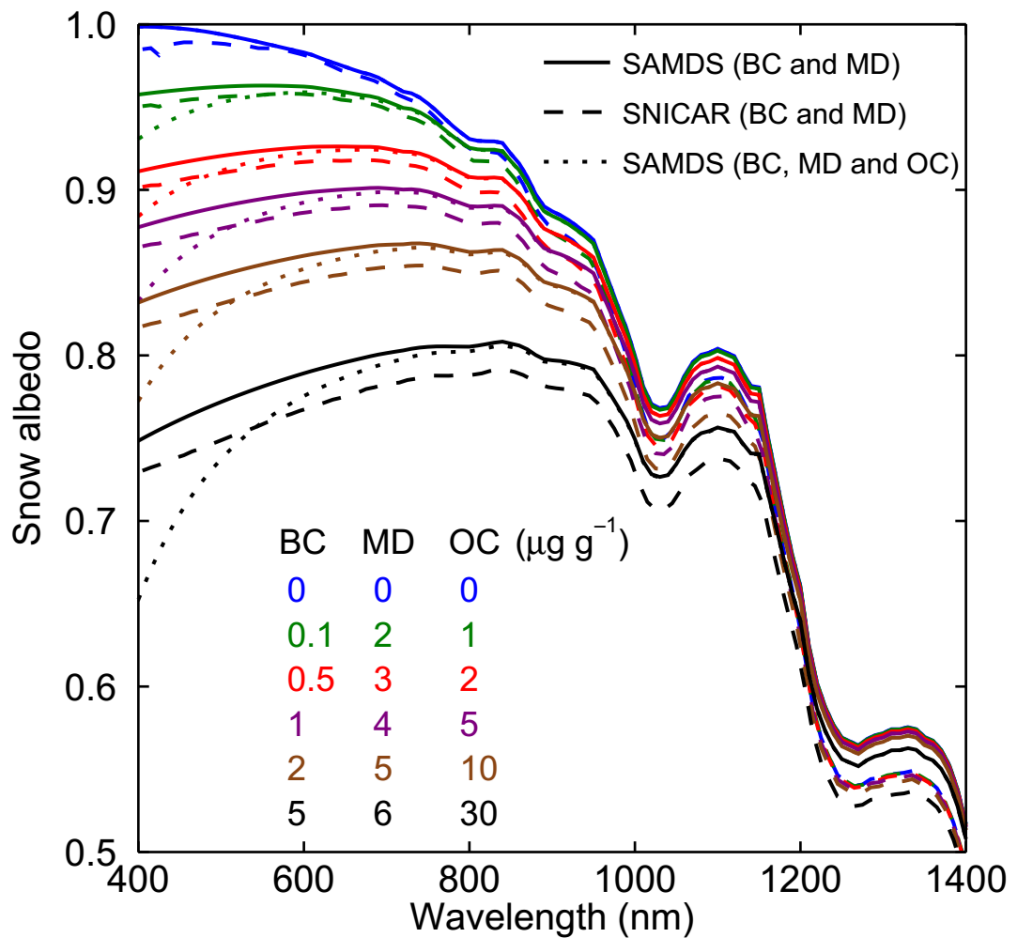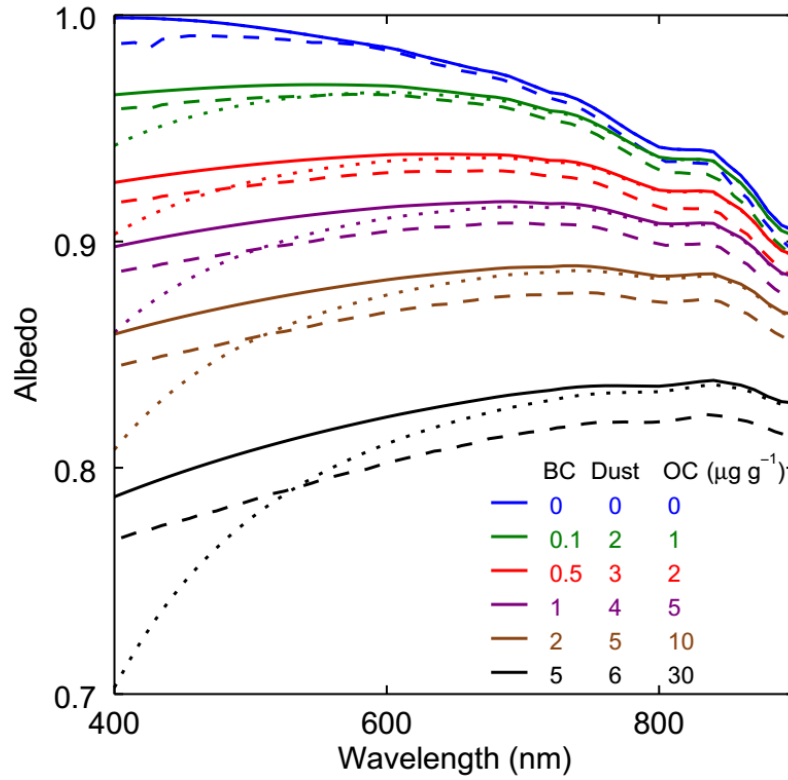
Fig. 89. Spectral albedo of snow with different contaminants for a 60° solar zenith angle and a 1070 μm ~~snow grain radius~~R_{eff}~~—~~. (Solid and dashed lines show the

SAMDS and SNICAR model predictions forof BC and mineral dustMD. Dotted lines show the SAMDS model predictions for all ILAPs, including BC, mineral dustMD, and OC).
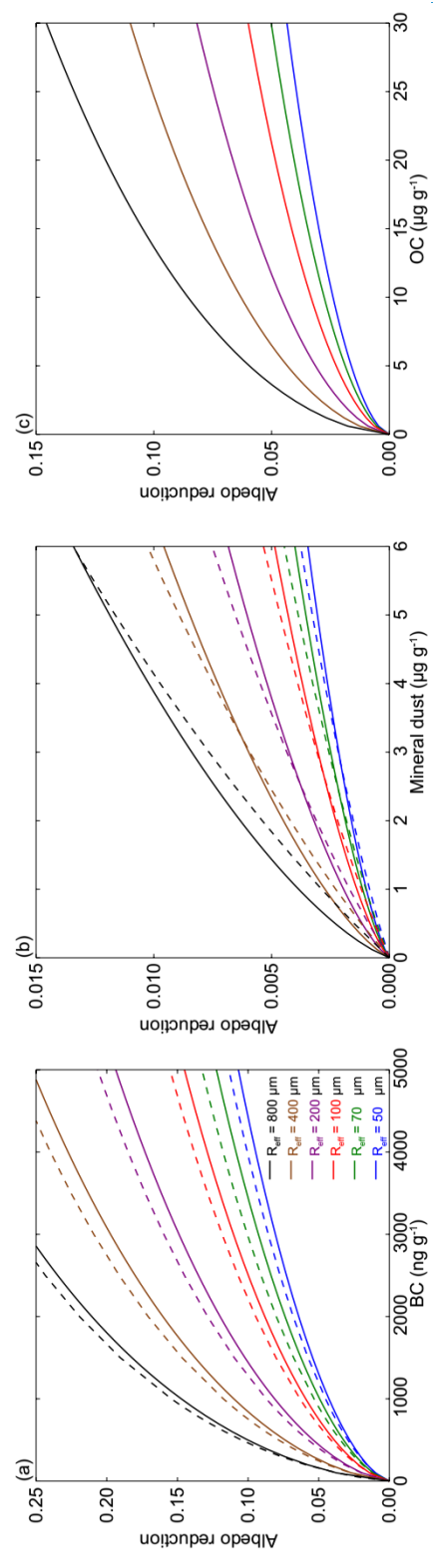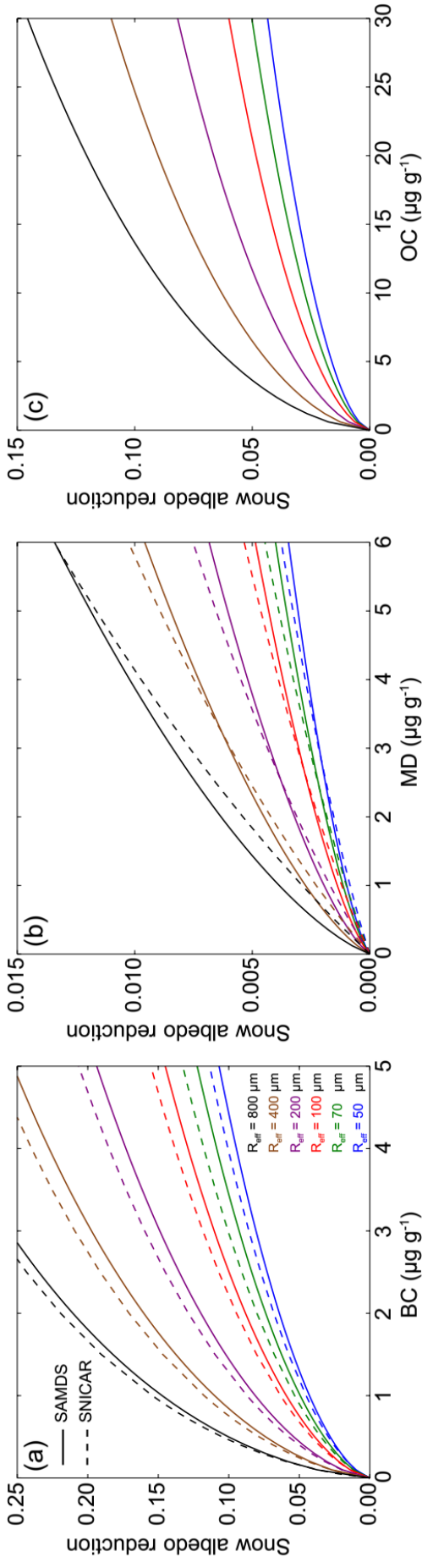
Fig. 910. Spectrally weighted snow albedo reduction over the 400–1400 nm solar spectrum attributed to (a) BC, (b) ~~mineral dust~~MD, and (c) OC computed as the albedo of contaminated snow minus the albedo of pure snow for a 60° solar zenith angle. ~~(~~Solid and dashed lines show the SAMDS and SNICAR models predictions. The MAC values of BC, ~~Fe~~OC, and ~~Fe~~OC were assumed to be 7.5 m^2 g^{-1}, 0.~~9~~3 m^2 g^{-1}, and 0.~~3~~9 m^2 g^{-1} at 550 nm, respectively, in SAMDS model).

(a)

fractal particles
hexagonal ice columns and plates
spheres

(b)

Spectral averages (0.4 - 1.4 μm)
$q = 60°$
$MAC(BC) = 7.5 \ m^2 \ g^{-1}$
$R_{eff}(snow) = 70 \ \mu m$
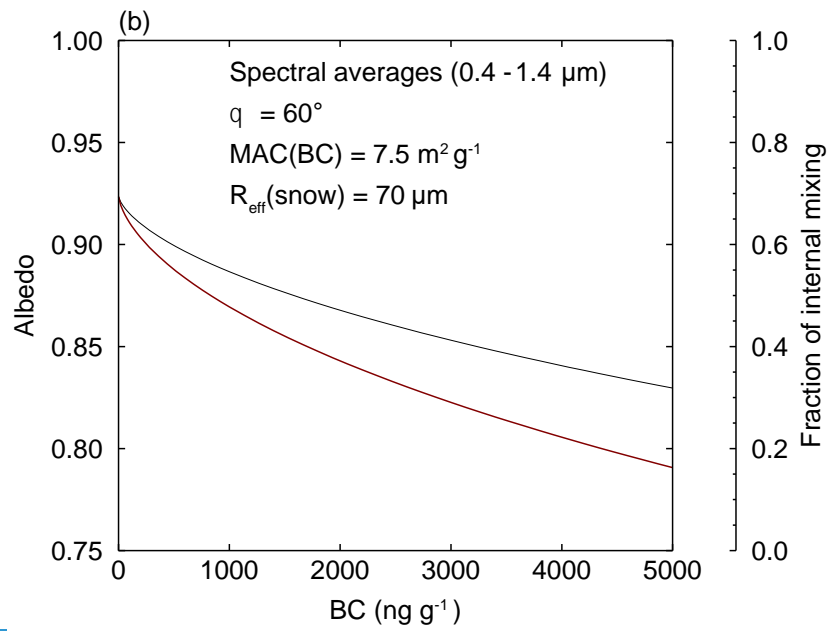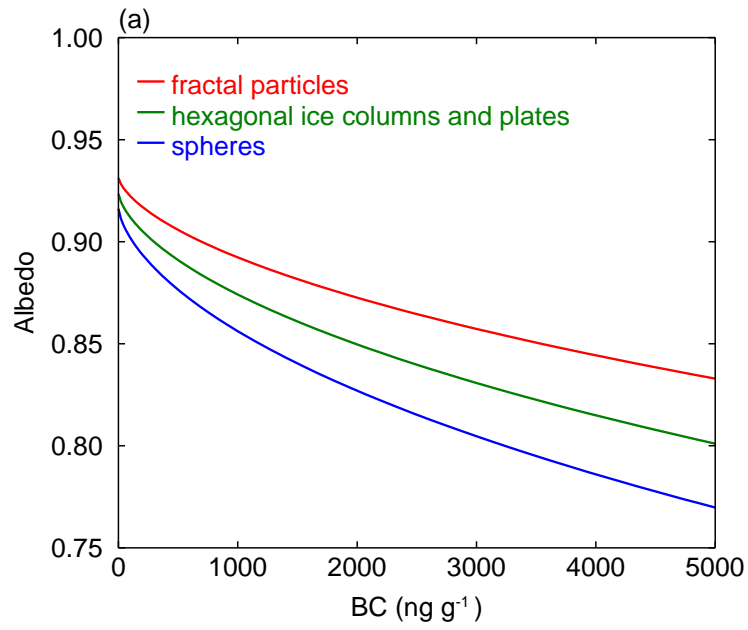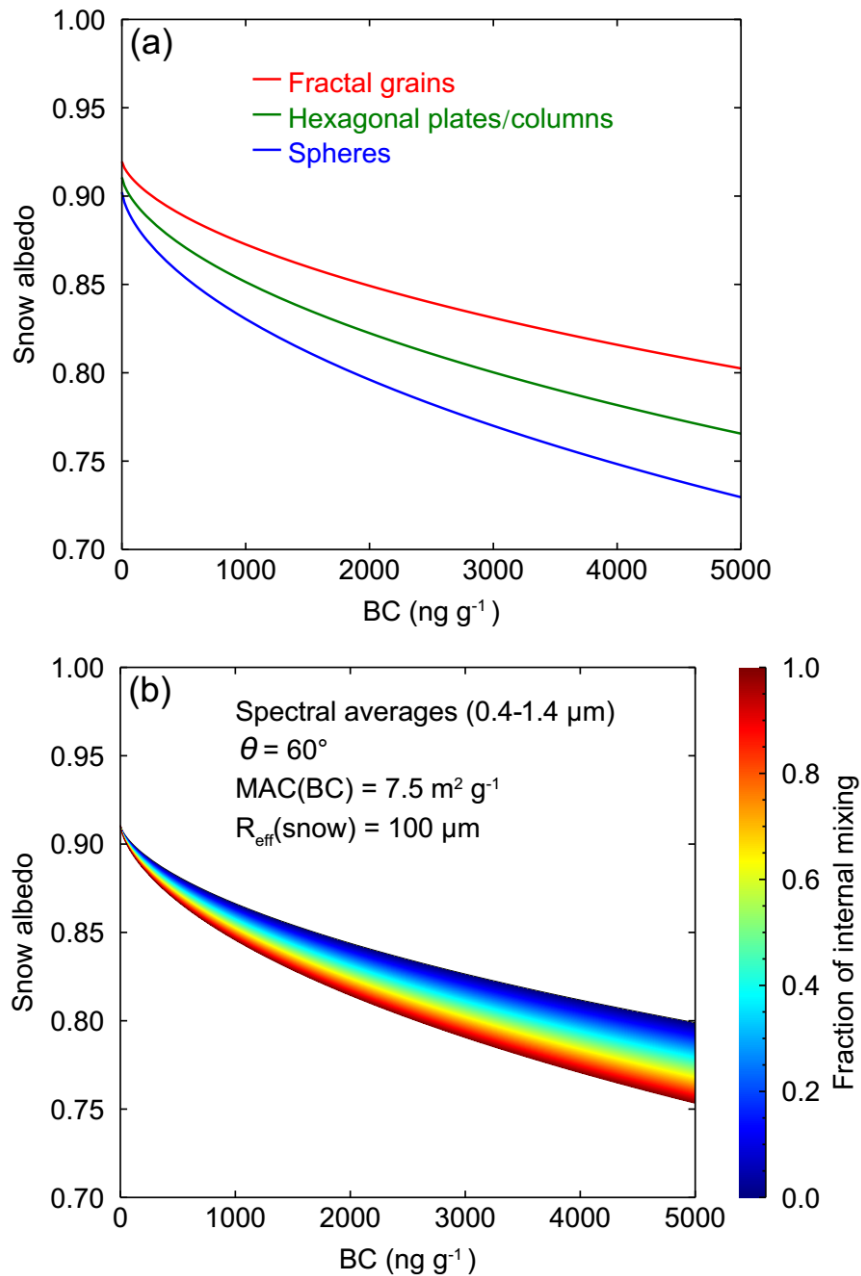
Fig. 1011 . Spectral albedoSnow albedo of snow reduction as a function of BC concentrationmixing ratios in snow by using SMDAS model for: (a) the irregular morphology of snow grains (fractal particlesgrains, hexagonal plates/columns, and spheres), (b) internal/ and external mixing of BC withand hexagonal plates/columns mixed with BCsnow grains. Also shown are model parameters includinge integrate spectral wavelengths (400-1400 nm), solar zenith angle (θ), mass absorption coefficient (MAC) of BC, and snow grain optical effective radius (R_eff).
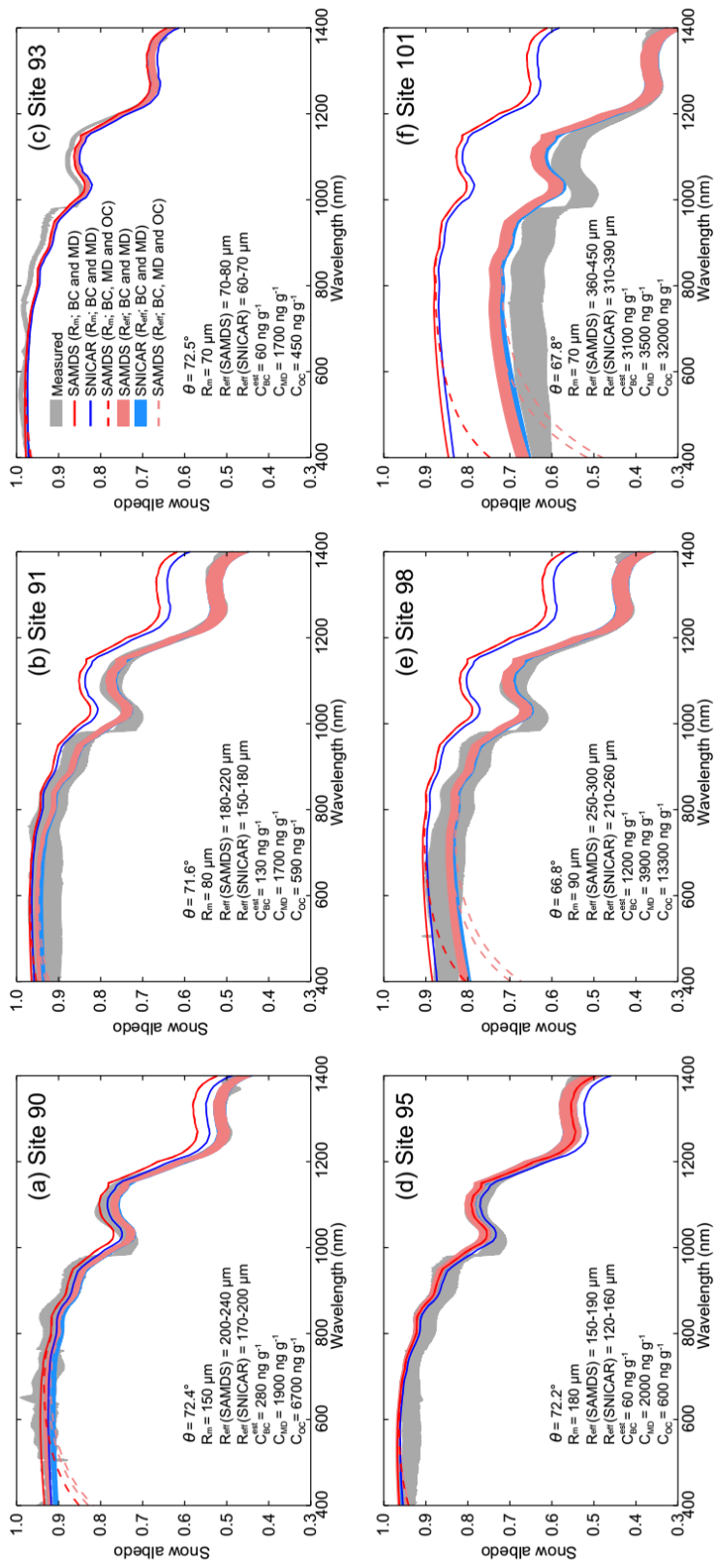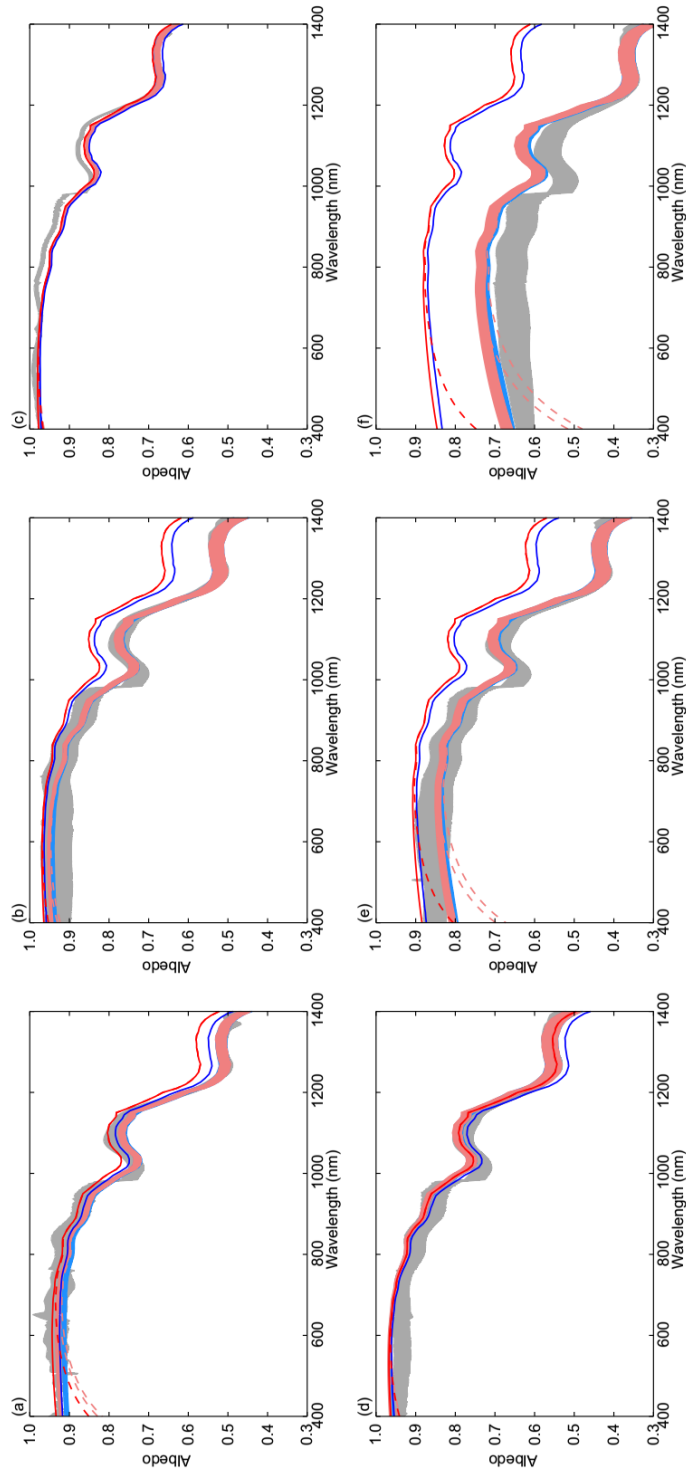
Fig. 1121. Measured and modeled spectral albedos of snow at sites (a) 90, (b) 91, (c) 93, (d) 95, (e) 98, and (f) 101. (Gray shaded bands correspond to measured spectral albedos using an spectroradiometer from the SAMDS and SNICAR models., Rred and blue solid lines correspond to spectral albedos from simulated by the SAMDS and SNICAR models with measured snow grain radii (R_m), and light red and blue shaded bands correspond to the albedos from the SAMDS and SNICAR models with calculated snow grain optical effective radii (R_{eff}). Contaminants only include BC and mineral dustMD in the SAMDS and SNICAR models. In the SNICAR model, the ratio of Fe in dust was found assumed to be 2.8%. Dashed red lines are similar to solid red lines, although OC should be added to the list of contaminants in the SAMDS model.

80

References

Acosta, J. A., Faz, A., Kalbitz, K., Jansen, B., and Martinez-Martinez, S.: Heavy metal concentrations in particle size fractions from street dust of Murcia (Spain) as the basis for risk assessment, J. Environ. Monitor., 13, 3087-3096, 2011.

Aleksandropoulou, V., Torseth, K., and Lazaridis, M.: Atmospheric Emission Inventory for Natural and Anthropogenic Sources and Spatial Emission Mapping for the Greater Athens Area, Water Air Soil Pollut., 219, 507-526, 2011.

Alfaro, S. C., Lafon, S., Rajot, J. L., Formenti, P., Gaudichet, A., and Maille, M.: Iron oxides and light absorption by pure desert dust: An experimental study, J. Geophys. Res.-Atmos., 109, D08208, 2004.

Arhami, M., Kuhn, T., Fine, P. M., Delfino, R. J., and Sioutas, C.: Effects of sampling artifacts and operating parameters on the performance of a semicontinuous particulate elemental carbon/organic carbon monitor, Environ. Sci. Technol., 40, 945-954, 2006.

Ax, W., Malchow, H., Koren, H., and Fischer, H.: Studies on immunological reactions in vitro, Sbornik vedeckych praci Lekarske fakulty Karlovy university v Hradci Kralove, 13, 287-292, 1970.

Bergstrom, R. W., Russell, P. B., and Hignett, P.: Wavelength dependence of the absorption of black carbon particles: Predictions and results from the TARFOX experiment and implications for the aerosol single scattering albedo, J. Atmos. Sci., 59, 567-577, 2002.

Bi, J. R., Huang, J. P., Hu, Z. Y., Holben, B. N., and Guo, Z. Q.: Investigating the aerosol optical and radiative characteristics of heavy haze episodes in Beijing during January of 2013, J. Geophys. Res.-Atmos., 119, 9884-9900, 2014.

Bond, T. C., and Bergstrom, R. W.: Light absorption by carbonaceous particles: An investigative review, Aerosol Sci. Tech., 40, 27-67, 2006.

Bond, T. C., Bussemer, M., Wehner, B., Keller, S., Charlson, R. J., and Heintzenberg, J.: Light absorption by primary particle emissions from a lignite burning plant, Environ. Sci. Technol., 33, 3887-3891, 1999.

Bond, T. C., Doherty, S. J., Fahey, D. W., Forster, P. M., Berntsen, T., DeAngelo, B. J., Flanner, M. G., Ghan, S., Karcher, B., Koch, D., Kinne, S., Kondo, Y., Quinn, P. K., Sarofim, M. C., Schultz, M. G., Schulz, M., Venkataraman, C., Zhang, H., Zhang, S., Bellouin, N., Guttikunda, S. K., Hopke, P. K., Jacobson, M. Z., Kaiser, J. W., Klimont, Z., Lohmann, U., Schwarz, J. P., Shindell, D., Storelvmo, T., Warren, S. G., and Zender, C. S.: Bounding the role of black carbon in the climate system: A scientific assessment, J. Geophys. Res.-Atmos., 118, 5380-5552, 2013.

Brandt, R. E., Warren, S. G., and Clarke, A. D.: A controlled snowmaking experiment testing the relation between black carbon content and reduction of snow albedo, J. Geophys. Res.-Atmos., 116, D08109, 2011.

Cappa, C. D., Onasch, T. B., Massoli, P., Worsnop, D. R., Bates, T. S., Cross, E. S., Davidovits, P., Hakala, J., Hayden, K. L., Jobson, B. T., Kolesar, K. R., Lack, D. A., Lerner, B. M., Li, S. M., Mellon, D., Nuaaman, I., Olfert, J. S., Petaja, T., Quinn, P. K., Song, C., Subramanian, R., Williams, E. J., and Zaveri, R. A.: Radiative Absorption Enhancements Due to the Mixing State of Atmospheric Black Carbon, Science, 337, 1078-1081, 2012.

Carmagnola, C. M., Domine, F., Dumont, M., Wright, P., Strellis, B., Bergin, M., Dibb, J., Picard, G., Libois, Q., Arnaud, L., and Morin, S.: Snow spectral albedo at Summit, Greenland: measurements and numerical simulations based on

physical and chemical properties of the snowpack, Cryosphere, 7, 1139-1160, 2013.

Che, H. Z., Wang, Y. Q., and Sun, J. Y.: Aerosol optical properties at Mt. Waliguan Observatory, China, Atmos. Environ., 45, 6004-6009, 2011.

Che, H. Z., Wang, Y. Q., Sun, J. Y., Zhang, X. C., Zhang, X. Y., and Guo, J. P.: Variation of Aerosol Optical Properties over the Taklimakan Desert in China, Aerosol Air Qual. Res., 13, 777-785, 2013.

Che, H. Z., Yang, Z. F., Zhang, X. Y., Zhu, C. Z., Ma, Q. L., Zhou, H. G., and Wang, P.: Study on the aerosol optical properties and their relationship with aerosol chemical compositions over three regional background stations in China, Atmos. Environ., 43, 1093-1099, 2009.

Che, H., Zhang, X. Y., Xia, X., Goloub, P., Holben, B., Zhao, H., Wang, Y., Zhang, X. C., Wang, H., Blarel, L., Damiri, B., Zhang, R., Deng, X., Ma, Y., Wang, T., Geng, F., Qi, B., Zhu, J., Yu, J., Chen, Q., and Shi, G.: Ground-based aerosol climatology of China: aerosol optical depths from the China Aerosol Remote Sensing Network (CARSNET) 2002-2013, Atmos. Chem. Phys., 15, 7619-7652, 2015a.

Che, H. Z., Zhao, H. J., Wu, Y. F., Xia, X. G., Zhu, J., Wang, H., Wang, Y. Q., Sun, J. Y., Yu, J., Zhang, X. Y., and Shi, G. Y.: Analyses of aerosol optical properties and direct radiative forcing over urban and industrial regions in Northeast China, Meteorol. Atmos. Phys., 127, 345-354, 2015b.

Chen, S. Y., Huang, J. P., Zhao, C., Qian, Y., Leung, L. R., and Yang, B.: Modeling the transport and radiative forcing of Taklimakan dust over the Tibetan Plateau: A case study in the summer of 2006, J. Geophys. Res.-Atmos., 118, 797-812, 2013.

Chu, D. A., Kaufman, Y. J., Ichoku, C., Remer, L. A., Tanre, D., and Holben, B. N.: Validation of MODIS aerosol optical depth retrieval over land, Geophys. Res. Lett., 29, 1617, 2002.

Cong, Z., Kang, S., Kawamura, K., Liu, B., Wan, X., Wang, Z., Gao, S., and Fu, P.: Carbonaceous aerosols on the south edge of the Tibetan Plateau: concentrations, seasonality and sources, Atmos. Chem. Phys., 15, 1573-1584, 2015.

Coz, E., Casuccio, G., Lersch, T. L., Moreno, T., and Artinano, B.: Anthropogenic Influenced Mineral Dust Ambient Fine Particles At An Urban Site In Barcelona (Spain), Chem. Eng. Trans., 22, 101-106, 2010.

Dang, C., and Hegg, D. A.: Quantifying light absorption by organic carbon in Western North American snow by serial chemical extractions, J. Geophys. Res.-Atmos., 119, 10247-10261, 2014.

Dang, C., Brandt, R. E., and Warren, S. G.: Parameterizations for narrowband and broadband albedo of pure snow and snow containing mineral dust and black carbon, J. Geophys. Res.-Atmos., 120, 5446-5468, 2015.

Dang, C., Fu, Q., and Warren, S. G.: Effect of Snow Grain Shape on Snow Albedo, J. Atmos. Sci., 73, 3573-3583, 2016.

Doherty, S. J., Dang, C., Hegg, D. A., Zhang, R. D., and Warren, S. G.: Black carbon and other light-absorbing particles in snow of central North America, J. Geophys. Res.-Atmos., 119, 12807-12831, 2014.

Doherty, S. J., Grenfell, T. C., Forsstrom, S., Hegg, D. L., Brandt, R. E., and Warren, S. G.: Observed vertical redistribution of black carbon and other insoluble light-absorbing particles in melting snow, J. Geophys. Res.-Atmos., 118, 5553-5569, 2013.

Doherty, S. J., Warren, S. G., Grenfell, T. C., Clarke, A. D., and Brandt, R. E.: Light-absorbing impurities in Arctic snow, Atmos. Chem. Phys., 10, 11647-11680, 2010.

Fierce, L., Bond, T. C., Bauer, S. E., Mena, F., and Riemer, N.: Black carbon absorption at the global scale is affected by particle-scale diversity in composition, Nat. Commun., 7, 2016.

Flanner, M. G.: Arctic climate sensitivity to local black carbon, J. Geophys. Res.-Atmos., 118, 1840-1851, 2013.

Flanner, M. G., Liu, X., Zhou, C., Penner, J. E., and Jiao, C.: Enhanced solar energy absorption by internally-mixed black carbon in snow grains, Atmos. Chem. Phys., 12, 4699-4721, 2012.

Flanner, M. G., Zender, C. S., Hess, P. G., Mahowald, N. M., Painter, T. H., Ramanathan, V., and Rasch, P. J.: Springtime warming and reduced snow cover from carbonaceous particles, Atmos. Chem. Phys., 9, 2481-2497, 2009.

Flanner, M. G., Zender, C. S., Randerson, J. T., and Rasch, P. J.: Present-day climate forcing and response from black carbon in snow, J. Geophys. Res.-Atmos., 112, D11202, 2007.

Friedl, M. A., Sulla-Menashe, D., Tan, B., Schneider, A., Ramankutty, N., Sibley, A., and Huang, X. M.: MODIS Collection 5 global land cover: Algorithm refinements and characterization of new datasets, Remote Sens. Environ., 114, 168-182, 2010.

Fu, Q.: A New Parameterization of an Asymmetry Factor of Cirrus Clouds for Climate Models, J. Atmos. Sci., 64, 4140-4150, 2007.

Givati, A., and Rosenfeld, D.: Quantifying precipitation suppression due to air pollution, J. Appl. Meteorol., 43, 1038-1056, 2004.

Goudie, A. S., and Middleton, N. J.: Saharan dust storms: nature and consequences, Earth Sci. Rev., 56, 179-204, 2001.

Grenfell, T. C., Doherty, S. J., Clarke, A. D., and Warren, S. G.: Light absorption from particulate impurities in snow and ice determined by spectrophotometric analysis of filters, Appl. Opt., 50, 2037-2048, 2011.

Grenfell, T. C., Warren, S. G., and Mullen, P. C.: Reflection of Solar-Radiation by the Antarctic Snow Surface at Ultraviolet, Visible, and near-Infrared Wavelengths, J. Geophys. Res.-Atmos., 99, 18669-18684, 1994.

Guan, X. D., Huang, J. P., Zhang, Y. T., Xie, Y. K., and Liu, J. J.: The relationship between anthropogenic dust and population over global semi-arid regions, Atmos. Chem. Phys., 16, 5159-5169, 2016.

Guan, X., Huang, J., Guo, R., Yu, H., Lin, P., and Zhang, Y.: Role of radiatively forced temperature changes in enhanced semi-arid warming in the cold season over east Asia, Atmos. Chem. Phys., 15, 13777-13786, 2015.

Hadley, O. L., and Kirchstetter, T. W.: Black-carbon reduction of snow albedo, Nat. Clim. Change, 2, 437-440, 2012.

Hansen, J., and Nazarenko, L.: Soot climate forcing via snow and ice albedos, Proc. Nat. Acad. Sci. U.S.A., 101, 423-428, 2004.

Hansen, J., Sato, M., Ruedy, R., Nazarenko, L., Lacis, A., Schmidt, G. A., Russell, G., Aleinov, I., Bauer, M., Bauer, S., Bell, N., Cairns, B., Canuto, V., Chandler, M., Cheng, Y., Del Genio, A., Faluvegi, G., Fleming, E., Friend, A., Hall, T., Jackman, C., Kelley, M., Kiang, N., Koch, D., Lean, J., Lerner, J., Lo, K., Menon, S., Miller, R., Minnis, P., Novakov, T., Oinas, V., Perlwitz, J., Perlwitz, J., Rind, D., Romanou, A., Shindell, D., Stone, P., Sun, S., Tausnev, N., Thresher,

D., Wielicki, B., Wong, T., Yao, M., and Zhang, S.: Efficacy of climate forcings, J. Geophys. Res.-Atmos., 110, D18104, 2005.

He, C. L., Li, Q. B., Liou, K. N., Takano, Y., Gu, Y., Qi, L., Mao, Y. H., and Leung, L. R.: Black carbon radiative forcing over the Tibetan Plateau, Geophys. Res. Lett., 41, 7806-7813, 2014.

Hegg, D. A., Warren, S. G., Grenfell, T. C., Doherty, S. J., and Clarke, A. D.: Sources of light-absorbing aerosol in arctic snow and their seasonal variation, Atmos. Chem. Phys., 10, 10923-10938, 2010.

Hegg, D. A., Warren, S. G., Grenfell, T. C., Doherty, S. J., Larson, T. V., and Clarke, A. D.: Source Attribution of Black Carbon in Arctic Snow, Environ. Sci. Technol., 43, 4016-4021, 2009.

Holben, B. N., Eck, T. F., and Fraser, R. S.: Temporal and Spatial Variability of Aerosol Optical Depth in the Sahel Region in Relation to Vegetation Remote-Sensing, Int. J. Remote Sens., 12, 1147-1163, 1991.

Holben, B. N., Eck, T. F., Slutsker, I., Smirnov, A., Sinyuk, A., Schafer, J., Giles, D., and Dubovik, O.: AERONET's Version 2.0 quality assurance criteria - art. no. 64080Q, Remote Sensing of the Atmosphere and Clouds, 6408, 64080q, 2006.

Holben, B. N., Tanre, D., Smirnov, A., Eck, T. F., Slutsker, I., Abuhassan, N., Newcomb, W. W., Schafer, J. S., Chatenet, B., Lavenu, F., Kaufman, Y. J., Castle, J. V., Setzer, A., Markham, B., Clark, D., Frouin, R., Halthore, R., Karneli, A., O'Neill, N. T., Pietras, C., Pinker, R. T., Voss, K., and Zibordi, G.: An emerging ground-based aerosol climatology: Aerosol optical depth from AERONET, J. Geophys. Res.-Atmos., 106, 12067-12097, 2001.

Hsu, S. C., Liu, S. C., Huang, Y. T., Chou, C. C. K., Lung, S. C. C., Liu, T. H., Tu, J. Y., and Tsai, F. J.: Long-range southeastward transport of Asian biosmoke pollution: Signature detected by aerosol potassium in Northern Taiwan, J. Geophys. Res.-Atmos., 114, D14301, 2009.

Huang, J. P., Fu, Q. A., Zhang, W., Wang, X., Zhang, R. D., Ye, H., and Warren, S. G.: Dust and Black Carbon in Seasonal Snow across Northern China, Bull. Amer. Meteor. Soc., 92, 175-181, 2011.

Huang, J. P., Liu, J. J., Chen, B., and Nasiri, S. L.: Detection of anthropogenic dust using CALIPSO lidar measurements, Atmos. Chem. Phys., 15, 11653-11665, 2015a.

Huang, J. P., Minnis, P., Chen, B., Huang, Z. W., Liu, Z. Y., Zhao, Q. Y., Yi, Y. H., and Ayers, J. K.: Long-range transport and vertical structure of Asian dust from CALIPSO and surface measurements during PACDEX, J. Geophys. Res.-Atmos., 113, 2008.

Huang, J. P., Wang, T. H., Wang, W. C., Li, Z. Q., and Yan, H. R.: Climate effects of dust aerosols over East Asian arid and semiarid regions, J. Geophys. Res.-Atmos., 119, 11398-11416, 2014.

Huang, Z. W., Huang, J. P., Hayasaka, T., Wang, S. S., Zhou, T., and Jin, H. C.: Short-cut transport path for Asian dust directly to the Arctic: a case study, Environ. Res. Lett., 10, 114018, 2015b.

Ichoku, C., Chu, D. A., Mattoo, S., Kaufman, Y. J., Remer, L. A., Tanre, D., Slutsker, I., and Holben, B. N.: A spatio-temporal approach for global validation and analysis of MODIS aerosol products, Geophys. Res. Lett., 29, 1616, 2002a.

Ichoku, C., Levy, R., Kaufman, Y. J., Remer, L. A., Li, R. R., Martins, V. J., Holben, B. N., Abuhassan, N., Slutsker, I., Eck, T. F., and Pietras, C.: Analysis of the performance characteristics of the five-channel Microtops II Sun photometer for

measuring aerosol optical thickness and precipitable water vapor, J. Geophys. Res.-Atmos., 107, 4179, 2002b.

IPCC: Climate Change 2013: The Physical Science Basis. Contribution of Working Group I to the Fifth Assessment Report of the Intergovernmental Panel on Climate Change, Stocker, T. F., Qin, D., Plattner, G.-K., Tignor, M., Allen, S. K., Boschung, J., Nauels, A., Xia, Y., Bex, V., and Midgley, P. M., Cambridge Univ. Press, Cambridge, United Kingdom and New York, NY, USA, 2013.

Jacobson, M. Z.: Climate response of fossil fuel and biofuel soot, accounting for soot's feedback to snow and sea ice albedo and emissivity, J. Geophys. Res.-Atmos., 109, D21201, 2004.

Jaffe, D., Anderson, T., Covert, D., Kotchenruther, R., Trost, B., Danielson, J., Simpson, W., Berntsen, T., Karlsdottir, S., Blake, D., Harris, J., Carmichael, G., and Uno, I.: Transport of Asian air pollution to North America, Geophys. Res. Lett., 26, 711-714, 1999.

Kamani, H., Ashrafi, S. D., Isazadeh, S., Jaafari, J., Hoseini, M., Mostafapour, F. K., Bazrafshan, E., Nazmara, S., and Mahvi, A. H.: Heavy Metal Contamination in Street Dusts with Various Land Uses in Zahedan, Iran, B. Environ. Contam. Tox., 94, 382-386, 2015.

Kang, L. T., Huang, J. P., Chen, S. Y., and Wang, X.: Long-term trends of dust events over Tibetan Plateau during 1961-2010, Atmos. Environ., 125, 188-198, 2016.

Kaufman, Y. J., Tanre, D., Gordon, H. R., Nakajima, T., Lenoble, J., Frouin, R., Grassl, H., Herman, B. M., King, M. D., and Teillet, P. M.: Passive remote sensing of tropospheric aerosol and atmospheric correction for the aerosol effect, J. Geophys. Res.-Atmos., 102, 16815-16830, 1997.

Kim, W., Doh, S. J., and Yu, Y.: Anthropogenic contribution of magnetic particulates in urban roadside dust, Atmos. Environ., 43, 3137-3144, 2009.

Koch, D., Menon, S., Del Genio, A., Ruedy, R., Alienov, I., and Schmidt, G. A.: Distinguishing Aerosol Impacts on Climate over the Past Century, J. Climate, 22, 2659-2677, 2009.

Kokhanovsky, A. A., and Zege, E. P.: Scattering optics of snow, Appl. Opt., 43, 1589-1602, 2004.

Lafon, S., Sokolik, I. N., Rajot, J. L., Caquineau, S., and Gaudichet, A.: Characterization of iron oxides in mineral dust aerosols: Implications for light absorption, J. Geophys. Res.-Atmos., 111, D21207. 2006.

Light, B., Eicken, H., Maykut, G. A., and Grenfell, T. C.: The effect of included particulates on the spectral albedo of sea ice, J. Geophys. Res.-Oceans, 103, 27739-27752, 1998.

Li, G. J., Chen, J., Ji, J. F., Yang, J. D., and Conway, T. M.: Natural and anthropogenic sources of East Asian dust, Geology, 37, 727-730, 2009.

Liou, K. N., Takano, Y., and Yang, P.: Light absorption and scattering by aggregates: Application to black carbon and snow grains, J. Quant. Spectrosc. Ra., 112, 1581-1594, 2011.

Liou, K. N., Takano, Y., He, C., Yang, P., Leung, L. R., Gu, Y., and Lee, W. L.: Stochastic parameterization for light absorption by internally mixed BC/dust in snow grains for application to climate models, J. Geophys. Res.-Atmos., 119, 7616-7632, 2014.

Li, S. Y., Lei, J. Q., Xu, X. W., Wang, H. F., and Gu, F.: Dust Source of Sandstorm in the Tarim Basin, Northwest China, Adv. Environ. Sci. Eng., 518-523, 4592-4598, 2012.

Li, Z., et al.: Aerosol and monsoon climate interactions over Asia, Rev. Geophys., 54, 2016.

Lorenz, K., Preston, C. M., and Kandeler, E.: Soil organic matter in urban soils: Estimation of elemental carbon by thermal oxidation and characterization of organic matter by solid-state C-13 nuclear magnetic resonance (NMR) spectroscopy, Geoderma, 130, 312-323, 2006.

Loveland, T. R., and Belward, A. S.: The IGBP-DIS global 1 km land cover data set, DISCover: first results, Int. J. Remote Sens., 18, 3291-3295, 1997.

Mahowald, N. M., and Luo, C.: A less dusty future?, Geophys. Res. Lett., 30, 1903, 2003.

Mahowald, N. M., Baker, A. R., Bergametti, G., Brooks, N., Duce, R. A., Jickells, T. D., Kubilay, N., Prospero, J. M., and Tegen, I.: Atmospheric global dust cycle and iron inputs to the ocean, Global Biogeochem. CY., 19, Gb4025, 2005.

McConnell, J. R., Edwards, R., Kok, G. L., Flanner, M. G., Zender, C. S., Saltzman, E. S., Banta, J. R., Pasteris, D. R., Carter, M. M., and Kahl, J. D. W.: 20th-century industrial black carbon emissions altered arctic climate forcing, Science, 317, 1381-1384, 2007.

More, S., Kumar, P. P., Gupta, P., Devara, P. C. S., and Aher, G. R.: Comparison of Aerosol Products Retrieved from AERONET, MICROTOPS and MODIS over a Tropical Urban City, Pune, India, Aerosol. Air. Qual. Res., 13, 107-121, 2013.

Morys, M., Mims, F. M., Hagerup, S., Anderson, S. E., Baker, A., Kia, J., and Walkup, T.: Design, calibration, and performance of MICROTOPS II handheld ozone monitor and Sun photometer, J. Geophys. Res.-Atmos., 106, 14573-14582, 2001.

Motoyoshi, H., Aoki, T., Hori, M., Abe, O., and Mochizuki, S.: Possible effect of anthropogenic aerosol deposition on snow albedo reduction at Shinjo, Japan, J. Meteorol. Soc. Jpn., 83A, 137-148, 2005.

Ofosu, F. G., Hopke, P. K., Aboh, I. J. K., and Bamford, S. A.: Characterization of fine particulate sources at Ashaiman in Greater Accra, Ghana, Atmos. Pollut. Res., 3, 301-310, 2012.

Painter, T. H., Bryant, A. C., and Skiles, S. M.: Radiative forcing by light absorbing impurities in snow from MODIS surface reflectance data, Geophys. Res. Lett., 39, L17502, 2012.

Painter, T. H., Barrett, A. P., Landry, C. C., Neff, J. C., Cassidy, M. P., Lawrence, C. R., McBride, K. E., and Farmer, G. L.: Impact of disturbed desert soils on duration of mountain snow cover, Geophys. Res. Lett., 34, L12502, 2007.

Painter, T. H., Deems, J. S., Belnap, J., Hamlet, A. F., Landry, C. C., and Udall, B.: Response of Colorado River runoff to dust radiative forcing in snow, Proc. Nat. Acad. Sci. U.S.A., 107, 17125-17130, 2010.

Painter, T. H., Seidel, F. C., Bryant, A. C., Skiles, S. M., and Rittger, K.: Imaging spectroscopy of albedo and radiative forcing by light-absorbing impurities in mountain snow, J. Geophys. Res.-Atmos., 118, 9511-9523, 2013.

Park, S. U., and Park, M. S.: Aerosol size distributions observed at Naiman in the Asian dust source region of Inner Mongolia, Atmos. Environ., 82, 17-23, 2014.

Pedersen, C. A., Gallet, J. C., Strom, J., Gerland, S., Hudson, S. R., Forsstrom, S., Isaksson, E., and Berntsen, T. K.: In situ observations of black carbon in snow and the corresponding spectral surface albedo reduction, J. Geophys. Res.-Atmos., 120, 1476-1489, 2015.

Pio, C. A., Legrand, M., Oliveira, T., Afonso, J., Santos, C., Caseiro, A., Fialho, P., Barata, F., Puxbaum, H., Sanchez-Ochoa, A., Kasper-Giebl, A., Gelencser, A.,

Preunkert, S., and Schock, M.: Climatology of aerosol composition (organic versus inorganic) at nonurban sites on a west-east transect across Europe, J. Geophys. Res.-Atmos., 112, D23s02, 2007.

Porter, J. N., Miller, M., Pietras, C., and Motell, C.: Ship-based sun photometer measurements using Microtops sun photometers, J. Atmos. Oceanic Technol., 18, 765-774, 2001.

Pu, W., Wang, X., Zhang, X. Y., Ren, Y., Shi, J. S., Bi, J. R., and Zhang, B. D.: Size Distribution and Optical Properties of Particulate Matter (PM10) and Black Carbon (BC) during Dust Storms and Local Air Pollution Events across a Loess Plateau Site, Aerosol Air Qual. Res., 15, 2212-2224, 2015.

Qian, Y., Wang, H. L., Zhang, R. D., Flanner, M. G., and Rasch, P. J.: A sensitivity study on modeling black carbon in snow and its radiative forcing over the Arctic and Northern China, Environ. Res. Lett., 9, 064001, 2014.

Qian, Y., Yasunari, T. J., Doherty, S. J., Flanner, M. G., Lau, W. K. M., Ming, J., Wang, H. L., Wang, M., Warren, S. G., and Zhang, R. D.: Light-absorbing Particles in Snow and Ice: Measurement and Modeling of Climatic and Hydrological impact, Adv. Atmos. Sci., 32, 64-91, 2015.

Qiao, Q. Q., Huang, B. C., Zhang, C. X., Piper, J. D. A., Pan, Y. P., and Sun, Y.: Assessment of heavy metal contamination of dustfall in northern China from integrated chemical and magnetic investigation, Atmos. Environ., 74, 182-193, 2013.

Remer, L. A., Tanre, D., Kaufman, Y. J., Ichoku, C., Mattoo, S., Levy, R., Chu, D. A., Holben, B., Dubovik, O., Smirnov, A., Martins, J. V., Li, R. R., and Ahmad, Z.: Validation of MODIS aerosol retrieval over ocean, Geophys. Res. Lett., 29, 1618, 2002.

Rosenfeld, D., Rudich, Y., and Lahav, R.: Desert dust suppressing precipitation: A possible desertification feedback loop, Proc. Nat. Acad. Sci. U.S.A., 98, 5975-5980, 2001.

Routray, A., Mohanty, U. C., Osuri, K. K., and Prasad, S. K.: Improvement of Monsoon Depressions Forecast with Assimilation of Indian DWR Data Using WRF-3DVAR Analysis System, Pure Appl. Geophys., 170, 2329-2350, 2013.

Rozenberg, G.: Optical characteristics of thick weakly absorbing scattering layers, Dokl. Akad. Nauk SSSR, 145, 775-777, 1962.

Smith, T. M., Gao, J. D., Calhoun, K. M., Stensrud, D. J., Manross, K. L., Ortega, K. L., Fu, C. H., Kingfield, D. M., Elmore, K. L., Lakshmanan, V., and Riedel, C.: Examination of a Real-Time 3DVAR Analysis System in the Hazardous Weather Testbed, Weather Forecast., 29, 63-77, 2014.

Sokolik, I. N., and Toon, O. B.: Incorporation of mineralogical composition into models of the radiative properties of mineral aerosol from UV to IR wavelengths, J. Geophys. Res.-Atmos., 104, 9423-9444, 1999.

Srivastava, K., and Bhardwaj, R.: Analysis and very short range forecast of cyclone "AILA" with radar data assimilation with rapid intermittent cycle using ARPS 3DVAR and cloud analysis techniques, Meteorol. Atmos. Phys., 124, 97-111, 2014.

Tegen, I., and Fung, I.: Contribution to the Atmospheric Mineral Aerosol Load from Land-Surface Modification, J. Geophys. Res.-Atmos., 100, 18707-18726, 1995.

Tegen, I., Harrison, S. P., Kohfeld, K. E., Engelstaedter, S., and Werner, M.: Emission of soil dust aerosol: Anthropogenic contribution and future changes, Geochimica Et Cosmochimica Acta, 66, A766-A766, 2002.

Tegen, I., Werner, M., Harrison, S. P., and Kohfeld, K. E.: Relative importance of climate and land use in determining present and future global soil dust emission, Geophys. Res. Lett., 31, L05105, 2004.

Thompson, L. G., Davis, M. E., Mosleythompson, E., and Liu, K. B.: Pre-Incan Agricultural Activity Recorded in Dust Layers in 2 Tropical Ice Cores, Nature, 336, 763-765, 1988.

Toon, O. B., Mckay, C. P., Ackerman, T. P., and Santhanam, K.: Rapid Calculation of Radiative Heating Rates and Photodissociation Rates in Inhomoge'neous Multiple-Scattering Atmospheres, J. Geophys. Res.-Atmos., 94, 16287-16301, 1989.

Wallach, D. F. H., and Fischer, H.: Membrane aspects of the immune response. Report of a workshop held in Titisee, Schwarzwald, Germany, October 13–15, 1969, FEBS Lett., 9, 129-135, 1970.

Wang, M., Xu, B. Q., Zhao, H. B., Cao, J. J., Joswiak, D., Wu, G. J., and Lin, S. B.: The Influence of Dust on Quantitative Measurements of Black Carbon in Ice and Snow when Using a Thermal Optical Method, Aerosol Sci. Tech., 46, 60-69, 2012.

Wang, P., Che, H. Z., Zhang, X. C., Song, Q. L., Wang, Y. Q., Zhang, Z. H., Dai, X., and Yu, D. J.: Aerosol optical properties of regional background atmosphere in Northeast China, Atmos. Environ., 44, 4404-4412, 2010a.

Wang, X., Doherty, S. J., and Huang, J. P.: Black carbon and other light-absorbing impurities in snow across Northern China, J. Geophys. Res.-Atmos., 118, 1471-1492, 2013a.

Wang, X. G., Parrish, D., Kleist, D., and Whitaker, J.: GSI 3DVar-Based Ensemble-Variational Hybrid Data Assimilation for NCEP Global Forecast System: Single-Resolution Experiments, Mon. Weather. Rev., 141, 4098-4117, 2013b.

Wang, X., Huang, J. P., Ji, M. X., and Higuchi, K.: Variability of East Asia dust events and their long-term trend, Atmos. Environ., 42, 3156-3165, 2008.

Wang, X., Huang, J. P., Zhang, R. D., Chen, B., and Bi, J. R.: Surface measurements of aerosol properties over northwest China during ARM China 2008 deployment, J. Geophys. Res.-Atmos., 115, D00k27, 2010b.

Wang, X., Pu, W., Zhang, X. Y., Ren, Y., and Huang, J. P.: Water-soluble ions and trace elements in surface snow and their potential source regions across northeastern China, Atmos. Environ., 114, 57-65, 2015.

Wang, X., Xu, B. Q., and Ming, J.: An Overview of the Studies on Black Carbon and Mineral Dust Deposition in Snow and Ice Cores in East Asia, J. Meteorol. Res.-Prc., 28, 354-370, 2014.

Warren, S. G., and Wiscombe, W. J.: A Model for the Spectral Albedo of Snow .2. Snow Containing Atmospheric Aerosols, J. Atmos. Sci., 37, 2734-2745, 1980.

Warren, S. G. and Wiscombe, W. J.: Dirty Snow after Nuclear-War, Nature, 313, 467-470, 1985.

Warren, S. G.: Optical-Properties of Snow, Rev. Geophys., 20, 67-89, 1982.

Wright, P., Bergin, M., Dibb, J., Lefer, B., Domine, F., Carman, T., Carmagnola, C., Dumont, M., Courville, Z., Schaaf, C., and Wang, Z. S.: Comparing MODIS daily snow albedo to spectral albedo field measurements in Central Greenland, Remote Sens. Environ., 140, 118-129, 2014.

Wuttke, S., Seckmeyer, G., and Konig-Lang, G.: Measurements of spectral snow albedo at Neumayer, Antarctica, Ann. Geophys., 24, 7-21, 2006b.

Wuttke, S., Seckmeyer, G., Bernhard, G., Ehramjian, J., McKenzie, R., Johnston, P., and O'Neill, M.: New spectroradiometers complying with the NDSC standards, J. Atmos. Oceanic Technol., 23, 241-251, 2006a.

Xia, X. A., Chen, H. B., Wang, P. C., Zong, X. M., Qiu, J. H., and Gouloub, P.: Aerosol properties and their spatial and temporal variations over North China in spring 2001, Tellus B., 57, 28-39, 2005.

Xia, X. G., Li, Z. Q., Holben, B., Wang, P., Eck, T., Chen, H. B., Cribb, M., and Zhao, Y. X.: Aerosol optical properties and radiative effects in the Yangtze Delta region of China, J. Geophys. Res.-Atmos., 112, D22s12, 2007.

Xu, B. Q., Cao, J. J., Hansen, J., Yao, T. D., Joswia, D. R., Wang, N. L., Wu, G. J., Wang, M., Zhao, H. B., Yang, W., Liu, X. Q., and He, J. Q.: Black soot and the survival of Tibetan glaciers, Proc. Nat. Acad. Sci. U.S.A., 106, 22114-22118, 2009.

Xu, B. Q., Cao, J. J., Joswiak, D. R., Liu, X. Q., Zhao, H. B., and He, J. Q.: Post-depositional enrichment of black soot in snow-pack and accelerated melting of Tibetan glaciers, Environ. Res. Lett., 7, 2012.

Yasunari, T. J., Bonasoni, P., Laj, P., Fujita, K., Vuillermoz, E., Marinoni, A., Cristofanelli, P., Duchi, R., Tartari, G., and Lau, K. M.: Estimated impact of black carbon deposition during pre-monsoon season from Nepal Climate Observatory - Pyramid data and snow albedo changes over Himalayan glaciers, Atmos. Chem. Phys., 10, 6603-6615, 2010.

Yasunari, T. J., Koster, R. D., Lau, W. K. M., and Kim, K. M.: Impact of snow darkening via dust, black carbon, and organic carbon on boreal spring climate in the Earth system, J. Geophys. Res.-Atmos., 120, 5485-5503, 2015.

Ye, H., Zhang, R. D., Shi, J. S., Huang, J. P., Warren, S. G., and Fu, Q.: Black carbon in seasonal snow across northern Xinjiang in northwestern China, Environ. Res. Lett., 7, 044002, 2012.

Yesubabu, V., Srinivas, C. V., Hariprasad, K. B. R. R., and Baskaran, R.: A Study on the Impact of Observation Assimilation on the Numerical Simulation of Tropical Cyclones JAL and THANE Using 3DVAR, Pure Appl. Geophys., 171, 2023-2042, 2014.

Zawadzka, O., Makuch, P., Markowicz, K. M., Zielinski, T., Petelski, T., Ulevicius, V., Strzalkowska, A., Rozwadowska, A., and Gutowska, D.: Studies of aerosol optical depth with the use of Microtops II sun photometers and MODIS detectors in coastal areas of the Baltic Sea, Acta Geophysica, 62, 400-422, 2014.

Zege, È. P., Ivanov, A. P., and Katsev, I. L.: Image transfer through a scattering medium, Springer Verlag, 1991.

Zhang, R., Hegg, D. A., Huang, J., and Fu, Q.: Source attribution of insoluble light-absorbing particles in seasonal snow across northern China, Atmos. Chem. Phys., 13, 6091-6099, 2013a.

Zhang, R. J., Arimoto, R., An, J. L., Yabuki, S., and Sun, J. H.: Ground observations of a strong dust storm in Beijing in March 2002, J. Geophys. Res.-Atmos., 110, D18, 2005.

Zhang, R., Jing, J., Tao, J., Hsu, S. C., Wang, G., Cao, J., Lee, C. S. L., Zhu, L., Chen, Z., Zhao, Y., and Shen, Z.: Chemical characterization and source apportionment of PM2.5 in Beijing: seasonal perspective, Atmos. Chem. Phys., 13, 7053-7074, 2013b.

Zhang, X. L., Wu, G. J., Kokhanovsky, A., Yao, T. D., and Tong D.: Spectral albedo parameterization for dirty snow with considering mirco-physicochemical

properties of impurities - Part I: Theory and preliminary evaluation, 2016 (preparation).

Zhang, X. Y., Gong, S. L., Shen, Z. X., Mei, F. M., Xi, X. X., Liu, L. C., Zhou, Z. J., Wang, D., Wang, Y. Q., and Cheng, Y.: Characterization of soil dust aerosol in China and its transport and distribution during 2001 ACE-Asia: 1. Network observations, J. Geophys. Res.-Atmos., 108, 4261, 2003.

Zhao, C., Hu, Z., Qian, Y., Leung, L. R., Huang, J., Huang, M., Jin, J., Flanner, M. G., Zhang, R., Wang, H., Yan, H., Lu, Z., and Streets, D. G.: Simulating black carbon and dust and their radiative forcing in seasonal snow: a case study over North China with field campaign measurements, Atmos. Chem. Phys., 14, 11475-11491, 2014.

Acosta, J. A., Faz, A., Kalbitz, K., Jansen, B., and Martinez-Martinez, S.: Heavy metal concentrations in particle size fractions from street dust of Murcia (Spain) as the basis for risk assessment, J. Environ. Monitor., 13, 3087-3096, 10.1039/c1em10364d, 2011.

Aleksandropoulou, V., Torseth, K., and Lazaridis, M.: Atmospheric Emission Inventory for Natural and Anthropogenic Sources and Spatial Emission Mapping for the Greater Athens Area, Water Air Soil Pollut., 219, 507-526, 10.1007/s11270-010-0724-2, 2011.

Arhami, M., Kuhn, T., Fine, P. M., Delfino, R. J., and Sioutas, C.: Effects of sampling artifacts and operating parameters on the performance of a semicontinuous particulate elemental carbon/organic carbon monitor, Environ. Sci. Technol., 40, 945-954, 10.1021/es0510313, 2006.

Ax, W., Malchow, H., Koren, H., and Fischer, H.: Studies on immunological reactions in vitro, Sbornik vedeckych praci Lekarske fakulty Karlovy university v Hradci Kralove, 13, 287-292, 1970.

Bergstrom, R. W., Russell, P. B., and Hignett, P.: Wavelength dependence of the absorption of black carbon particles: Predictions and results from the TARFOX experiment and implications for the aerosol single scattering albedo, J. Atmos. Sci., 59, 567-577, Doi 10.1175/1520-0469(2002)059<0567:Wdotao>2.0.Co;2, 2002.

Bi, J. R., Huang, J. P., Hu, Z. Y., Holben, B. N., and Guo, Z. Q.: Investigating the aerosol optical and radiative characteristics of heavy haze episodes in Beijing during January of 2013, J. Geophys. Res.-Atmos., 119, 9884-9900, 10.1002/2014JD021757, 2014.

Bond, T. C., Bussemer, M., Wehner, B., Keller, S., Charlson, R. J., and Heintzenberg, J.: Light absorption by primary particle emissions from a lignite burning plant, Environ. Sci. Technol., 33, 3887-3891, Doi 10.1021/Es9810538, 1999.

Bond, T. C., and Bergstrom, R. W.: Light absorption by carbonaceous particles: An investigative review, Aerosol Sci. Tech., 40, 27-67, 10.1080/02786820500421521, 2006.

Bond, T. C., Doherty, S. J., Fahey, D. W., Forster, P. M., Berntsen, T., DeAngelo, B. J., Flanner, M. G., Ghan, S., Karcher, B., Koch, D., Kinne, S., Kondo, Y., Quinn, P. K., Sarofim, M. C., Schultz, M. G., Schulz, M., Venkataraman, C., Zhang, H., Zhang, S., Bellouin, N., Guttikunda, S. K., Hopke, P. K., Jacobson, M. Z., Kaiser, J. W., Klimont, Z., Lohmann, U., Schwarz, J. P., Shindell, D., Storelvmo, T., Warren, S. G., and Zender, C. S.: Bounding the role of black carbon in the climate system: A scientific assessment, J. Geophys. Res. Atmos., 118, 5380-5552, 10.1002/jgrd.50171, 2013.

Brandt, R. E., Warren, S. G., and Clarke, A. D.: A controlled snowmaking experiment testing the relation between black carbon content and reduction of snow albedo, J. Geophys. Res.-Atmos., 116, Artn D08109, 10.1029/2010jd015330, 2011.

Cachier, H., Liousse, C., Buatmenard, P., and Gaudichet, A.: Particulate Content of Savanna Fire Emissions, J. Atmos. Chem., 22, 123-148, Doi 10.1007/Bf00708185, 1995.

Cao, J. J., Lee, S. C., Chow, J. C., Watson, J. G., Ho, K. F., Zhang, R. J., Jin, Z. D., Shen, Z. X., Chen, G. C., Kang, Y. M., Zou, S. C., Zhang, L. Z., Qi, S. H., Dai, M. H., Cheng, Y., and Hu, K.: Spatial and seasonal distributions of carbonaceous aerosols over China, J. Geophys. Res. Atmos., 112, Artn D22s11, 10.1029/2006jd008205, 2007.

Carmagnola, C. M., Domine, F., Dumont, M., Wright, P., Strellis, B., Bergin, M., Dibb, J., Picard, G., Libois, Q., Arnaud, L., and Morin, S.: Snow spectral albedo at Summit, Greenland: measurements and numerical simulations based on physical and chemical properties of the snowpack, Cryosphere, 7, 1139-1160, 10.5194/tc-7-1139-2013, 2013.

Che, H., Zhang, X. Y., Xia, X., Goloub, P., Holben, B., Zhao, H., Wang, Y., Zhang, X. C., Wang, H., Blarel, L., Damiri, B., Zhang, R., Deng, X., Ma, Y., Wang, T., Geng, F., Qi, B., Zhu, J., Yu, J., Chen, Q., and Shi, G.: Ground-based aerosol climatology of China: aerosol optical depths from the China Aerosol Remote Sensing Network (CARSNET) 2002-2013, Atmos. Chem. Phys., 15, 7619-7652, 10.5194/acp-15-7619-2015, 2015a.

Che, H. Z., Yang, Z. F., Zhang, X. Y., Zhu, C. Z., Ma, Q. L., Zhou, H. G., and Wang, P.: Study on the aerosol optical properties and their relationship with aerosol chemical compositions over three regional background stations in China, Atmos. Environ., 43, 1093-1099, 10.1016/j.atmosenv.2008.11.010, 2009.

Che, H. Z., Wang, Y. Q., and Sun, J. Y.: Aerosol optical properties at Mt. Waliguan Observatory, China, Atmos. Environ., 45, 6004-6009, 10.1016/j.atmosenv.2011.07.050, 2011.

Che, H. Z., Wang, Y. Q., Sun, J. Y., Zhang, X. C., Zhang, X. Y., and Guo, J. P.: Variation of Aerosol Optical Properties over the Taklimakan Desert in China, Aerosol Air Qual. Res., 13, 777-785, 10.4209/aaqr.2012.07.0200, 2013.

Che, H. Z., Zhao, H. J., Wu, Y. F., Xia, X. G., Zhu, J., Wang, H., Wang, Y. Q., Sun, J. Y., Yu, J., Zhang, X. Y., and Shi, G. Y.: Analyses of aerosol optical properties and direct radiative forcing over urban and industrial regions in Northeast China, Meteorol. Atmos. Phys., 127, 345-354, 10.1007/s00703-015-0367-3, 2015b.

Chen, S. Y., Huang, J. P., Zhao, C., Qian, Y., Leung, L. R., and Yang, B.: Modeling the transport and radiative forcing of Taklimakan dust over the Tibetan Plateau: A case study in the summer of 2006, J. Geophys. Res.-Atmos., 118, 797-812, 10.1002/jgrd.50122, 2013.

Chu, D. A., Kaufman, Y. J., Ichoku, C., Remer, L. A., Tanre, D., and Holben, B. N.: Validation of MODIS aerosol optical depth retrieval over land, Geophys. Res. Lett., 29, Artn 1617, 10.1029/2001gl013205, 2002.

Cong, Z., Kang, S., Kawamura, K., Liu, B., Wan, X., Wang, Z., Gao, S., and Fu, P.: Carbonaceous aerosols on the south edge of the Tibetan Plateau: concentrations, seasonality and sources, Atmos. Chem. Phys., 15, 1573-1584, 10.5194/acp-15-1573-2015, 2015.

Coz, E., Casuccio, G., Lersch, T. L., Moreno, T., and Artinano, B.: Anthropogenic Influenced Mineral Dust Ambient Fine Particles At An Urban Site In Barcelona (Spain), Chem. Eng. Trans., 22, 101-106, 10.3303/Cet1022016, 2010.

Dang, C., and Hegg, D. A.: Quantifying light absorption by organic carbon in Western North American snow by serial chemical extractions, J. Geophys. Res.-Atmos., 119, 10.1002/2014JD022156, 2014.

de Mourgues, G., Fischer, L., and Felman, D.: Salter's" innominate osteotomy" of the pelvis for inequality of inferior limbs in a child, after complex injuries of the pelvis and one femur, Lyon chirurgical, 66, 62, 1970.

Doherty, S. J., Warren, S. G., Grenfell, T. C., Clarke, A. D., and Brandt, R. E.: Light-absorbing impurities in Arctic snow, Atmos. Chem. Phys., 10, 11647-11680, 10.5194/acp-10-11647-2010, 2010.

Doherty, S. J., Grenfell, T. C., Forsstrom, S., Hegg, D. L., Brandt, R. E., and Warren, S. G.: Observed vertical redistribution of black carbon and other insoluble light-absorbing particles in melting snow, J. Geophys. Res.-Atmos., 118, 5553-5569, 10.1002/jgrd.50235, 2013.

Doherty, S. J., Dang, C., Hegg, D. A., Zhang, R. D., and Warren, S. G.: Black carbon and other light-absorbing particles in snow of central North America, J. Geophys. Res.-Atmos., 119, 12807-12831, 10.1002/2014JD022350, 2014.

Flanner, M. G., Zender, C. S., Randerson, J. T., and Rasch, P. J.: Present-day climate forcing and response from black carbon in snow, J. Geophys. Res.-Atmos., 112, Artn D11202, 10.1029/2006jd008003, 2007.

Flanner, M. G., Zender, C. S., Hess, P. G., Mahowald, N. M., Painter, T. H., Ramanathan, V., and Rasch, P. J.: Springtime warming and reduced snow cover from carbonaceous particles, Atmos. Chem. Phys., 9, 2481-2497, 2009.

Flanner, M. G.: Arctic climate sensitivity to local black carbon, J. Geophys. Res.-Atmos., 118, 1840-1851, 10.1002/jgrd.50176, 2013.

Friedl, M. A., Sulla Menashe, D., Tan, B., Schneider, A., Ramankutty, N., Sibley, A., and Huang, X. M.: MODIS Collection 5 global land cover: Algorithm refinements and characterization of new datasets, Remote Sens. Environ., 114, 168-182, 10.1016/j.rse.2009.08.016, 2010.

Ginoux, P., Garbuzov, D., and Hsu, N. C.: Identification of anthropogenic and natural dust sources using Moderate Resolution Imaging Spectroradiometer (MODIS) Deep Blue level 2 data, J. Geophys. Res.-Atmos., 115, Artn D05204, 10.1029/2009jd012398, 2010.

Givati, A., and Rosenfeld, D.: Quantifying precipitation suppression due to air pollution, J. Appl. Meteorol., 43, 1038-1056, Doi 10.1175/1520-0450(2004)043<1038:Qpsdta>2.0.Co;2, 2004.

Goudie, A. S., and Middleton, N. J.: Saharan dust storms: nature and consequences, Earth Sci. Rev., 56, 179-204, Doi 10.1016/S0012-8252(01)00067-8, 2001.

Grenfell, T. C., Doherty, S. J., Clarke, A. D., and Warren, S. G.: Light absorption from particulate impurities in snow and ice determined by spectrophotometric analysis of filters, Appl. Opt., 50, 2037-2048, 10.1364/Ao.50.002037, 2011.

Guan, X., Huang, J., Guo, R., Yu, H., Lin, P., and Zhang, Y.: Role of radiatively forced temperature changes in enhanced semi-arid warming in the cold season over east Asia, Atmos. Chem. Phys., 15, 13777-13786, 10.5194/acp-15-13777-2015, 2015.

Hadley, O. L., and Kirchstetter, T. W.: Black-carbon reduction of snow albedo, Nat. Clim. Change, 2, 437-440, 10.1038/Nclimate1433, 2012.

Hansen, J., and Nazarenko, L.: Soot climate forcing via snow and ice albedos, Proc. Nat. Acad. Sci. U.S.A., PNAS 101, 423-428, 10.1073/pnas.2237157100, 2004.

Hansen, J., Sato, M., Ruedy, R., Nazarenko, L., Lacis, A., Schmidt, G. A., Russell, G., Aleinov, I., Bauer, M., Bauer, S., Bell, N., Cairns, B., Canuto, V., Chandler, M.,

Cheng, Y., Del Genio, A., Faluvegi, G., Fleming, E., Friend, A., Hall, T., Jackman, C., Kelley, M., Kiang, N., Koch, D., Lean, J., Lerner, J., Lo, K., Menon, S., Miller, R., Minnis, P., Novakov, T., Oinas, V., Perlwitz, J., Perlwitz, J., Rind, D., Romanou, A., Shindell, D., Stone, P., Sun, S., Tausnev, N., Thresher, D., Wielicki, B., Wong, T., Yao, M., and Zhang, S.: Efficacy of climate forcings, J. Geophys. Res.-Atmos., 110, Artn D18104, 10.1029/2005jd005776, 2005.

Hegg, D. A., Warren, S. G., Grenfell, T. C., Doherty, S. J., Larson, T. V., and Clarke, A. D.: Source Attribution of Black Carbon in Arctic Snow, Environ. Sci. Technol., 43, 4016-4021, 10.1021/es803623f, 2009.

Hegg, D. A., Warren, S. G., Grenfell, T. C., Doherty, S. J., and Clarke, A. D.: Sources of light-absorbing aerosol in arctic snow and their seasonal variation, Atmos. Chem. Phys., 10, 10923-10938, 10.5194/acp-10-10923-2010, 2010.

Holben, B. N., Eck, T. F., and Fraser, R. S.: Temporal and Spatial Variability of Aerosol Optical Depth in the Sahel Region in Relation to Vegetation Remote Sensing, Int. J. Remote Sens., 12, 1147-1163, 1991.

Holben, B. N., Tanre, D., Smirnov, A., Eck, T. F., Slutsker, I., Abuhassan, N., Newcomb, W. W., Schafer, J. S., Chatenet, B., Lavenu, F., Kaufman, Y. J., Castle, J. V., Setzer, A., Markham, B., Clark, D., Frouin, R., Halthore, R., Karneli, A., O'Neill, N. T., Pietras, C., Pinker, R. T., Voss, K., and Zibordi, G.: An emerging ground-based aerosol climatology: Aerosol optical depth from AERONET, J. Geophys. Res.-Atmos., 106, 12067-12097, Doi 10.1029/2001jd900014, 2001.

Holben, B. N., Eck, T. F., Slutsker, I., Smirnov, A., Sinyuk, A., Schafer, J., Giles, D., and Dubovik, O.: AERONET's Version 2.0 quality assurance criteria - art. no. 64080Q, Remote Sensing of the Atmosphere and Clouds, 6408, Q4080-Q4080, Artn 64080q, 10.1117/12.706524, 2006.

Hsu, S. C., Liu, S. C., Huang, Y. T., Chou, C. C. K., Lung, S. C. C., Liu, T. H., Tu, J. Y., and Tsai, F. J.: Long-range southeastward transport of Asian biosmoke pollution: Signature detected by aerosol potassium in Northern Taiwan, J. Geophys. Res.-Atmos., 114, Artn D14301, 10.1029/2009jd011725, 2009.

Huang, J. P., Fu, Q. A., Zhang, W., Wang, X., Zhang, R. D., Ye, H., and Warren, S. G.: Dust and Black Carbon in Seasonal Snow across Northern China, Bull. Amer. Meteor. Soc., 92, 175-181, 10.1175/2010BAMS3064.1, 2011.

Huang, J. P., Wang, T. H., Wang, W. C., Li, Z. Q., and Yan, H. R.: Climate effects of dust aerosols over East Asian arid and semiarid regions, J. Geophys. Res.-Atmos., 119, 11398-11416, 10.1002/2014JD021796, 2014.

Huang, J. P., Liu, J. J., Chen, B., and Nasiri, S. L.: Detection of anthropogenic dust using CALIPSO lidar measurements, Atmos. Chem. Phys., 15, 11653-11665, 10.5194/acp-15-11653-2015, 2015a.

Huang, Z. W., Huang, J. P., Hayasaka, T., Wang, S. S., Zhou, T., and Jin, H. C.: Short-cut transport path for Asian dust directly to the Arctic: a case study, Environ. Res. Lett., 10, Artn 114018, 10.1088/1748-9326/10/11/114018, 2015b.

Ianniello, A., Spataro, F., Esposito, G., Allegrini, I., Hu, M., and Zhu, T.: Chemical characteristics of inorganic ammonium salts in PM2.5 in the atmosphere of Beijing (China), Atmos. Chem. Phys., 11, 10803-10822, 10.5194/acp-11-10803-2011, 2011.

Ichoku, C., Chu, D. A., Mattoo, S., Kaufman, Y. J., Remer, L. A., Tanre, D., Slutsker, I., and Holben, B. N.: A spatio-temporal approach for global validation and analysis of MODIS aerosol products, Geophys. Res. Lett., 29, Artn 1616, 10.1029/2001gl013206, 2002a.

Ichoku, C., Levy, R., Kaufman, Y. J., Remer, L. A., Li, R. R., Martins, V. J., Holben, B. N., Abuhassan, N., Slutsker, I., Eck, T. F., and Pietras, C.: Analysis of the performance characteristics of the five-channel Microtops II Sun photometer for measuring aerosol optical thickness and precipitable water vapor, J. Geophys. Res. Atmos., 107, Artn 4179, 10.1029/2001jd001302, 2002b.

IPCC: Climate Change 2013: The Physical Science Basis. Contribution of Working Group I to the Fifth Assessment Report of the Intergovernmental Panel on Climate Change, Stocker, T. F., Qin, D., Plattner, G.-K., Tignor, M., Allen, S. K., Boschung, J., Nauels, A., Xia, Y., Bex, V., and Midgley, P. M., Cambridge Univ. Press, Cambridge, United Kingdom and New York, NY, USA, 2013.

Jacobson, M. Z.: Climate response of fossil fuel and biofuel soot, accounting for soot's feedback to snow and sea ice albedo and emissivity, J. Geophys. Res. Atmos., 109, Artn D21201, 10.1029/2004jd004945, 2004.

Jaffe, D., Anderson, T., Covert, D., Kotchenruther, R., Trost, B., Danielson, J., Simpson, W., Berntsen, T., Karlsdottir, S., Blake, D., Harris, J., Carmichael, G., and Uno, I.: Transport of Asian air pollution to North America, Geophys. Res. Lett., 26, 711-714, Doi 10.1029/1999gl900100, 1999.

Kamani, H., Ashrafi, S. D., Isazadeh, S., Jaafari, J., Hoseini, M., Mostafapour, F. K., Bazrafshan, E., Nazmara, S., and Mahvi, A. H.: Heavy Metal Contamination in Street Dusts with Various Land Uses in Zahedan, Iran, B. Environ. Contam. Tox., 94, 382-386, 10.1007/s00128-014-1453-9, 2015.

Kang, L. T., Huang, J. P., Chen, S. Y., and Wang, X.: Long-term trends of dust events over Tibetan Plateau during 1961-2010, Atmos. Environ., 125, 188-198, 10.1016/j.atmosenv.2015.10.085, 2016.

Kaufman, Y. J., Tanre, D., Gordon, H. R., Nakajima, T., Lenoble, J., Frouin, R., Grassl, H., Herman, B. M., King, M. D., and Teillet, P. M.: Passive remote sensing of tropospheric aerosol and atmospheric correction for the aerosol effect, J. Geophys. Res. Atmos., 102, 16815-16830, Doi 10.1029/97jd01496, 1997.

Kim, W., Doh, S. J., and Yu, Y.: Anthropogenic contribution of magnetic particulates in urban roadside dust, Atmos. Environ., 43, 3137-3144, 10.1016/j.atmosenv.2009.02.056, 2009.

Koch, D., Menon, S., Del Genio, A., Ruedy, R., Alienov, I., and Schmidt, G. A.: Distinguishing Aerosol Impacts on Climate over the Past Century, J. Climate, 22, 2659-2677, 10.1175/2008JCLI2573.1, 2009.

Kokhanovsky, A. A., and Zege, E. P.: Scattering optics of snow, Appl. Opt., 43, 1589-1602, Doi 10.1364/Ao.43.001589, 2004.

Kotthaus, S., Smith, T. E. L., Wooster, M. J., and Grimmond, C. S. B.: Derivation of an urban materials spectral library through emittance and reflectance spectroscopy, Isprs J. Photogramm., 94, 194-212, 10.1016/j.isprsjprs.2014.05.005, 2014.

Lafon, S., Sokolik, I. N., Rajot, J. L., Caquineau, S., and Gaudichet, A.: Characterization of iron oxides in mineral dust aerosols: Implications for light absorption, J. Geophys. Res. Atmos., 111, Artn D21207. 10.1029/2005jd007016, 2006.

Li, G. J., Chen, J., Ji, J. F., Yang, J. D., and Conway, T. M.: Natural and anthropogenic sources of East Asian dust, Geology, 37, 727-730, 10.1130/G30031a.1, 2009.

Li, S. Y., Lei, J. Q., Xu, X. W., Wang, H. F., and Gu, F.: Dust Source of Sandstorm in the Tarim Basin, Northwest China, Adv. Environ. Sci. Eng., 518-523, 4592-4598, 10.4028/www.scientific.net/AMR.518-523.4592, 2012.

Li, X. Y., Liu, L. J., Wang, Y. G., Luo, G. P., Chen, X., Yang, X. L., Hall, M. H. P., Guo, R. C., Wang, H. J., Cui, J. H., and He, X. Y.: Heavy metal contamination of urban soil in an old industrial city (Shenyang) in Northeast China, Geoderma, 192, 50-58, 10.1016/j.geoderma.2012.08.011, 2013.

Light, B., Eicken, H., Maykut, G. A., and Grenfell, T. C.: The effect of included particulates on the spectral albedo of sea ice, J. Geophys. Res.-Oceans, 103, 27739-27752, Doi 10.1029/98jc02587, 1998.

Lorenz, K., Preston, C. M., and Kandeler, E.: Soil organic matter in urban soils: Estimation of elemental carbon by thermal oxidation and characterization of organic matter by solid-state C-13 nuclear magnetic resonance (NMR) spectroscopy, Geoderma, 130, 312-323, 10.1016/j.geoderma.2005.02.004, 2006.

Loveland, T. R., and Belward, A. S.: The IGBP-DIS global 1 km land cover data set, DISCover: first results, Int. J. Remote Sens., 18, 3291-3295, 1997.

Mahowald, N. M., and Luo, C.: A less dusty future?, Geophys. Res. Lett., 30, Artn 1903, 10.1029/2003gl017880, 2003.

Mahowald, N. M., Baker, A. R., Bergametti, G., Brooks, N., Duce, R. A., Jickells, T. D., Kubilay, N., Prospero, J. M., and Tegen, I.: Atmospheric global dust cycle and iron inputs to the ocean, Global Biogeochem. CY., 19, Artn Gb4025, 10.1029/2004gb002402, 2005.

Ming, J., Xiao, C. D., Sun, J. Y., Kang, S. C., and Bonasoni, P.: Carbonaceous particles in the atmosphere and precipitation of the Nam Co region, central Tibet, J. Environ. Sci., 22, 1748-1756, 10.1016/S1001-0742(09)60315-6, 2010.

Morys, M., Mims, F. M., Hagerup, S., Anderson, S. E., Baker, A., Kia, J., and Walkup, T.: Design, calibration, and performance of MICROTOPS II handheld ozone monitor and Sun photometer, J. Geophys. Res. Atmos., 106, 14573-14582, Doi 10.1029/2001jd900103, 2001.

Motoyoshi, H., Aoki, T., Hori, M., Abe, O., and Mochizuki, S.: Possible effect of anthropogenic aerosol deposition on snow albedo reduction at Shinjo, Japan, J. Meteorol. Soc. Jpn., 83A, 137-148, Doi 10.2151/Jmsj.83a.137, 2005.

Novakov, T., Menon, S., Kirchstetter, T. W., Koch, D., and Hansen, J. E.: Aerosol organic carbon to black carbon ratios: Analysis of published data and implications for climate forcing, J. Geophys. Res. Atmos., 110, Artn D21205, 10.1029/2005jd005977, 2005.

Painter, T. H., Barrett, A. P., Landry, C. C., Neff, J. C., Cassidy, M. P., Lawrence, C. R., McBride, K. E., and Farmer, G. L.: Impact of disturbed desert soils on duration of mountain snow cover, Geophys. Res. Lett., 34, Artn L12502, 10.1029/2007gl030284, 2007.

Painter, T. H., Deems, J. S., Belnap, J., Hamlet, A. F., Landry, C. C., and Udall, B.: Response of Colorado River runoff to dust radiative forcing in snow, Proc. Nat. Acad. Sci. U.S.A., PNAS 107, 17125-17130, 10.1073/pnas.0913139107, 2010.

Painter, T. H., Bryant, A. C., and Skiles, S. M.: Radiative forcing by light absorbing impurities in snow from MODIS surface reflectance data, Geophys. Res. Lett., 39, Artn L17502, 10.1029/2012gl052457, 2012.

Painter, T. H., Seidel, F. C., Bryant, A. C., Skiles, S. M., and Rittger, K.: Imaging spectroscopy of albedo and radiative forcing by light-absorbing impurities in mountain snow, J. Geophys. Res.-Atmos., 118, 9511-9523, 10.1002/jgrd.50520, 2013.

Park, S. U., and Park, M. S.: Aerosol size distributions observed at Naiman in the Asian dust source region of Inner Mongolia, Atmos. Environ., 82, 17-23, 10.1016/j.atmosenv.2013.09.054, 2014.

Pedersen, C. A., Gallet, J. C., Strom, J., Gerland, S., Hudson, S. R., Forsstrom, S., Isaksson, E., and Berntsen, T. K.: In situ observations of black carbon in snow and the corresponding spectral surface albedo reduction, J. Geophys. Res. Atmos., 120, 1476-1489, 10.1002/2014JD022407, 2015.

Pio, C. A., Legrand, M., Oliveira, T., Afonso, J., Santos, C., Caseiro, A., Fialho, P., Barata, F., Puxbaum, H., Sanchez-Ochoa, A., Kasper-Giebl, A., Gelencser, A., Preunkert, S., and Schock, M.: Climatology of aerosol composition (organic versus inorganic) at nonurban sites on a west-east transect across Europe, J. Geophys. Res. Atmos., 112, Artn D23s02, 10.1029/2006jd008038, 2007.

Porter, J. N., Miller, M., Pietras, C., and Motell, C.: Ship-based sun photometer measurements using Microtops sun photometers, J. Atmos. Oceanic Technol., 18, 765-774, Doi 10.1175/1520-0426(2001)018<0765:Sbspmu>2.0.Co;2, 2001.

Pu, W., Wang, X., Zhang, X. Y., Ren, Y., Shi, J. S., Bi, J. R., and Zhang, B. D.: Size Distribution and Optical Properties of Particulate Matter (PM10) and Black Carbon (BC) during Dust Storms and Local Air Pollution Events across a Loess Plateau Site, Aerosol Air Qual. Res., 15, 2212-2224, 10.4209/aaqr.2015.02.0109, 2015.

Qian, Y., Wang, H. L., Zhang, R. D., Flanner, M. G., and Rasch, P. J.: A sensitivity study on modeling black carbon in snow and its radiative forcing over the Arctic and Northern China, Environ. Res. Lett., 9, Artn 064001, 10.1088/1748-9326/9/6/064001, 2014.

Qian, Y., Yasunari, T. J., Doherty, S. J., Flanner, M. G., Lau, W. K. M., Ming, J., Wang, H. L., Wang, M., Warren, S. G., and Zhang, R. D.: Light-absorbing Particles in Snow and Ice: Measurement and Modeling of Climatic and Hydrological impact, Adv. Atmos. Sci., 32, 64-91, 10.1007/s00376-014-0010-0, 2015.

Qiao, Q. Q., Huang, B. C., Zhang, C. X., Piper, J. D. A., Pan, Y. P., and Sun, Y.: Assessment of heavy metal contamination of dustfall in northern China from integrated chemical and magnetic investigation, Atmos. Environ., 74, 182-193, 10.1016/j.atmosenv.2013.03.039, 2013.

Remer, L. A., Tanre, D., Kaufman, Y. J., Ichoku, C., Mattoo, S., Levy, R., Chu, D. A., Holben, B., Dubovik, O., Smirnov, A., Martins, J. V., Li, R. R., and Ahmad, Z.: Validation of MODIS aerosol retrieval over ocean, Geophys. Res. Lett., 29, Artn 1618, 10.1029/2001gl013204, 2002.

Rosenfeld, D., Rudich, Y., and Lahav, R.: Desert dust suppressing precipitation: A possible desertification feedback loop, Proc. Nat. Acad. Sci. U.S.A.,PNAS 98, 5975-5980, DOI 10.1073/pnas.101122798, 2001.

Routray, A., Mohanty, U. C., Osuri, K. K., and Prasad, S. K.: Improvement of Monsoon Depressions Forecast with Assimilation of Indian DWR Data Using WRF-3DVAR Analysis System, Pure Appl. Geophys., 170, 2329-2350, 10.1007/s00024-013-0648-z, 2013.

Rozenberg, G.: Optical characteristics of thick weakly absorbing scattering layers, Dokl. Akad. Nauk SSSR, 145, 775-777,1962.

Smith, T. M., Gao, J. D., Calhoun, K. M., Stensrud, D. J., Manross, K. L., Ortega, K. L., Fu, C. H., Kingfield, D. M., Elmore, K. L., Lakshmanan, V., and Riedel, C.: Examination of a Real-Time 3DVAR Analysis System in the Hazardous Weather Testbed, Weather Forecast., 29, 63-77, 10.1175/Waf-D-13-00044.1, 2014.

Srivastava, K., and Bhardwaj, R.: Analysis and very short range forecast of cyclone "AILA" with radar data assimilation with rapid intermittent cycle using ARPS

3DVAR and cloud analysis techniques, Meteorol. Atmos. Phys., 124, 97-111, 10.1007/s00703-014-0307-7, 2014.

Tegen, I., and Fung, I.: Contribution to the Atmospheric Mineral Aerosol Load from Land Surface Modification, J. Geophys. Res. Atmos., 100, 18707-18726, Doi 10.1029/95jd02051, 1995.

Tegen, I., Harrison, S. P., Kohfeld, K. E., Engelstaedter, S., and Werner, M.: Emission of soil dust aerosol: Anthropogenic contribution and future changes, Geochimica Et Cosmochimica Acta, 66, A766-A766, 2002.

Tegen, I., Werner, M., Harrison, S. P., and Kohfeld, K. E.: Relative importance of climate and land use in determining present and future global soil dust emission, Geophys. Res. Lett., 31, Artn L05105, 10.1029/2003gl019216, 2004.

Thompson, L. G., Davis, M. E., Mosleythompson, E., and Liu, K. B.: Pre-Incan Agricultural Activity Recorded in Dust Layers in 2 Tropical Ice Cores, Nature, 336, 763-765, Doi 10.1038/336763a0, 1988.

Toon, O. B., Mckay, C. P., Ackerman, T. P., and Santhanam, K.: Rapid Calculation of Radiative Heating Rates and Photodissociation Rates in Inhomogeneous Multiple-Scattering Atmospheres, J. Geophys. Res. Atmos., 94, 16287-16301, Doi 10.1029/Jd094id13p16287, 1989.

Wallach, D. F. H., and Fischer, H.: Membrane aspects of the immune response. Report of a workshop held in Titisee, Schwarzwald, Germany, October 13-15, 1969, FEBS Lett. , 9, 129-135, 1970.

Wang, M., Xu, B. Q., Zhao, H. B., Cao, J. J., Joswiak, D., Wu, G. J., and Lin, S. B.: The Influence of Dust on Quantitative Measurements of Black Carbon in Ice and Snow when Using a Thermal Optical Method, Aerosol Sci. Tech., 46, 60-69, 10.1080/02786826.2011.605815, 2012.

Wang, P., Che, H. Z., Zhang, X. C., Song, Q. L., Wang, Y. Q., Zhang, Z. H., Dai, X., and Yu, D. J.: Aerosol optical properties of regional background atmosphere in Northeast China, Atmos. Environ., 44, 4404-4412, 10.1016/j.atmosenv.2010.07.043, 2010a.

Wang, X., Huang, J. P., Ji, M. X., and Higuchi, K.: Variability of East Asia dust events and their long-term trend, Atmos. Environ., 42, 3156-3165, 10.1016/j.atmosenv.2007.07.046, 2008.

Wang, X., Huang, J. P., Zhang, R. D., Chen, B., and Bi, J. R.: Surface measurements of aerosol properties over northwest China during ARM China 2008 deployment, J. Geophys. Res.-Atmos., 115, Artn D00k27, 10.1029/2009jd013467, 2010b.

Wang, X., Doherty, S. J., and Huang, J. P.: Black carbon and other light-absorbing impurities in snow across Northern China, J. Geophys. Res. Atmos., 118, 1471-1492, 10.1029/2012JD018291, 2013a.

Wang, X., Pu, W., Zhang, X. Y., Ren, Y., and Huang, J. P.: Water-soluble ions and trace elements in surface snow and their potential source regions across northeastern China, Atmos. Environ., 114, 57-65, 10.1016/j.atmosenv.2015.05.012, 2015.

Wang, X. G., Parrish, D., Kleist, D., and Whitaker, J.: GSI 3DVar-Based Ensemble-Variational Hybrid Data Assimilation for NCEP Global Forecast System: Single-Resolution Experiments, Mon. Weather. Rev., 141, 4098-4117, 10.1175/Mwr-D-12-00141.1, 2013b.

Wang, Z. W., Gallet, J. C., Pedersen, C. A., Zhang, X. S., Strom, J., and Ci, Z. J.: Elemental carbon in snow at Changbai Mountain, northeastern China: concentrations, scavenging ratios, and dry deposition velocities, Atmos. Chem. Phys., 14, 629-640, 10.5194/acp-14-629-2014, 2014.

Wang, X., Xu, B. Q., and Ming, J.: An Overview of the Studies on Black Carbon and Mineral Dust Deposition in Snow and Ice Cores in East Asia, J Meteorol Res-Prc, 28, 354-370, 2014.

Warren, S. G., and Wiscombe, W. J.: A Model for the Spectral Albedo of Snow .2. Snow Containing Atmospheric Aerosols, J. Atmos. Sci., 37, 2734-2745, Doi 10.1175/1520-0469(1980)037<2734:Amftsa>2.0.Co;2, 1980.

Warren, S. G. and Wiscombe, W. J.: Dirty Snow after Nuclear-War, Nature, 313, 467-470, 1985.

Warren, S. G.: Optical-Properties of Snow, Rev. Geophys., 20, 67-89, Doi 10.1029/Rg020i001p00067, 1982.

Wedepohl, K. H.: The Composition of the Continental Crust, Geochimica Et Cosmochimica Acta, 59, 1217-1232, 1995.

Wright, P., Bergin, M., Dibb, J., Lefer, B., Domine, F., Carman, T., Carmagnola, C., Dumont, M., Courville, Z., Schaaf, C., and Wang, Z. S.: Comparing MODIS daily snow albedo to spectral albedo field measurements in Central Greenland, Remote Sens. Environ., 140, 118-129, 10.1016/j.rse.2013.08.044, 2014.

Wuttke, S., Seckmeyer, G., Bernhard, G., Ehramjian, J., McKenzie, R., Johnston, P., and O'Neill, M.: New spectroradiometers complying with the NDSC standards, J. Atmos. Oceanic Technol., 23, 241-251, 2006a.

Wuttke, S., Seckmeyer, G., and Konig-Lang, G.: Measurements of spectral snow albedo at Neumayer, Antarctica, Ann. Geophys., 24, 7-21, 2006b.

Xia, X. A., Chen, H. B., Wang, P. C., Zong, X. M., Qiu, J. H., and Gouloub, P.: Aerosol properties and their spatial and temporal variations over North China in spring 2001, Tellus B., 57, 28-39, 2005.

Xia, X. G., Li, Z. Q., Holben, B., Wang, P., Eck, T., Chen, H. B., Cribb, M., and Zhao, Y. X.: Aerosol optical properties and radiative effects in the Yangtze Delta region of China, J. Geophys. Res. Atmos., 112, Artn D22s12, 10.1029/2007jd008859, 2007.

Xu, B. Q., Cao, J. J., Hansen, J., Yao, T. D., Joswia, D. R., Wang, N. L., Wu, G. J., Wang, M., Zhao, H. B., Yang, W., Liu, X. Q., and He, J. Q.: Black soot and the survival of Tibetan glaciers, Proc. Nat. Acad. Sci. U.S.A., 106, 22114-22118, 10.1073/pnas.0910444106, 2009.

Xu, B. Q., Cao, J. J., Joswiak, D. R., Liu, X. Q., Zhao, H. B., and He, J. Q.: Post-depositional enrichment of black soot in snow-pack and accelerated melting of Tibetan glaciers, Environ. Res. Lett., 7, 10.1088/1748-9326/7/1/014022, 2012.

Yasunari, T. J., Bonasoni, P., Laj, P., Fujita, K., Vuillermoz, E., Marinoni, A., Cristofanelli, P., Duchi, R., Tartari, G., and Lau, K. M.: Estimated impact of black carbon deposition during pre-monsoon season from Nepal Climate Observatory - Pyramid data and snow albedo changes over Himalayan glaciers, Atmos. Chem. Phys., 10, 6603-6615, 10.5194/acp-10-6603-2010, 2010.

Yasunari, T. J., Koster, R. D., Lau, W. K. M., and Kim, K. M.: Impact of snow darkening via dust, black carbon, and organic carbon on boreal spring climate in the Earth system, J. Geophys. Res.-Atmos., 120, 5485-5503, 10.1002/2014jd022977, 2015.

Ye, H., Zhang, R. D., Shi, J. S., Huang, J. P., Warren, S. G., and Fu, Q.: Black carbon in seasonal snow across northern Xinjiang in northwestern China, Environ. Res. Lett., 7, Artn 044002, 10.1088/1748-9326/7/4/044002, 2012.

Yesubabu, V., Srinivas, C. V., Hariprasad, K. B. R. R., and Baskaran, R.: A Study on the Impact of Observation Assimilation on the Numerical Simulation of Tropical Cyclones JAL and THANE Using 3DVAR, Pure Appl. Geophys., 171, 2023-2042, 10.1007/s00024-013-0741-3, 2014.

Zawadzka, O., Makuch, P., Markowicz, K. M., Zielinski, T., Petelski, T., Ulevicius, V., Strzalkowska, A., Rozwadowska, A., and Gutowska, D.: Studies of aerosol optical depth with the use of Microtops II sun photometers and MODIS detectors in coastal areas of the Baltic Sea, Acta Geophysica, 62, 400-422, 10.2478/s11600-013-0182-5, 2014.

Zege, E. P., Ivanov, A. P., and Katsev, I. L.: Image transfer through a scattering medium, Springer Verlag, 1991.

Zhang, R., Hegg, D. A., Huang, J., and Fu, Q.: Source attribution of insoluble light-absorbing particles in seasonal snow across northern China, Atmos. Chem. Phys., 13, 6091-6099, 10.5194/acp-13-6091-2013, 2013.

Zhang, R., Jing, J., Tao, J., Hsu, S. C., Wang, G., Cao, J., Lee, C. S. L., Zhu, L., Chen, Z., Zhao, Y., and Shen, Z.: Chemical characterization and source apportionment of PM2.5 in Beijing: seasonal perspective, Atmos. Chem. Phys. , 13, 7053-7074, 10.5194/acp-13-7053-2013, 2013.

Zhang, R. J., Arimoto, R., An, J. L., Yabuki, S., and Sun, J. H.: Ground observations of a strong dust storm in Beijing in March 2002, J. Geophys. Res. Atmos., 110, 10.1029/2004jd004589, 2005.

Zhang, X. L., Wu, G. J., Kokhanovsky, A., Yao, T. D., and Tong D.: Spectral albedo parameterization for dirty snow with considering mirco-physicochemical properties of impurities - Part I: Theory and preliminary evaluation, 2016 (preparation).

Zhang, X. Y., Gong, S. L., Shen, Z. X., Mei, F. M., Xi, X. X., Liu, L. C., Zhou, Z. J., Wang, D., Wang, Y. Q., and Cheng, Y.: Characterization of soil dust aerosol in China and its transport and distribution during 2001 ACE-Asia: 1. Network observations, J. Geophys. Res. Atmos., 108, Artn 4261, 10.1029/2002jd002632, 2003.

Zhao, C., Hu, Z., Qian, Y., Leung, L. R., Huang, J., Huang, M., Jin, J., Flanner, M. G., Zhang, R., Wang, H., Yan, H., Lu, Z., and Streets, D. G.: Simulating black carbon and dust and their radiative forcing in seasonal snow: a case study over North China with field campaign measurements, Atmos. Chem. Phys., 14, 11475-11491, 10.5194/acp-14-11475-2014, 2014.

Ofosu, F. G., Hopke, P. K., Aboh, I. J. K., and Bamford, S. A.: Characterization of fine particulate sources at Ashaiman in Greater Accra, Ghana, Atmos Pollut Res, 3, 301-310, 2012.